Functional characterization of the US3 serine/threonine kinase during BHV-1 infection

A Thesis

Submitted to the College of Graduate Studies and Research

In Partial Fulfillment of the Requirements

For the Degree of Master of Science

In the Department of Vaccinology and Immunotherapeutics, School of Public Health

University of Saskatchewan

By

Tara Jean Donovan

PERMISSION TO USE

In presenting this thesis as partial fulfillment of the requirements for a postgraduate degree from the University of Saskatchewan, I agree that the Libraries of this University may make it freely available for inspection. I further agree that permission for copying of this thesis in any matter, in whole or in part, for scholarly purposes, may be granted by the professors who supervised my thesis work or, in their absence, by the Head of the Department or the Dean of the College in which my thesis work was done. It is understood that copying or publication of this thesis or parts thereof for financial gain shall not be allowed without my written permission. It is also understood that due recognition shall be given to me and to the University of Saskatchewan in any scholarly use which may be made of any materials in my thesis.

Request for permission to copy or to make use of other materials in this thesis, in whole or in part, should be addressed to:

Head of the Department of Vaccinology & Immunotherapeutics

School of Public Health

University of Saskatchewan

ABSTRACT

Bovine herpesvirus 1 (BHV-1) is a member of the *Alphaherpesvirinae* subfamily and is the prototype ruminant herpesvirus. BHV-1 causes a number of complications in cattle including upper respiratory tract disorders, conjunctivitis, genital disorders, abortions, and immune suppression. Like all herpesviruses, reactivation from latency can occur throughout the animal's life. Of particular economic importance is the bovine respiratory disease complex (BRDC) or 'shipping fever', in which BHV-1 plays a major role. BRDC is an enormous economic concern as it costs the US cattle industry approximately one billion dollars annually.

In order to generate improved gene-deleted vaccines against BHV-1, there is a need to understand the contributions of viral gene products during infection. US3 is a serine/threonine kinase present in BHV-1 and is thought to play major roles during viral infection. As in other herpesviruses, US3 in BHV-1 is expected to phosphorylate several cellular and/or viral proteins. We recently presented evidence that BHV-1 US3 phosphorylates both VP8 and VP22; however, further functional characteristics of BHV-1 US3 during viral infection have not been elucidated.

The hypothesis of this project is that the deletion of the US3 gene leads to reduced BHV-1 fitness. To explore this hypothesis, we generated a US3-deleted (ΔUS3) and subsequent US3-rescued (US3R) BHV-1 virus. Using these viral mutants, we characterized the growth properties of the viruses, evaluated the effect of the US3 deletion on major structural BHV-1 proteins, characterized the protein composition of the mature virions, and, identified viral processes that were impaired in the deletion mutant.

Initially, the ΔUS3 virus was generated through a 3-step PCR strategy which replaced the gene of interest with an antibiotic resistance cassette. Following this, the US3 gene was rescued via a two-step *en passant* mutagenesis strategy which has been previously used to generate

insertions, deletions, and substitutions in herpesvirus-containing bacterial artificial chromosome (BAC) DNA.

In vitro characterization of ΔUS3 BHV-1 has demonstrated that US3 deletion affects BHV-1 growth characteristics, expression kinetics of major structural proteins, mature virion composition, cell to cell spread, and the subcellular localization of key viral proteins during infection. Growth kinetics of ΔUS3 BHV-1 were impaired compared to wild-type (WT) BHV-1, especially at late times post-infection. Plaque sizes formed by ΔUS3 BHV-1 were significantly smaller than those formed by either WT or US3R BHV-1, demonstrating that US3 is important for cell to cell spread. The expression kinetics of major structural and regulatory BHV-1 proteins were different between cells infected with ΔUS3 or WT BHV-1, and incorporation of these proteins into the mature viruses differed, demonstrating that US3 is instrumental in ensuring proper protein expression and mature virus composition *in vitro*.

Of particular importance, glycoprotein B (gB), was shown to be expressed in higher quantities earlier during infection in the absence of US3, and that this protein was incorporated in significantly higher amounts in mature virions which lacked US3. Qualitative analysis of ΔUS3 BHV-1 infected monolayers suggested the abolishment of cell to cell projections characteristic of WT BHV-1 infection. Finally, the disruption of gB in ΔUS3 BHV-1 infected cells was confirmed by confocal microscopy and fluorescence-activated cell sorting (FACS) analysis. Through confocal microscopy, evidence was provided that infection with ΔUS3 BHV-1 possibly results in earlier expression of gB on the surface of cells and less intracellular accumulation of this protein during late stages of infection. The observed effect on the localization of intracellular gB in ΔUS3 BHV-1 infected cells was quantified by flow cytometry. ΔUS3 BHV-1 infected cells had approximately 25% higher gB expression on the surface of cells and a corresponding 25%

decrease in intracellular gB. Although these differences have not yet been demonstrated to be statistically significant and not confirmed through infection with US3R BHV-1, this suggests that US3 may influence the synthesis and cellular trafficking of gB *in vitro.*

ACKNOWLEDGEMENTS

First off, I would like to thank my graduate supervisor, Dr. Sylvia van Drunen Littel – van den Hurk for her supervision. I have appreciated the opportunity to study in such a diverse field and have valued her guidance, expertise, and resourcefulness throughout the course of my research. Additionally, I would like to thank my advisory committee, Dr. Joyce Wilson and Dr. Suresh Tikoo for their guidance and encouragement throughout this project. Funding for this project was provided by the Canadian Institutes of Health Research and Natural Sciences and Engineering Research Council, as well as from a scholarship through the Department of Vaccinology and Immunotherapeutics.

I would like to extend many thanks to all of the friends and colleagues I have made while studying at VIDO. Not only is there a great wealth of knowledge in the building, it houses some of the greatest people that I've ever had the pleasure of working with. Specifically, I would like to thank Dr. Robert Brownlie for his molecular expertise and assistance with my project. I would also like to thank Marlene Snider for her technical expertise and support during my confocal studies. Not only have these people made me into a more skilled researcher, they have both become great friends of mine. Finally, I would like to thank Natasa Arsic and Ravendra Garg for their assistance with my FACS analyses and for the time they have devoted to my project.

There are too many past and present lab mates to thank, but specifically I would like to extend my gratitude to Dr. Vladislav Lobanov, Dr. Karl Robinson, and Luana Dummer for their help with this project. I have enjoyed the time I have spent with all of the people from A321, and will miss all the laughs, camaraderie, and stories that we shared on a daily basis.

Lastly, I would like to thank my greatest support during this project: My family. Thanks to my parents, Robert and Janet Lee, for their unwavering encouragement and belief in me and

my dreams. You have given me the confidence and strength to believe that anything is possible if I put my mind to it. Thanks to my in-laws for their love and support. Lastly, I owe the greatest thanks to my wonderful husband, Andrew, who has been there every step of the way through this journey called graduate school.

DEDICATION

This thesis is dedicated to my family.

Tables of Contents

LIST OF TABLES

LIST OF FIGURES

LIST OF ABBREVIATIONS

˚C	degree Celsius
a.a.	amino acid
AP	adaptor protein
APS	ammonium persulfate
ATP	adenosine triphosphate
BAC	bacterial artificial chromosome
BCIP	5-bromo-4-chloro-3-indolylphosphate
BHV-1	bovine herpesvirus type 1
BHV-5	bovine herpesvirus type 5
bp	base pairs
BRDC	bovine respiratory disease complex
BRSV	bovine respiratory syncytial virus
BVDV	bovine viral diarrhea virus
CD	cluster of differentiation
Cdc42	cell division control protein 42 homolog
CK2	cellular casein kinase 2
cm	centimetres
CMI	cell-mediated immunity
CO_2	carbon dioxide
ddH20	double distilled water
DNA	deoxyribonucleic acid
DTT	dithiothreitol
E	early
FACS	fluorescence-activated cell sorting
FBS	fetal bovine serum
FBT	Fetal Bovine Tracheal cells
gB	glycoprotein B. All viral glycoproteins are designated with the prefix ‘g.’
GFP	green fluorescent protein
GTP	guanosine triphosphate
HCL	hydrochloric acid
HSV-1	herpes simplex virus type 1

HSV-2	herpes simplex virus type 2
IBRD	infectious bovine rhinotracheitis disorder
IE	immediate-early
IFN-γ	interferon gamma
Ig	immunoglobulin
IR	internal repeat
I-SceI	inducible homing endonuclease SceI
kb	kilobase
kD	kilodalton
KV	killed vaccine
kV	kilovolts
L	late
LAT	latency-associated transcript
LT	linear transgene
MAb	monoclonal antibody
mAmps	milliamps
MDBK	Madin Darby Bovine Kidney cells
MDV	Marek's Disease virus
MFI	mean fluorescent intensity
MHC	major histocompatibility complex
ml	millilitre
MLV	modified live vaccine
mm	millimetre
MOI	multiplicity of infection
mRNA	messenger ribonucleic acid
NBT	nitroblue tetrazolium
ng	nanograms
ORF	open reading frame
PAb	polyclonal antibody
PAK	serine/threonine protein kinase
PBS	phosphate buffered saline
PCR	polymerase chain reaction
PFU	plaque-forming units

PMSF	phenylmethylsulfonyl fluoride
PRV	pseudorabiesvirus
Rac1	Ras-related C3 botulinum toxin substrate 1
RCF	relative centrifugal force
Rho	ρ factor
RPM	revolutions per minute
SDS-PAGE	sodium dodecyl sulphate polyacrylamide gel electrophoresis
TEMED	N,N,N’,N’-tetramethylethylenediamine
Thr-887	threonine residue 887
TR	terminal repeat
Tyr-889	tyrosine residue 889
UL	unique long
US	unique short
US3R	US3-rescued
v/v	volume per volume
w/v	weight per volume
WT	wild-type
ΔUS3	US3-deleted
μg	micrograms
Ω	ohm
μF	microfarads
μl	microlitres

1.0 Literature Review

1.1 Introduction to BHV-1

1.1.1 Nomenclature and Classification

BHV-1 is a member of the *Varicellovirus* genus and *Alphaherpesvirinae* subfamily and is the prototype ruminant herpesvirus (125). It is the causative agent of *infectious bovine rhinotracheitis disorder* (IBRD) and *shipping fever*, which cause a number of complications in cattle worldwide.

BHV-1 is classified into subtypes 1.1, 1.2a, and 1.2b. Each of the subtypes has different DNA restriction endonuclease profiles (89), cause different clinical manifestations in their hosts (98), and has different geographical distributions (51). Subtype 1.1 is the most pathogenic and is typically isolated from cattle with BHV-1-induced respiratory disease, causing bovine rhinotracheitis and abortions. This subtype is most prevalent in North America, Europe, and South America. Subtype 1.2a (2a) is geographically restricted to Brazil and causes a broad range of symptoms, including genital and respiratory infections, and abortions (142). Subtype 1.2b (2b) is found in Australia and Europe and is associated with milder clinical disease, causing respiratory and genital infections in cattle (51). Subtypes 1.1 and 1.2a are capable of causing abortion, where as subtype 1.2b is not (89).

1.1.2 Disease and Importance

1.1.2.1 Clinical Manifestations

Clinical manifestations of BHV-1 were primarily restricted to genital disorders in the early 19th century (98). In the early 1950's, however, a more severe form of the disease showed up in North American feedlots. This form of the disease affected the upper respiratory tract of

cattle, leading to IBRD (123). IBRD spread rapidly across North America and to Europe due to importation of dairy cattle from infected feedlots (98).

Since its discovery, BHV-1 has been further characterized as a multifaceted disease affecting a wide range of tissues and causing symptoms in cattle ranging from upper respiratory tract disorders, conjunctivitis, genital disorders, abortions, to immune suppression in cattle (51, 98). Primary infection with BHV-1 includes inoculation at a mucosal surface and a 1-6 day incubation period depending on the strain and mode of transmission (51, 133). After incubation, virus-loaded lesions appear in the infected areas and usually resolve within 4-5 days for respiratory infections, and about two weeks for genital infections. BHV-1 induced respiratory infections cause high fever, salivation, nasal and ocular discharge, anorexia, coughing, and numerous nasal lesions on the septal mucosa (51). Although abortions often occur in parallel with acute respiratory infection, they can also occur through BHV-1 reactivation up to 100 days after acute infection. Symptoms caused by genital infections with subtypes 2a and 2b often begin as an increased urination frequency followed by the appearance of lesions on the genitals of infected animals. Infections with BHV-1 tend to be complicated by secondary infections caused by a weakened immune system in the infected animal and usually require antibiotics (155).

Although a multifactorial disease, BHV-1 is known to play a primary role in the development of full BRDC. In addition to BHV-1, stress and other viral pathogens, such as parainfluenza-3 virus, bovine respiratory syncytial virus (BRSV), and bovine viral diarrhoea virus (BVDV), contribute to the formation of BRDC through immune suppression which eventually leads to secondary infections caused by *M. haemolytica* and *P. multocida* (51, 155). BRDC is characterized by high fever, anorexia, coughing, excessive salivation, nasal discharge,

inflamed nares, pneumonia and dyspneae (51, 155). BHV-1 is thought to cause BRDC through immunosuppression of the host due to down regulation of the major histocompatibility complex (MHC) class I (40, 51, 101) and through apoptosis of infected CD4+ T cells early in infection (152).

Similar to all primary alphaherpesvirus infections, BHV-1 gains access to the local sensory neurons and establishes latency in the ganglia (2, 3). Reactivation of BHV-1 from latency can occur throughout the animal's life and can cause serious respiratory disease, abortion of the fetus, and transmission of the virus to disease-free animals.

1.1.2.2 Epidemiology

BHV-1 is widely distributed throughout the world. Australia, New Zealand, Canada, and the USA have variable but high seroprevalence rates (1). Despite control measures, BHV-1 is endemic in many European and South American countries (21). Complicating the problem further, BHV-1 and BHV-5 have been shown to co-infect cattle in countries such as Argentina and Brazil, where vaccination against BHV-1 is not mandatory and where BHV-5 infections are prevalent (15).

BHV-1 risk factors include sex (higher incidence in males), age, herd size, direct animal contact, and farm density (9, 129, 143, 147). Since BHV-1 is latent in its host and can reactivate at any point, latently infected animals are the major source of transmission to uninfected herds. Therefore, since cattle populations in North America are large, transmission of the virus from latently infected cattle to uninfected herds is difficult to control. The virus is easily spread via mating, birth, transport, and through the introduction of infected heifers into dairy cattle herds (98). Transmission of the virus through a non-cattle ruminant reservoir is not likely to be a major source of BHV-1 transmission (132).

1.1.2.3 Cell Tropisms

BHV-1 has limited cell tropisms, infecting the epithelial cells of the upper respiratory tract, the genital tract, and the conjunctiva (98), and can infect CD4+ cells (152). Infection of the upper respiratory tract most commonly occurs through direct nose to nose contact, but can occur through aerosol droplets at short distances (81). Entry of the virus through the genitals usually occurs through mating or through artificial insemination by virus-infected semen (63). After replication in the epithelial mucosa, the virus gains access to the ganglia to establish latent infection in neurons (105). Systemic spread of the virus is possible when the mucosal barriers are compromised (82), and the resulting viremia is associated with abortion of the unborn fetus (18) and fatal systemic infection in calves (42).

1.1.2.4 Economic Importance of BRDC

BHV-1 is of particular economic importance due to the role that it plays in the development of BRDC or 'shipping fever' (51). BRDC is an enormous economic concern as it costs the US cattle industry approximately 640 million annually due to weight loss, decreased milk production, abortions, and restrictions on international trade (11, 100). Since recovered cattle remain lifetime carriers of the virus, they are considered dangerous to disease-free herds since they can introduce the virus under immunosuppressive conditions (108, 142).

1.1.3 Vaccines

BHV-1 has been eradicated from a number of European countries including Denmark, Switzerland, Austria, Finland, Sweden, and Norway by culling of seropositive herds (102, 130). This method is acceptable in countries which harbour small cattle populations that can be controlled. A similar method, however, is unfeasible for countries with large cattle populations,

such as those present in North America. In these countries, vaccination remains the most feasible method of BHV-1 eradication, however, vaccination programs to date have been largely unsuccessful (1).

There are two types of commercially available vaccines against BHV-1, namely modified live vaccines (MLV) and inactivated vaccines (51). Although considerable efforts have been made to generate vaccines against BHV-1, all have been shown to have problems with efficacy or safety (98). Currently, subunit vaccines, DNA vaccines, gene-deleted, and vector based vaccines are in pre-clinical development.

Vaccines against BHV-1 are generally evaluated based on absence of clinical symptoms, low viral shedding upon challenge and high neutralizing antibody titer (51). Recently, it was demonstrated that in addition to a high IFN-γ response by T cells, increased expression of CD25 is indicative of BHV-1 immunity (27).

Early studies on BHV-1 vaccines were focused on generating MLV and killed vaccines (KV). MLV are able to replicate in cells, therefore inducing rapid and long-lasting humoral and cell-mediated immune (CMI) responses (150). Although quite efficient, MLV have problems with safety, including inducing immunosuppression in calves and abortion in pregnant cows due to reactivation from latency (100). Furthermore, it has been noted that there have been a number of BRDC outbreaks in feedlot cattle which were previously immunized with MLV (139).

Although a safe alternative to MLV, KV only elicit a humoral response and are incapable of inducing a CMI response. Other drawbacks to KV include requiring more than one dose, the need for adjuvants, and the possibility of the antigenic structures becoming denatured during the inactivation process, which may affect immunogenicity (51).

Due to the problems associated with commercial MLV and KV, genetically engineered gene-deleted, subunit, and vectored BHV-1 vaccines are being investigated as potentially more efficient and safe for use in cattle. Furthermore, gene-deleted, subunit, and vectored vaccines have the added advantage of differentiating vaccinated from non-vaccinated animals. Various gene-deleted vaccines have been constructed, but most have had issues with reactivation from latency or virulence (50). A glycoprotein E (gE)-deleted vaccine, however, was shown to be extremely safe and has been successful in eradicating BHV-1 from several European countries. Although it has an excellent safety profile, this vaccine has been shown to be less efficacious than other glycoprotein-deleted vaccines (53). Efforts are being made to identify immunosuppressive BHV-1 motifs that can be deleted along with gE to improve the vaccine efficacy (50). A glycoprotein D (gD) subunit vaccine has been demonstrated to be highly protective when formulated with adjuvants such as a mineral oil emulsion and a CpG oligodeoxynucleotide (46, 140). Vectored vaccines which express gD using either DNA or bovine adenovirus have been shown to be successful and may be useful in immunizing neonates due to resilience in the face of maternal antibodies (137, 156).

BHV-1 is ideal as a vaccine vector due to its large size, which easily accommodates foreign genes, and its limited host range (6, 79). The virus been used successfully as a vaccine vector to immunize cattle against pathogens such as BVDV and BRSV (64, 120). To continue to improve BHV-1 subunit and marker vaccines, as well as increase the potential for BHV-1 to be an effective vaccine vector, more research is needed to understand the contributions of individual BHV-1 gene products to viral fitness and pathogenicity in the host.

1.2 BHV-1 genome and virus composition

Like other *Herpesviridae*, BHV-1 is a large, pleomorphic virus that contains four morphologically distinct compartments (114). These compartments include the genome-containing core inside the icosahedral capsid, surrounded by the proteinaceous tegument layer that links the capsid to the outer cell-derived envelope (85, 86).

Together, the icosahedral capsid and the viral genome make up the viral nucleocapsid. The 136 kilobase (kb) BHV-1 genome contains linear double-stranded DNA encoding approximately 70 proteins, with 33 known structural proteins and 15 non-structural proteins (91, 98, 125) (Table 1.1). In 2008, a random insertional mutagenesis study by Robinson et al. demonstrated that in cell culture, BHV-1 has 33 essential open reading frames (ORF) and 36 non-essential ORF (113). The genome is extremely guanine and cytosine rich (72%) and many proteins are conserved within the *Alphaherpesvirinae* subfamily (146).

Belonging to class D herpesvirus genomes, the BHV-1 genome contains a unique long (UL) and unique short (US) region with two inverted repeat sequences that flank the US region, called the internal repeat (IR) and the terminal repeat (TR) (127) (Figure 1.1). During genome replication, the repeats result in packaging of equimolar amounts of two isomers in which the US region is in either orientation and the UL region is fixed (114). These isomeric forms are created as a consequence of homologous recombination between the inverted repeats.

Type	Gene	Protein	Remarks
Glycoproteins	UL27	gB	major glycoprotein, attachment, entry, intracellular spread, fusion
	UL44	gC	major glycoprotein, attachment, virulence
	US6	gD	major glycoprotein, entry, intracellular spread
	US8	gE	intracellular spread, neuroinvasion
	US7	gI	intracellular spread, virulence
	UL22	gH	entry, intracellular spread, egress
	UL1	gL	entry, cooperates with gH
	US4	gG	chemokine binding activity, intracellular spread
	UL53	gK	syncytium formation
	UL10	gM	central nervous system spread
	UL49.5	gN	membrane, involved in virulence
Envelope	UL34	UL34	membrane
Tegument	UL11	UL11	myristylated protein
	UL36	UL36	very large tegument protein
	UL37	UL37	complexes with UL36
	UL47	VP8	most abundant tegument protein, viral RNA shuttling
	UL48	VP16	alpha trans-inducing factor
	UL49	VP22	major player in intracellular spread
	US9	US9	involved in neurovirulence
Capsid	UL19	VP5	major capsid protein
Enzyme	UL23	UL23	thymidine kinase
	UL13	UL13	serine/threonine kinase
	US3	US3	serine/threonine kinase
Regulatory	BICP0	BICP0	immediate-early transactivator protein
	BICP4	BICP4	immediate-early transactivator protein
Unknown	UL31	UL31	complexes with UL34
BHV-1 specific	UL3.5	UL3.5	interacts with VP16 for efficient nuclear egress

Table 1.1: Major BHV-1 genes discussed or investigated in this study (91, 99, 125, 132)

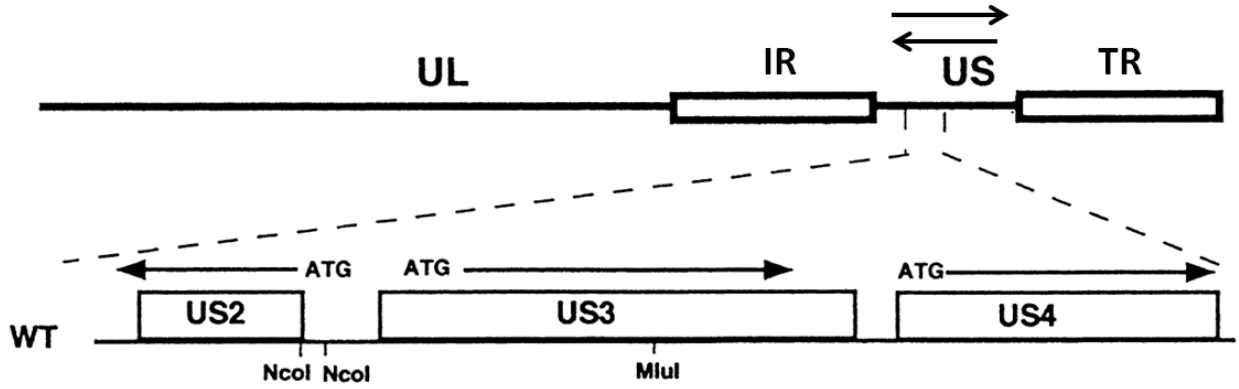

Figure 1.1: Schematic of the BHV-1 genome and the US2, US3, and US4 gene organization.

Adapted from Takashima et al. (131)

The majority of proteins encoded by BHV-1 are involved in nucleic acid metabolism, DNA synthesis, and protein processing (115). Of the 33 structural proteins, 11 are glycoproteins (125). The major envelope glycoproteins are gB, C (gC), and D (gD) (5), and the minor glycoproteins include E (gE), G (gG), H (gH), I (gI), K (gK), L (gL), M (gM), and N (gN). Some of these glycoproteins play essential roles in viral pathogenicity and viability, as they regulate virus attachment, entry, egress, and cell to cell spread of the virus (28, 110, 125). The five glycoproteins that are essential for growth in cell culture are gB, gD, gH, gL, and gK (51). Other major structural and regulatory proteins include the capsid protein, VP5 (103); VP8 and VP16, which are involved in gene regulation (16, 138); VP22, which has been implicated in BHV-1 cell to cell spread (54); and bICP4 and bICP0, which are key regulatory elements of viral transcription (61).

Surrounding the nucleocapid is a specialized electron-dense layer called the tegument that contains approximately 15 viral proteins (84). After fusion of the virus, the tegument proteins dissociate from the nucleocapsid and play important roles such as modulating the host immune response (62) and activating the viral replication cycle (16). After viral replication, these proteins have important roles in generating infectious progeny through various regulatory functions, which are not yet completely understood.

1.3 Alphaherpesvirus replication cycle

The alphaherpesvirus lifecycle is separated into the following stages: entry, uncoating, translocation to the nucleus, replication of the genome, packaging, nuclear egress, envelopment, tegumentation, and cellular egress (Figure 1.2). BHV-1 mediates attachment to permissive cells through gB, gC, and gD (72, 75). To facilitate entry, gC attaches to the heparin sulfate

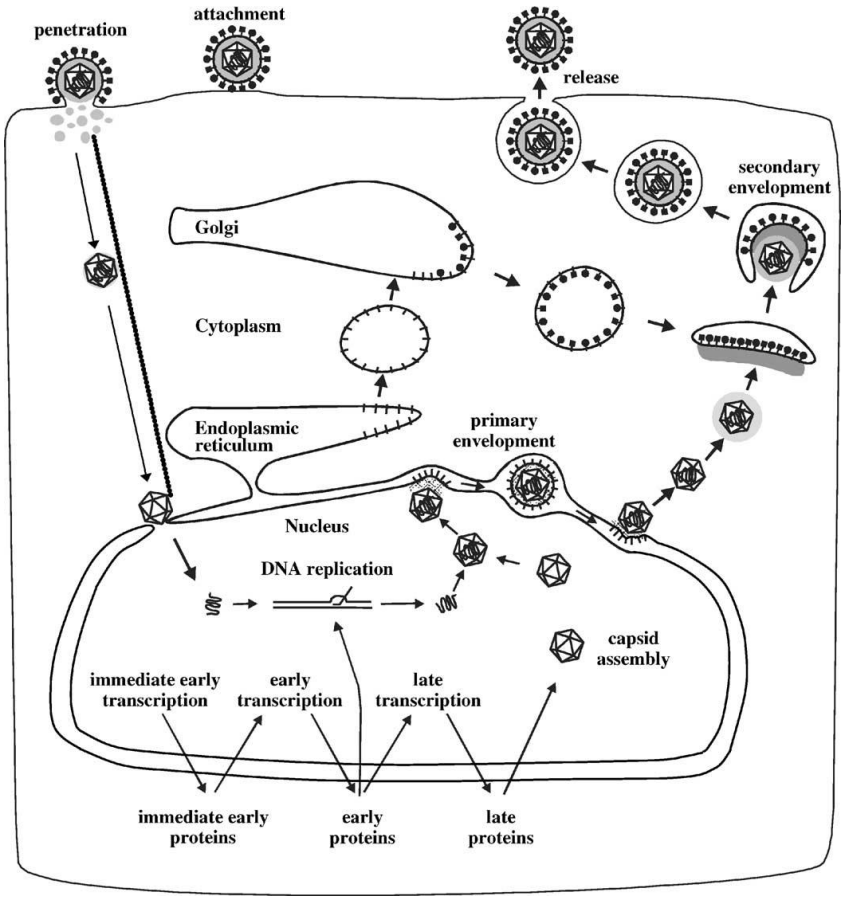

Figure 1.2: Schematic of the alphaherpesvirus replication cycle.

The alphaherpesvirus virus replication cycle includes entry, uncoating, translocation to the nucleus, replication of the genome, packaging, nuclear egress, envelopment, tegumentation, and cellular egress. This figure is used with permission from Thomas C. Mettenleiter (84).

proteoglycan residue on the surface of cells, and when deleted, attachment can be mediated through gB (72, 104). After attachment, viral fusion occurs though interaction of gD with the nectin 1 receptor (HveC) (19), likely in cooperation with either gB or gH/gL (51, 83). Although interaction of gD with nectin 1 is required for entry, a compensatory mutation in gH at amino acid (a.a.) residue 450 can rescue gD-deleted BHV-1 viruses (121).

After fusion of the virus with the cellular membrane, many of the tegument proteins are dissociated from the capsid to play a variety of roles including facilitating degradation of host mRNAs (65) and priming the cell for viral replication (85, 86). Of importance, BHV-1 VP16 and its homologous protein in herpes simplex virus type 1 (HSV-1) dissociates from the tegument to transactivate immediate-early gene expression, likely in collaboration with VP8 (92, 93, 157). After fusion, the capsid travels to the nucleus along microtubules until the viral DNA translocates through a nuclear pore. While most of the tegument proteins dissociate after fusion, some proteins remain with the capsid until it docks at the nuclear pore. Specifically, in pseudorabies virus (PRV), UL36, UL37, and US3 have been shown to remain with the capsid until docking at the nuclear pore occurs (38).

Once the viral DNA enters the nucleus, it circularizes and the DNA is replicated and transcribed. The genome is replicated through a rolling-circle mechanism using both viral and cellular proteins (71). Similar to other alphaherpesviruses, the BHV-1 genome is transcribed in a cascade which results in immediate-early (IE), early (E), and late (L) viral mRNAs. The IE genes are transcribed immediately after infection by host transcription factors which are enhanced by VP16 and VP8 (84, 126). The IE proteins are then shuttled into the nucleus to transcribe the E mRNAs. Following this, the E mRNAs are shuttled into the cytoplasm for translation before the resulting proteins are shuttled back into the nucleus for trans-activation of the L genes. Once the

L proteins are translated, they are translocated back into the nucleus where the capsid autocatalytically assembles and encapsulates the viral DNA (84, 85).

All *Herpesviridae* undergo a series of budding and de-envelopment events to acquire the tegument proteins and the cellular derived viral membrane (85, 86). Nuclear egress is a complicated process which requires the capsid to first bud through the inner leaflet of the nuclear membrane, a step called primary envelopment. Viral proteins UL31 and UL34 are essential for this process and deletions in either of these genes results in the accumulation of capsids in the nucleus of HSV-1 infected cells (116). In addition to these proteins, cellular protein kinases and US3 have been shown to aid in primary envelopment, possibly through phosphorylation (112, 128).

After primary envelopment, the capsid buds through the outer nuclear membrane in a process called de-envelopment. This process involves fusion of the primary viral envelope with the outer nuclear membrane. De-envelopment releases the viral capsids into the cytoplasm. US3 in HSV-1 plays an important role in this process since US3-deleted mutants have been shown to accumulate the virions in the perinuclear space (59, 111).

Once in the cytoplasm, the virions undergo a secondary envelopment process where they acquire their tegument and envelope before cellular egress. Although complex and not well understood, the process of tegumentation is thought to be facilitated through a series of protein-protein interactions which begins with UL36 (159). Two layers of the tegument are added, with some proteins being capsid-associated and others being membrane-associated. The viral glycoproteins are thought to be key players in this process, and in PRV, gE and gM have been demonstrated to be required for incorporation of the major tegument protein, UL49 (34). Similarly, in HSV-1, gE and gD are required to incorporate the UL49 protein (29). US3 has been

shown to be a component of primary and mature PRV and HSV-1 virions and remains tightly associated with the capsid during the process of tegumentation. It is thought that US3 may play a role in facilitating alphaherpesvirus egress from the nucleus, since US3-deleted PRV are impaired during secondary envelopment (39, 112).

The glycoproteins and tegument proteins assemble with the capsid through vesicles of the *trans* Golgi network (85). The vesicles eventually comprise the envelope of mature virions. Recruiting and retaining the virions at Golgi-derived vesicles has been shown to depend on UL11 and gM (12, 20), with deletions in these genes in PRV causing large intracytoplasmic accumulations of capsids embedded in Golgi-derived vesicles (60). In BHV-1, UL3.5 has been shown to interact with VP16 for efficient secondary envelopment and release (33, 69).

Once the virus has acquired its tegument and envelope, the virus is transported to the cellular membrane in a vesicle where it fuses with the plasma membrane and the virus is released through exocytosis. Alternatively, alphaherpesviruses can enter adjacent cells through cell to cell spread using gD and gE/gI (122, 135).

1.4 Latency

As is a hallmark of all herpesviruses, BHV-1 establishes lifelong latency in its host following acute infection. The primary site for latency is the sensory neuron of the ganglia, into which the virus gains access to through cell to cell spread (51). The circularized genome is maintained extrachromosomally in latently-infected neurons through high expression of the latency-associated transcript (LAT) and open reading frame (ORF) E, which prevent apoptosis, transcription of other viral genes, and regulate the latency-reactivation cycle (45, 49, 51Jones, 1990 #1305, 52).

Environmental stressors on the host which result in increased cortisol levels and immunosuppression lead to virus reactivation and subsequent proliferative infection. Three factors are associated with reactivation from latency, which include decreased expression of LAT and ORF-E, productive viral gene expression, and infectious virus released from nasal or ocular orifices (51).

1.5 Alphaherpesvirus US3 serine/threonine kinase

US3 has been identified in both BHV-1 and HSV-1 as being a 58 kilodalton (kD) serine/threonine kinase (131), and along with UL13, is one of the two serine/threonine kinases present in alphaherpesviruses (114). The multifunctional protein is conserved amongst the alphaherpesviruses, with low amino acid similarity but high functional conservation (Table 2). Furthermore, the kinase domain contains two invariant residues which are conserved among US3 orthologues and correspond to the adenosine triphosphate (ATP)-binding domains and the catalytic sites (22) (Table 2). Although the protein is non-essential for viral replication, it has proven to play key roles throughout the subfamily in viral fitness and pathogenicity. The US3 protein has been studied extensively in PRV and HSV-1, but the specific roles that US3 plays in BHV-1 infection have not been elucidated.

1.5.1 Function of US3 in HSV-1 and PRV

The roles that US3 plays in HSV-1 and PRV infections have been well-characterized. In HSV-1, US3 helps evade the antiviral host response through disrupted interferon signaling (73, 106) and helps establish latent infections in the sensory ganglia of its host (4). HSV-1 US3 has also been shown to regulate viral gene expression through independent blocking of histone deacetylation (107). Nuclear egress in HSV-1 is facilitated by US3 (57, 97) through

phosphorylation of gB (153), which downregulates the surface expression of gB (55), resulting in decreased antigen presentation at the cell surface (44, 55). Kato et al. have determined a number of viral substrates for US3, which include UL34, ICP22, US9, and the major tegument protein, UL47 (57). Recently, US3 has been demonstrated to play a role in regulating the subcellular localization of UL47 (56).

PRV US3 plays a role in the downregulation of MHC-I surface expression (23), and similar to HSV-1 US3, blocks apoptosis during infection (35, 149). For the purposes of this review, only the functions that were investigated in BHV-1 during this project will be discussed.

The role that US3 plays in PRV and HSV-1 virion morphogenesis has been studied extensively. US3 has been shown to play an integral role in viral egress from the nucleus after encapsidation. Nuclear egress is a multifaceted process which is mediated through US3 phosphorylation of various cellular and viral proteins. Two of the major players in this process are the viral proteins, UL31 and UL34, which together form a transmembrane complex that facilitates primary envelopment and subsequent nuclear egress (57, 59, 96, 109). US3 phosphorylation of these proteins in HSV-1 is regulated by the UL13 serine/threonine kinase, which uses US3 as a substrate (58). In recombinant HSV-1 viruses lacking the US3 gene, the UL31/UL34 complex appeared at the nuclear rim in punctuate patterns as opposed to the distributed phenotype seen during WT infection (58, 111). Through the generation of a kinase-dead mutant or mutating the corresponding serine/threonine targets in UL34, Rychman and Roller showed that proper distribution of the HSV-1 UL34/UL31 complex is due to US3-mediated phosphorylation of UL34 in specific cell types (117).

	HSV-1	HSV-2	VZV	PRV	BoHV-1	BoHV-5	EHV-1	EHV-4	MDV
HSV-1	100								
HSV-2	74 (84)	100							
VZV	37 (45)	35 (44)	100						
PRV	33 (40)	32 (40)	29 (40)	100					
BoHV-1	29 (43)	30 (40)	33 (45)	41 (49)	100				
BoHV-5	31 (42)	31 (40)	33 (43)	41 (48)	81 (89)	100			
EHV-1	34 (41)	34 (40)	36 (45)	38 (46)	40 (47)	40 (46)	100		
EHV-4	36 (43)	36 (42)	36 (44)	39 (48)	39 (48)	40 (48)	86 (91)	100	
MDV	31 (41)	30 (40)	28 (38)	27 (37)	29 (37)	29 (36)	29 (37)	29 (37)	100

Table 1.2: Amino acid sequence similarities between various US3 orthologues

The table denotes the amino acid similarities of the US3 ORF between various alphaherpesviruses and displays the homology of the kinase regions in parentheses. Homologies between BHV-1 US3 and other US3 homologues within the alphaherpesvirus subfamily have been circled. Table adapted from (22).

To further aid in primary envelopment of the virions, HSV-1 US3 has been shown to direct capsids to the inner nuclear membrane and facilitate budding through phosphorylation of nuclear membrane proteins. This process is facilitated through the phosphorylation of lamin A/C proteins which are present in the nuclear lamina, and also emerin, an inner nuclear membrane protein that interacts with lamins (22, 95). It has recently been demonstrated that hyperphosphorylation of emerin via US3, in collaboration with UL34, results in increased mobility of emerin in the inner nuclear membrane. This causes disrupted connections between emerin and lamin, ultimately resulting in the nuclear lamina becoming compromised, which allows the virus to bud into the perinuclear space (70, 94).

A predominant phenotype of US3-deleted PRV and HSV-1 viruses is the accumulation of capsids in the perinuclear space in large inner membrane blebs due to impaired de-envelopment (59, 112, 148). This phenotype has also been observed in cells infected with Marek's Disease Virus (MDV) when US3 is deleted (124). In HSV-1, the phenotype is dependent on the catalytic region of US3, since kinase-dead mutants have the same phenotype as US3-deleted viruses (117). The mechanism behind impaired egress in kinase-dead mutants may be the lack of phosphorylation of gB, since gB is important in the fusion of the outer nuclear membrane with the envelope surrounding perinuclear HSV-1 virions (153). The model suggested by Wisner et al. is that US3 phosphorylates the cytoplasmic tail of gB in the virion and triggers fusion between the outer nuclear membrane and the virion envelope (153).

Further to its role in nuclear egress, US3-mediated phosphorylation of the major antigenic epitope, gB, has also been implicated as a mechanism by which alphaherpesviruses evade the host immune response (7, 119). Cell surface expression of gB has been shown to directly correlate with cell lysis of infected cells (8). To prevent excess expression of gB at the

surface of infected cells, herpesviruses have developed an intricate system to recycle the protein from the surface through endocytosis after being modified into an active form (13). Typically, intracellular trafficking of gB occurs from the cytoplasm to the cell membrane, where it is recycled through endocytosis before being directed to the trans-Golgi network for viral envelope assembly. Endocytosis is dependent on two motifs that are present in the cytoplasmic tail of gB. These motifs are recognized by subunits of the clatherin adaptor protein (AP) which make up the endocytotic vesicles (10).

Recent studies in HSV-1 have shown that US3 phosphorylates gB at threonine residue 887 (Thr-887), and that this modification results in a conformational change that may increase recognition of the endocytosis motif by AP (55, 153). Through mutations at Thr-887 in gB and inactivation of US3, Kato et al. were able to demonstrate that the surface expression of gB is markedly increased in HSV-1 infected cells (55). These results support the hypothesis that US3 phosphorylation of gB at residue Thr-887 is required for optimal endocytosis of gB from the infected cell surface.

To determine the effect that US3 has on pathogenicity and replication of HSV-1 *in vivo* due to the down-regulation of gB at the cell surface, Imai et al. used recombinant HSV-1 expressing mutated Thr-887 gB for infection in a mouse model (44). Consistent with previous studies, where a kinase-dead HSV-1 US3 mutant was used for infection, Imai et al. showed that mutating the US3 phosphorylation target on gB significantly reduced both viral titres and the development of herpes stroma keratitis and periocular skin disease in infected mice (118). Furthermore, this group also developed a monoclonal antibody which reacts specifically with phosphorylated Thr-887 and was able to demonstrate that endocytosis of gB from the cell surface is dependent on phosphorylation at this residue. Taken together, these results show that the

phosphorylation of gB at residue Thr-887 by US3 is required for efficient down regulation of gB from the cell surface in HSV-1-infected cells, as well as for effective replication and pathogenicity in a mouse stromal keratitis model. Follow-up studies by Imai et al. have characterized two other sequences that are necessary for optimal gB trafficking during HSV-1 infection (43), which include tyrosine residue 889 (Tyr-889) and a dileucine residue at 871/ 872. The Tyr-889 residue was found to play the most critical role in regulating the intracellular transport of gB, expression of the protein on the surface of infected cells, and neurovirulence in mice.

US3 in HSV-1 and PRV has also been demonstrated to induce cytoskeletal rearrangements that result in actin stress fiber breakdown and long microtubule-rich extensions from the cell that can be several cell diameters in length (22). These extensions often make intimate contact with host cells, and in PRV, have been implicated in cell to cell spread of the virus (30). Through transfection assays, Van Minnebruggen et al. have demonstrated that in PRV, cytoskeleton actin stress fiber breakdown is dependent solely on US3 (141). Van der Broeke et al. have shed some light on the mechanisms behind the dramatic alphaherpesvirus US3-mediated cytoskeleton rearrangements (136) by demonstrating that the p21-kinases play an essential roles in both actin stress fiber breakdown and filamentous process formation when phosphorylated (activated) by US3. The cellular p21-activated kinases are key regulators of Cdc42/Rac1 Rho GTPase actin-modifying signaling pathways. Using gene-knockout mouse fibroblast cells, the group identified two components of the pathway that are essential for either US3-mediated stress fiber breakdown or filamentous process formation. These constituents are PAK2 and PAK1, respectively. US3 has been implicated in other herpesviruses as the main

driver of cytoskeleton rearrangements during viral infection, including BHV-5, herpes simplex viruse 2 (HSV-2), and most recently, BHV-1 (14, 32, 68).

Interestingly, US3 and UL47 have recently been shown to reciprocally regulate their subcellular location within HSV-1 infected cells (56). Typically in HSV-1 infection, UL47 shuttles between the nucleus and the cytoplasm to carry out various functions, including shuttling mRNAs into the nucleus during early infection (24) Through a systematic process of mutating serine and threonine residues near the nuclear localization site, serine at residue 77 (Ser-77) was shown to be phosphorylated by US3 and mutation of this residue resulted in accumulation of pUL47 at the nuclear rim of infected cells. Conversely, mutating the catalytic region in US3 had a similar phenotype. Pathogenesis studies showed that mutating either Ser-77 in UL47 or the catalytic site in US3 resulted in decreased viral replication and the development of herpes stromal keratitis in a mouse model. Furthermore, the nuclear localization of US3 was shown to be impaired in the absence of UL47 (43). These results demonstrate an important role for HSV-1 US3 in both the phosphorylation and intracellular localization of the major tegument protein, UL47, and a role for US3 in the pathogenesis of HSV-1.

1.5.2 Putative functions of US3 in BHV-1

1.5.2.1 Known substrates

Although much is known about the functions of US3 during HSV-1 and PRV infections, the role(s) that this protein plays in BHV-1 infection has not been fully characterized. The first report that identified BHV-1 US3 as a 58kD serine/threonine protein kinase demonstrated that unlike the orthologous protein in HSV-1 and PRV, BHV-1 US3 is not directly involved in blocking apoptosis in infected cells (131). Labiuk et al. recently identified VP8 and VP22 as

substrates of BHV-1 US3 (66, 67). The tegument protein, VP22, was shown to be phosphorylated by BHV-1 US3 as well as by the cellular casein kinase 2 (CK2). VP22 plays essential roles in the fitness of BHV-1 *in vitro*, including trafficking from infected to non-infected cells in the absence of other viral proteins (41, 74). In addition to identifying VP22 as a minor substrate for US3, Labiuk et al. determined the catalytic region in the protein and determined that US3 autophosphorylates itself (66).

Like in HSV-1, the BHV-1 UL47 gene product, VP8, is phosphorylated by US3 (67). Similar to its role in HSV-1, BHV-1 VP8 shuttles between the nucleus and cytoplasm and may bind viral mRNA (24, 25, 138, 145), while playing an important role in immunogenicity (131). Through a combination of immunoprecipitation and mass spectroscopy, Labiuk et al. were able to identify two kinases which contribute to the phosphorylation of VP8. US3 was found to play a minor role and CK2 was demonstrated to play a major role in the phosphorylation of VP8 (67). It is still unknown whether phosphorylation of VP8 in BHV-1 regulates its intracellular localization as has been demonstrated in HSV-1.

Recently, using a recombinant baculovirus, BHV-1 US3 was shown to produce cytoskeleton changes in transfected cells that are characteristic of BHV-1 infection. These cytoskeleton modifications are similar to those seen in HSV-1 and PRV, which are dependent on the activity of US3. In the study by Brzozowska et al., microtubule-rich projections were formed in both BHV-1-permissive and non-permissive cells following transfection with the US3-expressing baculovirus (14). Using confocal microscopy, the group was able to identify US3 localizing in the nucleus early after transduction and throughout the cytoplasm as time progressed. Mutating the catalytic region in US3 demonstrated that the kinase activity is required for modification of the cytoskeleton in this system. It still remains to be elucidated whether

cytoskeleton remodeling in the context of BHV-1 infection is dependent on US3 and whether there are other viral proteins involved.

Additional functions that BHV-1 US3 plays *in vitro* were recently elucidated (90) in an attempt to determine the role that it plays in the pathogenicity of BHV-1. To investigate this, the Schönböken and Aus12 strains were compared, which are low and high passage number, respectively. The objectives of this study were to compare the growth characteristics of the two virus strains, determine the significance of the aminoterminal domain of US3, and the subcellular location of US3-deleted BHV-1 virions. The role that BHV-1 US3 plays in apoptosis was also investigated and the function of the cellular SET protein in productive BHV-1 infection was observed. When the US3 gene was deleted in the highly passaged strain (Aus12), the group observed a large defect in cell to cell spread while the minimally passaged strain (Schönböken) had a minimal defect in cell to cell spread. It was hypothesized that point mutations elsewhere in the genome in the Schönböken strain had complemented the inhibitory effects of the US3 deletion. Growth characteristics were slightly impaired (about a 10-fold difference) with the US3 deleted viruses compared to their wild-type parent virus, but were independent of the strain used (i.e. Schönböken vs Aus12). Interestingly, ultrastructural analysis showed that US3-deletion results in nuclear accumulation of aggregates which contain viral nucleocapsids. This nuclear accumulation of nucleocapsids is distinct from the perinuclear accumulation of nucleocapsids that is seen in HSV-1, PRV and MDV (59, 96, 112, 124, 153), and may elude to a different mode of egress facilitated by BHV-1 US3.

Recent studies on BHV-1 US3 have therefore shown the significance during viral infection (22). While BHV-1 US3 has been shown to be non-essential, it has a substantial impact on the growth kinetics and possibly cell to cell spread of the virus. Distinct functions of US3 in

the cell and its interactions with other viral proteins need to be elucidated to determine the exact role of US3 in BHV-1 pathogenesis. Expression kinetics of major structural and regulatory proteins and mature virion composition assays will be useful in determining which proteins may be affected and/or involved in the phenotypical changes that are seen upon US3 deletion in BHV-1. Kinetics assays will also help to determine at which stage in the viral cycle these phenotypical changes arise. Furthermore, confocal microscopy using antibodies against important proteins identified may elucidate a role for US3 in the viral lifecycle of BHV-1.

2.0 HYPOTHESIS AND OBJECTIVES

Based on previous work on the role(s) of US3 serine/threonine kinase homologues during alphaherpesvirus infection, our hypothesis is that BHV-1 US3 contributes to viral fitness *in vitro*. To validate this hypothesis, five main objectives were explored.

The first objective was to generate a US3-deleted and subsequent US3-rescued BHV-1 virus. This was carried out using a homologous cloning strategy with a BHV-1-containing BAC.

The second objective of this project was to characterize growth properties of the mutant viruses by performing a single-step growth assay. This standard growth assay was used to determine whether BHV-1 US3 plays a role during *in vitro* growth kinetics.

Our third objective was to evaluate the effect of BHV-1 US3-deletion on the expression kinetics of major structural and regulatory BHV-1 proteins. This was carried out in an effort to identify the role that BHV-1 US3 plays on the expression of key viral proteins *in vitro*. Identifying proteins which are affected by US3-deletion also helps to identify roles that BHV-1 US3 plays in the viral lifecycle.

Our fourth objective was to characterize the composition of the mutant virions. This assay was used to identify putative roles that BHV-1 US3 may play in tegument acquisition and maturation of the BHV-1 virion in general.

The fifth objective of this project was to identify viral process(es) impaired by US3-deletion and other proteins which may be involved. This was a broad objective, which allowed us to explore potential roles that BHV-1 US3 may play in the viral lifecycle. The effect that BHV-1 US3 has on cellular morphology during infection was explored along with the role that the protein plays in cell to cell spread of BHV-1. Lastly, the role that US3 plays in the cellular

localization of α-tubulin, gB, and substrates VP22 and VP8, during BHV-1 infection was determined.

3.0 MATERIALS AND METHODS

3.1 Cloning

3.1.1 Construction of ΔUS3 pBHV-1 BAC

To generate a ΔUS3 BHV-1, a 2-step PCR strategy was used to generate the knockout fragment, along with a homologous recombination system in DH10b cells which harbored the Colorado-1 strain (Cooper) bacterial artificial chromosome (BAC) (76) (Figure 3.1). The first step of the strategy was to PCR-amplify the 1246 bp kanamycin resistance cassette from pUC4K, and fragments upstream (325 bp) and downstream (470 bp) of US3 in pCooper BAC. Primers kan-F and kan-R (Table 3.1) were used to amplify the kanamycin cassette, primers US3up-F and US3up-R (Table 3.1) were used to amplify the upstream cassette, and primers US3down-F and US3down-R (Table 3.1) were used to amplify the downstream cassette. The resulting cassettes contained ~50 bp of homology to the kanamycin cassette. All cassettes were amplified using 500 ng of the template plasmid on the PTC-225 Tetrad DNA Thermal Cycler (MJ Research) using the PCR program outlined in Table 3.2. The cassettes were then gel-purified using the QIAquick Gel Extraction Kit (Qiagen) according to the manufacturer's instructions. The full-length linear transgene (2041 bp) was generated by using all three cassettes and two primers which bind to the outside of either the upstream fragment (US3up-F) or the downstream fragment (US3down-R) (Table 3.1). The resulting 2041 bp fragment was gel purified as described above and used for homologous recombination.

The homologous recombination system used in this study included *E. coli* DH10B cells containing the pCooper BAC which harbors the green fluorescent protein (GFP) and chloramphenicol resistance cassettes. The pML300 plasmid, which contains the proteins necessary for homologous recombination, was used to transform DH10B cells by electroporation

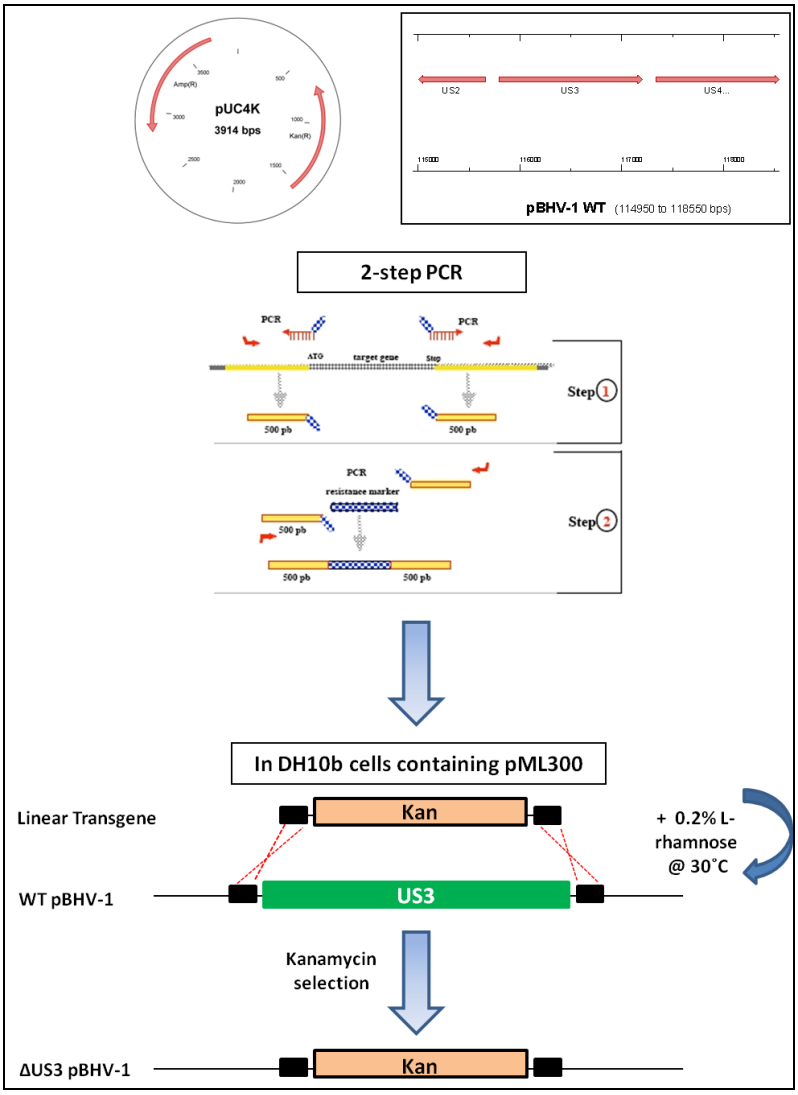

Figure 3.1: Generation of a ΔUS3 pBHV-1 mutant.

The kanamycin-containing linear transgene was initially generated through a 2-step PCR strategy. The linear transgene was then used to transform electrocompetent DH10b cells containing the lambda-red-expressing pML300 maintained at 30˚C. Homologous recombination was induced between the linear transgene and the WT US3 gene in WT pBHV-1 BAC through the addition of 0.2% L-rhamnose. The resulting ΔUS3 pBHV-1 clones were selected on 50 μg/ml kanamycin.

in a 1 mm cuvette (Sigma) using the Gene Pulser XCell (BioRad) at the following settings: 2.5 kV, 25 μF, and 200 Ω. pML300 harbors the recombinase driven, temperature sensitive, rhamnose inducible PrHaB-gbexo promoter. The PrHaB-gbexo promoter controls the lambda-red genes and is inhibited by glucose. pML300 is permissible at 30˚C and is spectinomycin selectable.

To isolate a ΔUS3 pBHV-1 BAC clone, electrocompetent DH10b cells harboring both the pCooper BAC and pML300 were transformed with the 2041 bp linear transgene, and recombination was induced through the addition of 0.1% rhamnose to activate the lambda-red genes on pML300. Throughout the course of these studies, all DH10b cells harboring pML300 were grown at 30˚C to ensure that pML300 was maintained.

To select for the ΔUS3 pBHV-1 BAC clones, cells that were transformed with the linear transgene were plated on 25 μg/ml chloramphenicol to select for the BAC, 50 μg/ml spectinomycin to maintain pML300, and either 50 μg/ml or 15 μg/ml of kanamycin to select for ΔUS3 clones and determine which concentration was more suitable for selection. 50 μg/ml of kanamycin was able to inhibit bacteria not possessing the kanamycin-resistance cassette. Four ΔUS3 clones were isolated and used for Western Blot analysis, PCR amplification of the mutated region, and sequencing to determine the integrity.

3.1.2 Construction of US3R pBHV-1 BAC

To generate a US3R BHV-1 using the ΔUS3 BHV-1 mutant, the *en passant* mutagenesis strategy (134) was performed. This strategy has been used extensively in the field to generate point mutations, substitutions, deletions, and insertions in BAC DNA. The approach uses the inducible homing endonuclease, I-SceI, to induce site-specific cleavage of sequences containing

the 18 bp I-SceI recognition site (154). The strategy involves first generating a PCR product containing a positive selectable marker adjacent to an I-SceI recognition site and by regions of ≥50 bp homology. The PCR product can then be inserted into the BAC through lambda-red recombination. After insertion, the positive selection marker can be excised by inducing the I-SceI enzyme which will cleave the SceI site present in the insert. After cleavage, homologous recombination between the two flanking regions of the insert can be induced by induction of the lambda-red system (134). The GS1783 cell line used in this system was kindly given to our lab by Dr. Benedikt Kaufer in Berlin, Germany. This cell line has been used successfully in Dr. Kaufer's lab to generate insertions and deletions in BACs containing MDV clones.

The *en passant* mutagenesis strategy was used to rescue the original US3-deleted clone using the newly-obtained GS1783 cell line (Figure 3.2). The GS1783 cell line harbours the inducible (at 42˚C) lambda-red system and the inducible (via 0.1% L-arabinose) I-SceI enzyme. It is a derivative of the DY380 strain, which was used previously. To generate the US3R pBHV-1 BAC clone, a 2.9 kB linear transgene was first generated from pRescue-zeo (see Figure 3.2) which was kindly provided by Dr. Robert Brownlie. The insert was isolated through PCR amplification using primers pRescue-F and pRescue-R (Table 3.1), Dpn-1 (New England Biolabs)-treated, and gel purified (QIAquick Gel Extraction Kit) to ensure that that the template (pRescue-zeo) was removed to prevent contamination. The linear transgene contains the zeocin cassette adjacent to the I-SceI recognition site and is flanked by the US3 region which was removed in the ΔUS3 pBHV-1 BAC. The flanking regions, containing 300 bp of identical sequences, were used to facilitate homologous recombination and subsequent resolution of the inserted region to generate a US3R pBHV-1 BAC clone.

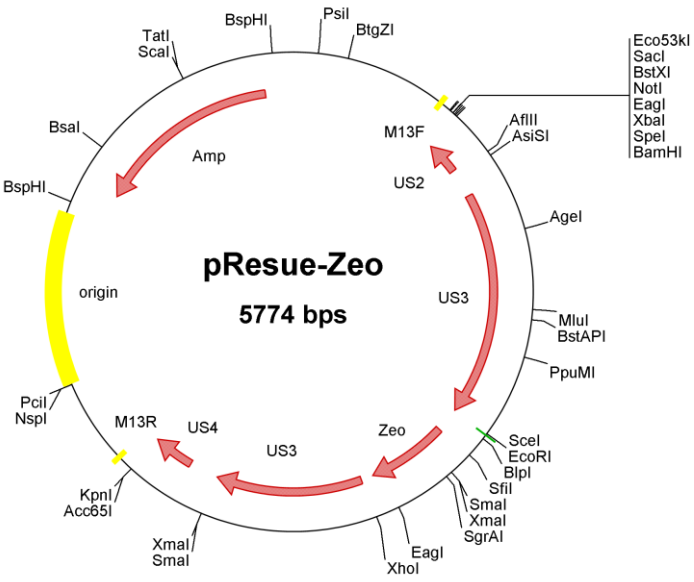
pResue-Zeo
5774 bps
Amp
origin
M13F
US2
US3
Zeo
US3
US4
M13R
Eco53kI
SacI
BstXI
NotI
EagI
XbaI
SpeI
BamHI
AflII
AsiSI
AgeI
MluI
BstAPI
PpuMI
SceI
EcoRI
BlpI
SfiI
SmaI
XmaI
SgrAI
EagI
XhoI
XmaI
SmaI
KpnI
Acc65I
PciI
NspI
BspHI
BsaI
TatI
ScaI
BspHI
PsiI
BtgZI

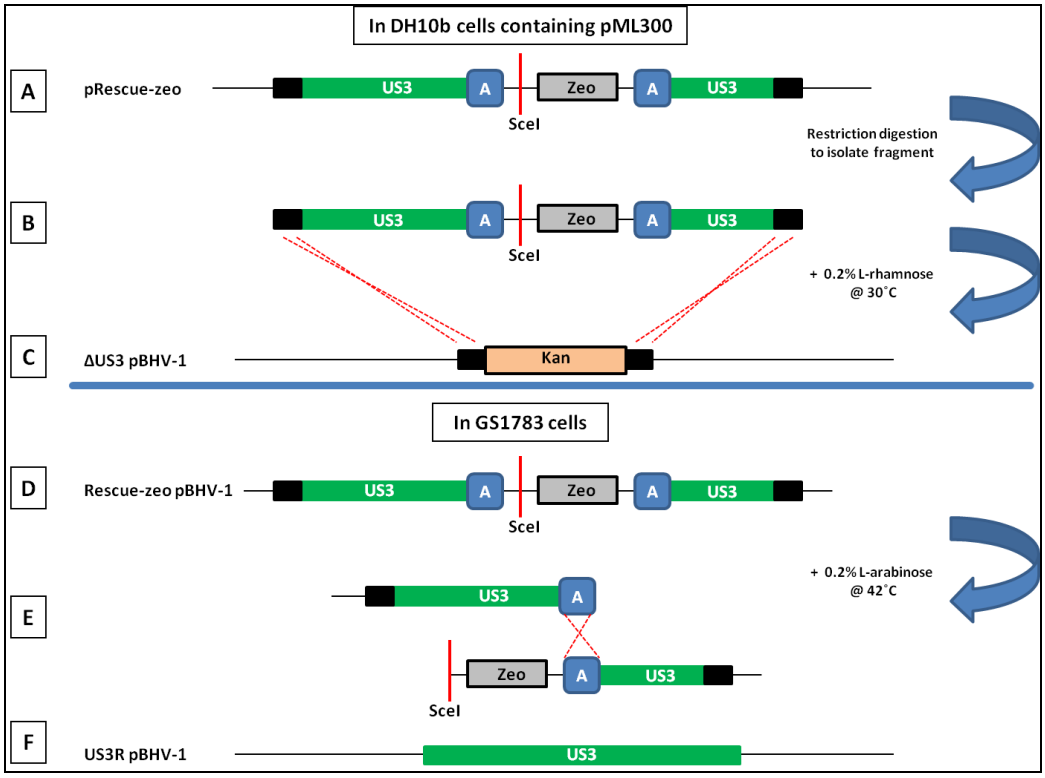

Figure 3.2: ΔUS3 pBHV-1 rescue using the *en passant* mutagenesis strategy (134).

A) The pRescue-zeo plasmid was generated which contains the zeomycin (zeo) cassette adjacent to the unique restriction site, SceI. The zeo cassette is flanked by redundant sequences ("A") and the deleted regions of US3. The distant ends of the fragment correspond to the WT US3 upstream and downstream regions that are present in the ΔUS3 pBHV-1 BAC (black squares). B) The linear rescue fragment was isolated from the vector through restriction digestion and used to transform electrocompetent, recombination-ready DH10b *E. coli* cells containing the ΔUS3 pBHV-1 BAC. C) Homologous recombination between the linear transgene from pRescue-zeo and the ΔUS3 pBHV-1 BAC was induced and recombinants were checked for integrity. D) The isolated Rescue-zeo pBHV-1 BAC clone was used to transform electrocompetent GS1783 *E. coli* cells. E) The WT US3 gene was resolved (F) through induction of the I-SceI enzyme by 0.2% L-arabinose and heat-shock at 42˚C to induce the lambda-red genes.

The overall rescue procedure included first electroporating the original ΔUS3 pBHV-1 BAC clone with the purified linear transgene present in DH10b cells containing the pML300 cassette, used previously. Briefly, rescued clones were selected on 25 μg/ml chloramphenicol to maintain the BAC and 25 μg/ml zeocin (Invitrogen) to select for the insert. Resulting clones were also counter-selected on 50 μg/ml of kanamycin to ensure that the kanamycin resistance cassette had been replaced and 100 μg/ml ampicillin to ensure that there was no pRescue-zeo carry-over in the new clones. Four clones were isolated using the Qiagen Large Construct Kit (Qiagen) according to the manufacturer's instructions and verified through PCR amplification of the 2.9 kB linear transgene. The altered BACs were then used to transform electrocompetent GS1783 cells using a 0.1 cm cuvette (settings: 15kV/cm, 25μF and 200Ω) which were maintained at 30˚C. To resolve the WT US3 region, the GS1783 cells were exposed to 1% L-arabinose to induce the I-SceI enzyme, followed by heat shock at 42˚C to induce the lambda-red genes and facilitate homologous recombination between the flanking regions.

Primer	5' to 3' Sequence
kan-F	ctg cag ggg ggg ggg ggc gct gag gtc tgc ctc g
kan-R	ctg cag ggg ggg ggg gga aag cca cgt tgt gtc
US3up-F	tac tag ggc gtg atc gaa gac aac
US3up-R	acg agg cag acc tca gcg ccc ccc ccc ccc tgc agg ggt gcc caa gaa cgt cgg gtc gt
US3down-F	aca caa cgt ggc ttt ccc ccc ccc ccc tgc agc ccc ggg ggt ttc ccg caa aac tga g
US3down-R	ata tgc cag agg cac cat gca gtc
pRescue-F	gaa gga tcc agg gcg tga tcg aag aca ac
pRescue-R	gga agg tac cga aac ccg cga ggt caa atc

Table 3.1: Primers used for PCR

Steps	Temperature (˚C)	Time (min)	Cycles
1	95	5	1
2	94	0.5	10
	62 (decreases by 0.5˚C/cycle)	1	10
	72	0.5-3	10
3	94	0.5	25
	57	0.5	25
	72	0.5-3	25
4	72	5	1
5	4	15	1

Table 3.2: PCR program used for amplification of oligonucleotides

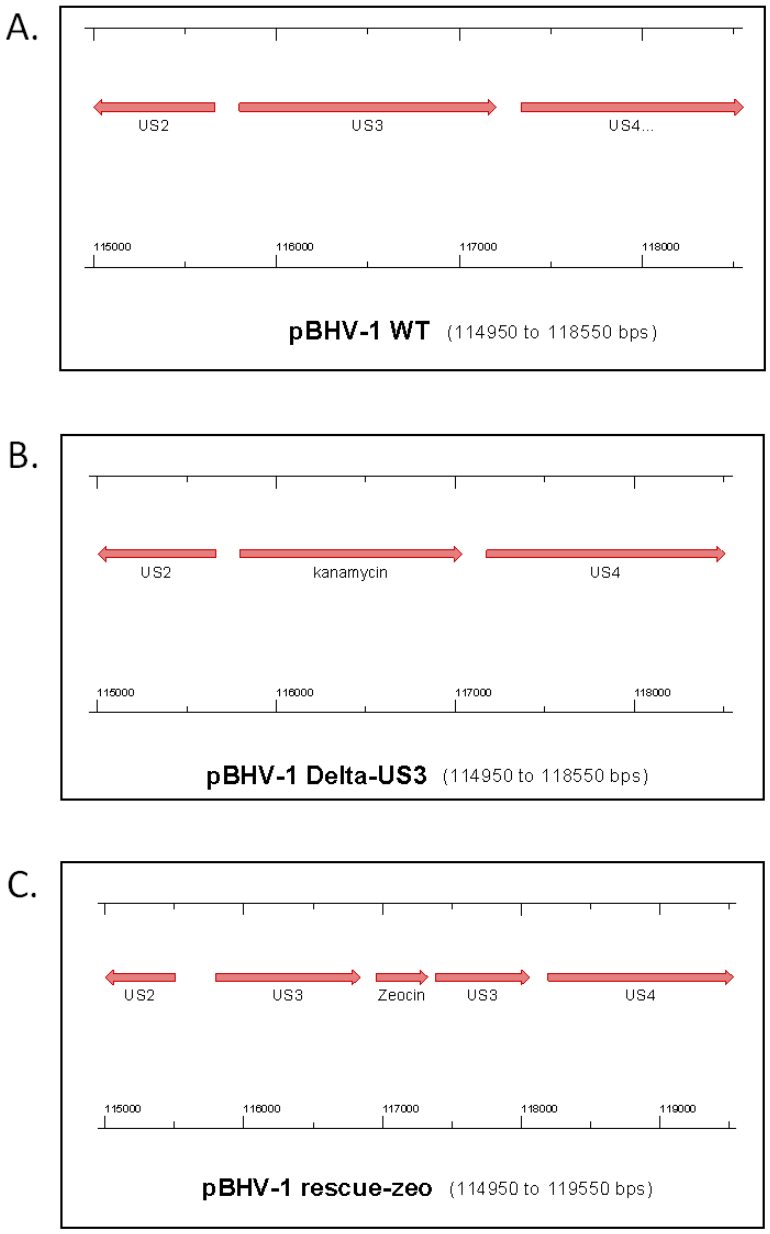

Figure 3.3: Maps of the altered US3 region in WT, ΔUS3, and Rescue-zeo pBHV-1.

A) WT pBHV-1 US3 gene is flanked by the US2 and US4 genes in the unique short region of pBHV-1. B) ΔUS3 pBHV-1 has the US3 gene replaced with a kanamycin resistance cassette C) Rescue-zeo pBHV-1 has the kanamycin cassette from ΔUS3 pBHV-1 replaced with a zeocin cassette that is flanked by the WT pBHV-1 US3 gene.

3.1.3 Verifying mutant virus integrity

After the resolution step, the resulting clones were selected for on 25 μg/ml chloramphenicol, and 25 μg/ml zeocin. >90% of the resulting clones were zeocin sensitive, indicating that the WT US3 fragments had resolved. To verify that the WT fragments were intact, PCR-amplification of the 4kB US2-US3-US4 region was carried out and the clones were sent for sequencing of the region in the WT, ΔUS3 and US3R pBHV-1 BAC clones. Sequencing confirmed that the US2-US3-US4 region was intact in the rescued clone and did not have any point mutations compared to WT. Interestingly, sequencing of the full US2 region confirmed a guanine insertion which renders the open reading frame non-functional. This insertion was present in all 3 clones (WT, ΔUS3, and US3R), and is likely the result of cell-culture adaptation of the virus (78).

To ensure that no spontaneous recombination events occurred in the viral genome, restriction fragment length polymorphisms were detected through digestion with HindIII. Briefly, two T-150 flasks containing confluent Madin-Darby Bovine Kidney (MDBK) cells that were infected with BHV-1 viruses at a multiplicity of infection (MOI) of 1 were harvested after 48 hours, or until cells showed significant cytopathic effects. Infected cells were scraped from the flasks and pelleted via low speed centrifugation, and the supernatants were collected. To concentrate the virus, supernatants were pelleted through a 30% (w/v) sucrose cushion in TNE buffer (10 mM Tris-HCl, pH 7.5, 150 mM NaCl, 1 mM EDTA) by ultracentrifugation using a Beckman S232Ti rotor at 24,000 rpm for 2 hours at 4˚C. After centrifugation, pellets were resuspended in 50 μl TNE buffer overnight at 4˚C. To isolate the viral genome from each preparation, the Gentra PureGene Cell Kit (Qiagen) was used according to the manufacturer's directions. After isolation of the genome, 1.5 μg of DNA from each suspension was digested

with HindIII (NEB) for 6 hours according to the manufacturer's directions. Following digestion, 50 μl of each sample was loaded on a 0.7% agarose gel containing 0.01% GelRed Nucleic Acid Gel Stain (Biotium) and fragments were electrophoretically separated at 35 volts (20 mAmps) for 18 hours. Fluorescent bands were detected using the Gel Doc XR+ System (BioRad) after post-staining with GelRed (Biotium).

3.2 Propagation and titration of viruses in cell culture

WT, ΔUS3 and US3R pBHV-1 BACs were isolated using the QIAGEN Large-Construct Kit (Qiagen), according to the manufacturer's instructions. All isolated pBHV-1 BACs were then used to transfect Fetal Bovine Testicular (FBT) cells. Briefly, varying concentrations of pBHV-1 BAC DNA and Lipofectamine 2000 (Invitrogen) were mixed according to the manufacturer's instructions, and allowed to interact at room temperature for 45 minutes. After incubation, the mixture was diluted in 50% reduced serum Minimal Essential Medium (MEM) (Invitrogen) and added to 80% confluent FBT cells in 6-well nunc assay plates (BD Falcon). The cells were incubated at 37˚C/5% CO_2 overnight to allow the DNA to enter the cells. The next morning, the DNA-containing medium was replaced with MEM with 10% fetal bovine serum (FBS). Transfection efficiency was determined at 48 hours post-transfection under the fluorescence microscope which detected the GFP in the virus.

At 72 hours post-transfection, or when the cell monolayers showed significant signs of BHV-1 infection, the monolayers were collected and frozen at -80˚C. After two freeze-thaw cycles and low-speed centrifugation, the virus-containing supernatants were collected and used to propagate the virus in MDBK cells. After viral propagation, stocks were either frozen at -80˚C or titred under overlay medium in 24-well Nunc assay plates (BD Falcon) containing 2x MEM (Gibco) with 2% FBS and 0.8% agarose type VII (Sigma-Aldrich).

3.3 Single-step growth curves

To investigate the growth kinetics of the viruses, MDBK cells were infected at a MOI of 5 in 35-mm cell culture dishes. Extracellular and intracellular fractions were isolated from each infection from 5-25 hours at 5 hour intervals. After the intracellular fractions were put through two freeze-thaw cycles, all samples were clarified via low-speed centrifugation. The resulting supernatants were frozen at -80˚C before being titred in MDBK cells under overlay medium as described previously (77).

3.4 Expression kinetics assay

3.4.1 Preparation of BHV-1 infected cell lysates

MDBK cells were either mock-infected or infected at MOI of 2 in T-25 flasks. Cells were harvested at 5-25 hours post-infection at 5-hour intervals by scraping the cells from the flasks with a rubber scraper. Cells were washed two times in ice-cold phosphate buffered saline (PBS) (3 mM KCl, 1.5 mM KH_2PO_4, 137 mM NaCl, 8 mM Na_2HPO_4, pH 7.3), and the pellets were resuspended in Triton-X phenylmethylsulfonyl fluoride (TX-PMSF) buffer (150 mM NaCl, 1 mM EDTA, 1% Triton X-100, 50 mM Tris/HCL, pH 7.4) supplemented with 1mM PMSF, 1 μg/ml aprotinin, 1 μg/ml leupeptin, and 1 mM dithiothreitol (DTT). Resuspended cells were incubated on ice for 30 minutes before centrifugation at 1600 RCF for 10 minutes at 4˚C to isolate the solubilised protein fraction.

3.4.2 SDS-PAGE

After determining the amount of protein in each sample using the Bio-Rad Protein Assay Kit (Bio-Rad) according to the manufacturer's directions, equal amounts of each sample were denatured and resolved through a 10% sodium dodecyl sulphate polyacrylamide gel electrophoresis

(SDS-PAGE) gel (10% bisacrylamide, 25% 1.5M Tris pH 8.8 (v/v), 0.1% SDS, 64.84% (v/v) ddH20, 0.05% APS, 0.01% TEMED) using 1.5 mm spacers with a 4% stacking gel (4% bisacrylamide, 25% (v/v) 0.5M Tris-HCL, pH 6.8, 0.1% SDS, 70.84% (v/v) ddH20, 0.05% APS, 0.01% TEMED) in 1x SDS running buffer (0.3% (w/v) Tris, 1.44% (w/v) glycine, 0.1% (w/v) SDS). Samples were run at 110 volts for 2 hours to separate all proteins of interest.

3.4.3 Western Blot

Proteins were electrophoretically transferred to a nitrocellulose membrane at 100 volts for 1 hour 10 minutes at 4˚C. Membranes were blocked in Odyssey Blocking Buffer (Li-Cor) diluted 1:1 in PBS for 2 hours at 4˚C with rocking. After blocking, membranes were incubated with primary antibodies overnight at 4˚C with rocking. Monoclonal antibodies (MAb) that were used included those against α-tubulin (Sigma-Aldrich), β-actin (Sigma-Aldrich), BHV-1 VP8, gC, gB, and gD. Polyclonal antibodies (PAb) that were used included those against BHV-1 US3, VP5, VP16, bICP4, and VP22. After thoroughly washing with PBS containing 0.1% Triton X-100, membranes were incubated with IRDye 680-conjugated goat anti-mouse IgG or IRDye 800CW-conjugated goat anti-rabbit IgG (Li-Cor). After thoroughly washing the membranes with PBS containing 0.1% Triton X-100, fluorescent bands were visualized using the Odyssey Imaging System and analyzed with the Odyssey 3.0.16 application software (Li-Cor).

Blots were re-probed up to two times by removing membrane-bound antibody complexes using the Newblot Nitro Stripping Buffer (Li-Cor) according to the manufacturer's instructions. Membranes were blocked in Odyssey Blocking Buffer (Li-Cor) for 2 hours before re-probing with new antibodies.

3.5 Purification of BHV-1 viruses

Nine to twelve T-150 flasks containing confluent MDBK cells were infected with WT, ΔUS3, or US3R viruses at $1x10^6$ pfu/flask. After cells displayed complete cytopathic effect (~ 48 hours post-infection), flasks were freeze-thawed twice to release intracellular virus. Cell debris were removed via low-speed centrifugation and supernatants were pelleted through a 30% (w/v) sucrose cushion in TNE buffer by ultracentrifugation using a Beckman S232Ti rotor at 24,000 rpm for 2 hours at 4˚C. To further purify the viruses, the pellets were resuspended in TNE buffer overnight at 4˚C before being sonicated and gently layered onto a 10-60% (w/v) potassium sodium tartrate gradient in TNE buffer present in 36 ml tubes. The gradient was generated using a Hoefer SG50 Gradient Maker (Amersham). The tubes containing the gradients and virus suspensions were centrifuged for 2 hours at 25,000 rpm in the SW32Ti rotor. To remove the purified viral suspension from the gradient, the tubes were punctured in the side using a 21-gauge needle and the thin virus-containing band was removed. Care was taken to avoid isolating any cell debris which trailed above the band containing the viral suspension. Purified virus was concentrated by resuspending in TNE followed by ultra-centrifugation at 25,000 rpm for 2 hours at 4˚ C in the SW32Ti rotor. After resuspending the concentrated, purified virus in TNE, samples were frozen at -80˚C.

3.5.1 Normalization of the purified virus

To normalize the amount of the three purified virus samples (i.e. WT, ΔUS3, and US3R) used in subsequent Western Blot analyses, varying amounts of purified virus samples were loaded onto a 10% SDS-PAGE gel and transferred to a nitrocellulose membrane. Rabbit VP5-specific serum (77) was used as the primary antibody and IRDYe 800CW-conjugated goat anti-rabbit IgG was used as the secondary antibody for detection of VP5. Bands were visualized using the Odyssey Imaging System and analyzed using the corresponding 3.0.16 application software.

In addition to Western Blot analysis, a BCA Protein Assay (Thermo Scientific) was used to determine the protein concentration in each purified virus sample.

3.6 Plaque-size quantification

To determine whether the ΔUS3 BHV-1 virus was impaired in cell to cell spread, a plaque-size analysis was performed for all viruses. Briefly, MDBK cells were cultured in six-well plates and infected with 50-100 PFU/well of WT, ΔUS3, or US3R BHV-1 viruses. After 48 hours, or until distinct plaques had formed, cells were fixed with a solution containing 75% ethanol and 25% glacial acetic acid. Following fixation, infected cells were stained using a cocktail of gB-specific MAbs, followed by incubation with alkaline phosphatase-conjugated goat anti-mouse IgG (Kirkegaard and Perry Laboratories). After washing, plaques were visualized by incubating cells with 5-bromo-4-chloro-3-indolylphosphate and nitroblue tetrazolium (BCIP/NBT) (Sigma).

To quantify plaque sizes, 50 discrete images of plaques were acquired using the Zeiss Axiovert 200M microscope. The average plaque diameters were calculated using the AxioVision AC 4.5 Software to make two perpendicular diameter measurements of each plaque. The plaque sizes were then ranked between all viruses and statistical analysis was performed using GraphPad Prism 5 software (GraphPad).

3.7 Light microscopy of BHV-1 infected MDBK cells

The morphologies of virus-infected cells were examined by light microscopy. MDBK cells were infected with each virus at MOIs from 2-5 and images were acquired from 5-35 hours post-infection with the Zeiss Axiovert 200M microscope.

3.8 Confocal microscopy of BHV-1 infected MDBK cells

MDBK cells grown on two-chamber Permanox slides (Lab-Tek) were infected with either WT or ΔUS3 BHV-1 at MOI of 3. At various times post infection, cells were fixed with 4% paraformaldehyde for 15 minutes at room temperature followed by blocking with 5% heat-inactivated goat serum in PBS with or without 0.1% Triton X-100 to permeabilize the cells. Cells were incubated with primary antibody and after washing, incubated with either Alexa Fluor 633 goat-anti rabbit IgG or Alexa Fluor 488 goat anti-mouse IgG (Invitrogen). 0.1% Triton X-100 was added to the staining solutions to permeabilized cells when necessary. Cells were air-dried overnight at room temperature in the dark and mounted the next day using Prolong Gold Antifade Reagent with Dapi (Invitrogen). Images were acquired using normalized settings on either the Zeiss LSM410 or the Leica DMI6000 confocal microscopes and enhanced under identical parameters using the ImageJ software system.

3.9 Fluorescence-Activated Cell Sorting (FACS)

The effect that US3 has on the total and cell surface expression of BHV-1 gB was analyzed by FACS. Briefly, MDBK cells were infected at an MOI of 3 and harvested at 4 hours post-infection by trypsinization and washed three times in ice-cold PBS. A cell suspension of $1x10^7$ cells/ml was generated, and 50 µl of cells were aliquoted into a 96-well round-bottom plate (Corning). To investigate the cell surface expression of gB, cells were blocked in 5% goat serum in PBS for 20 minutes at 4˚C. Cells were then incubated with gB-specific mouse IgG2a MAb (1:2000 dilution) for 20 minutes at 4˚C, followed by incubation with Alexa Fluor 633 goat anti-mouse IgG (Invitrogen) (1:2000 dilution) for 20 minutes at 4˚C. Each step was followed by thorough washing in PBS. Finally, cells were fixed with 2% formaldehyde.

To detect total gB expression in infected cells, cells were initially fixed and permeabilized using the BD Cytofix/Cytoperm Plus kit (BD Bioscience) according to the

manufacturer's protocol. Following fixation, cells were blocked in 5% goat serum in PBS for 20 minutes at 4˚C. After blocking, cells were incubated with gB-specific mouse IgG2a MAb (1:2000 dilution) for 20 minutes at 4˚C, followed by incubation with Alexa Fluor 633 goat anti-mouse IgG (Invitrogen) (1:2000 dilution) for 20 minutes at 4˚C. Since cell permeabilization is not stable, all washes and incubations were performed in the presence of a saponin-containing buffer included in the BD Cytofix/Cytoperm kit. After the final wash, cells were resuspended in PBS.

To ensure non-specific binding of the primary antibody did not result in false readings, purified mouse myeloma IgG2a (Invitrogen) was used as an isotype control. All samples were read on a FACSCalibur flow cytometer (BD Bioscience) and analyzed using Cell Quest software (BD Bioscience).

4.0 RESULTS

4.1 Construction and verification of ΔUS3 and US3R pBHV-1

To construct a ΔUS3 BHV-1 virus (Cooper-1 strain), a bacterial homologous recombination strategy was used. Briefly, DH10B cells containing pCooper in BAC (76) and the pML300 plasmid harboring the inducible lamda-red recombination cassette were electroporated with a 2.0 kB fragment that contained the full-length BHV-1 US3 cassette with sequences upstream and downstream to facilitate homologous recombination. The fragment was generated through a 2-step PCR strategy. After homologous recombination and recovery, DH10b cells were plated on chloramphenicol to select for the BAC, spectinomycin to maintain pML300, and kanamycin to select for the ΔUS3 recombinant BACs (Figure 3.1). Over 100 kanamycin-resistant colonies resulted from the recombination event, showing that homologous recombination using this system was highly effective.

To ensure that the phenotype of the ΔUS3 clones was due to US3 deletion alone, a US3R virus was generated. Briefly, a two-step *en passant* mutagenesis procedure was undertaken, which first replaced the kanamycin-resistance cassette in the ΔUS3 clone with a linear transgene containing the full-length US3 gene and a zeocin cassette, and second, resolved the WT US3 gene (134) (Figure 3.2). To ensure that a scar-less rescue would occur, an inducible SceI site (154) was incorporated upstream of the zeocin cassette in the linear transgene which, when cut, would result in homologous recombination between ~300 bp identical US3 sequences immediately upstream and downstream of the zeocin cassette. To replace the kanamycin-resistance cassette in the ΔUS3 clone, the zeocin-resistant linear transgene was amplified from pRescue-zeo (see Figure 3.2) and used to transform electrocompetent and recombination-ready DH10b cells containing pML300 and the ΔUS3 pBHV-1 BAC.

After selection on zeocin, the resulting pBHV-1 BAC was used to transform GS1783 cells. GS1783 cells contain the inducible lambda-red genes and the SceI enzyme, and were used to resolve the WT US3 gene in the pBHV-1 BAC through restriction digestion of the linear transgene with I-SceI, followed by lambda-red induction and homologous recombination between identical sequences within the transgene. The resulting US3R pBHV-1 BACs were selected based on chloramphenicol resistance and zeocin sensitivity.

To verify the integrity of ΔUS3 and US3R BHV-1, PCR analysis, sequencing, restriction digestion, and Western blotting using anti-US3 antibodies were carried out. Sequencing of the 4kB US2/US3/US4 region in the WT, ΔUS3, and US3R pBHV-1 showed that ΔUS3 pBHV-1 had no unexpected mutations and US3R pBHV-1 had reverted to an identical genotype compared to WT pBHV-1. Furthermore, sequencing elucidated that an insertional mutation was present in the US2 region in all clones, including WT pBHV-1. This may be due to the Cooper

strain's adaptation to cell culture, as US2 has been previously shown to be non-essential for HSV-1 growth under these conditions (78).

To verify that the ΔUS3 BHV-1 was only manipulated in the US3 region of the genome, restriction profiling was done using HindIII digestion on purified viral DNA. As demonstrated in Figure 4.1, the WT and US3R clones had restriction profiles which were identical to each other and representative of the expected WT profile as determined by Clone Manager 9 Professional Edition software program (Sci-Ed). The ΔUS3 BHV-1, on the other hand, had the expected restriction profile that corresponded to two different bands at 8231 bp and 6307 bp compared to WT or US3R BHV-1.

To verify that the ΔUS3 BHV-1 does not express US3 and that the US3R does, Western blot analysis was conducted by generating whole-cell extracts from infected MDBK cells and probing with a US3-specific rabbit PAb. As expected, the WT and US3R BHV-1 both expressed US3 during viral infection, whereas the ΔUS3 BHV-1 does not produce the 58 kD protein during infection (Figure 4.2). These results confirmed the integrity of the ΔUS3 and US3R BHV-1 clones.

4.2 Single-step growth curves of WT, ΔUS3 and US3R BHV-1

To investigate the growth kinetics of the WT, ΔUS3 and US3R BHV-1, a single-step growth assay was carried out. MDBK cells were infected at an MOI of 5 and harvested from 5-25 hours post-infection. Intracellular and extracellular viral titres were determined by quantifying plaque formation under BHV-1 neutralizing serum. Figure 4.3 a,b is a compiled figure containing the single-step growth curves from the three viruses titred in quadruplicate and is

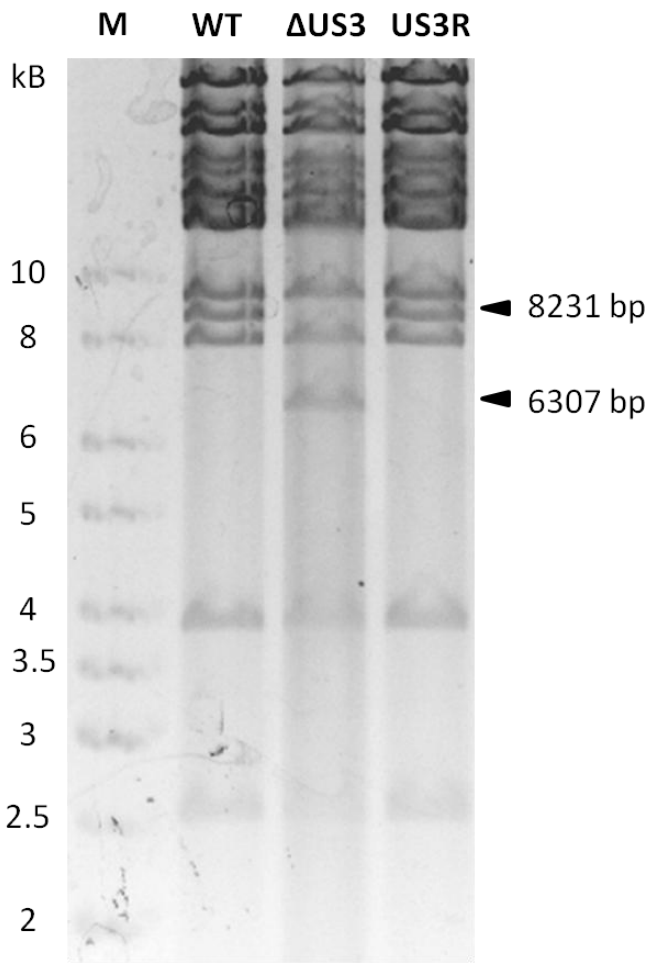

Figure 4.1: HindIII-digestion of ΔUS3, WT and US3R BHV-1.

Viral DNA preparations were digested with HindIII for 6 hours at 37˚C before being run on a 0.7% agarose gel for 18 hours at 35 volts (20 mAmps). The gel was then stained with GelRed Nucleic Acid Gel Stain (Biotium) for 30 minutes. Bands were visualized using the Gel Doc XR+ system (Bio Rad).

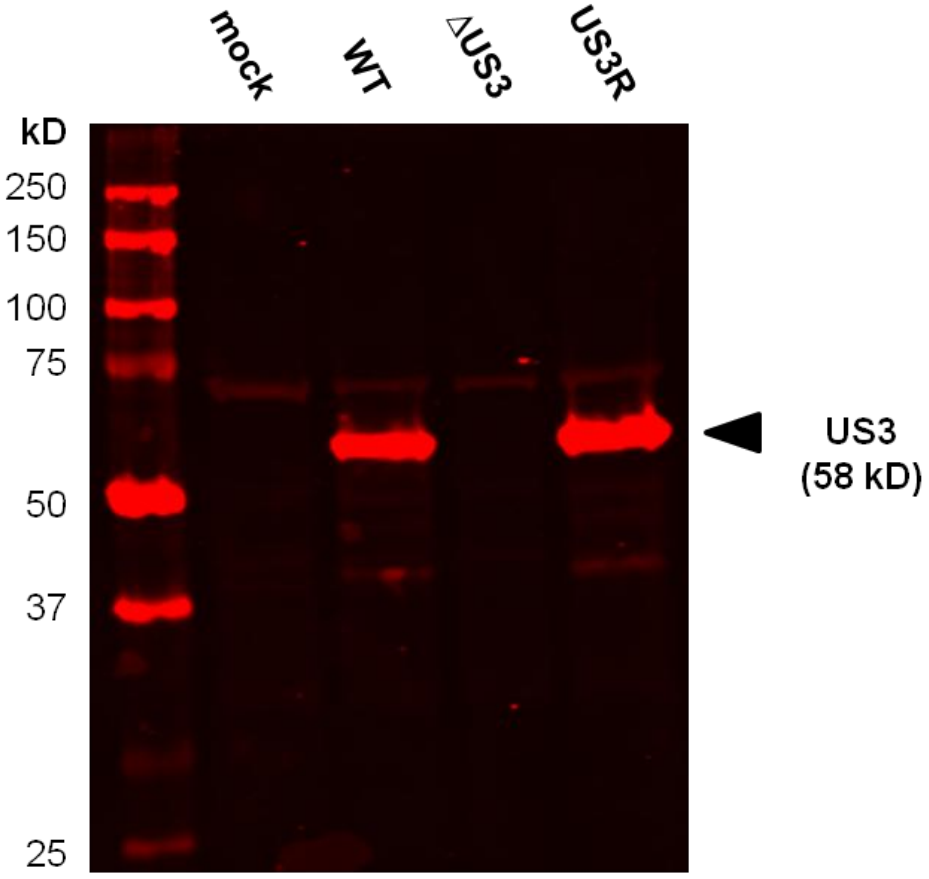

Figure 4.2: US3 expression profiles of WT, ΔUS3 and US3R BHV-1 infected cells.

MDBK cells were infected at an MOI of 2 for approximately 24 hours. Whole-cell extracts were prepared and low-speed centrifugation was used to collect the solubilised proteins. Equal amounts of total cell lysates were analyzed by Western blot using US3-specific PAbs. Proteins were visualized by probing with goat anti-rabbit IgG IRDye 680-conjugated secondary antibody (LI-COR Biosciences) and visualized using LI-COR's ODYSSEY infrared imaging system (LI-COR Biosciences).

a)

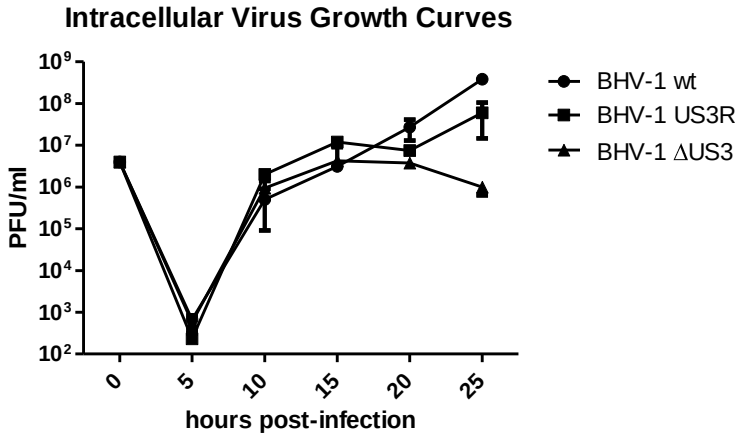

b)

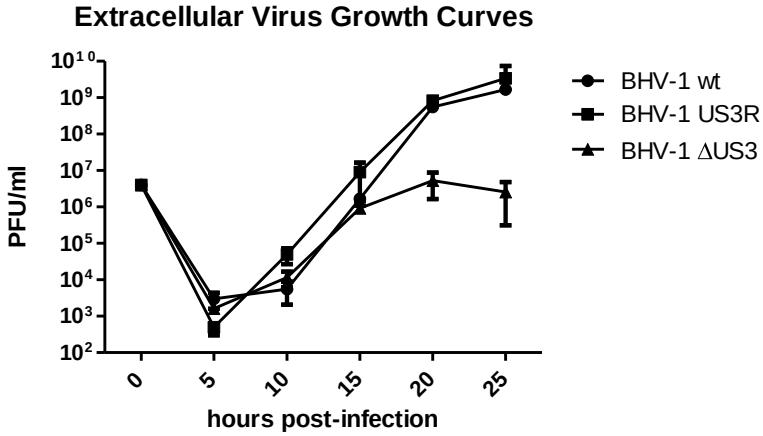

Figure 4.3 a, b: Growth characteristics of WT, ΔUS3 and US3R BHV-1.

Duplicate cultures of MDBK cells were infected with each virus at an MOI of 5. Virus-containing supernatants and infected cells were collected at 5-25 hours post infection at 5 hour intervals. The intracellular (a) and extracellular (b) titres of infectious progeny were determined using a standard plaque assay and BHV-1 neutralizing serum. Titres were determined based on plaque formation. The figures are representative of two independent experiments conducted under identical parameters.

representative of two independent experiments conducted previously.

The curves demonstrate that the growth kinetics of the ΔUS3 BHV-1 is impaired compared to both WT and US3R BHV-1, which are nearly identical. Both the intracellular and extracellular production of ΔUS3 BHV-1 was similar to that of WT until about 15 hours post-infection. After this time point, the titres of the ΔUS3 BHV-1 plateaued during the remainder of the infection, staying close to ~10^6 pfu/ml. This observed defect in growth kinetics of ΔUS3 BHV-1 could be due to a deficiency in cell to cell spread or egress of the virus *in vitro*.

4.3 Effect of US3 deletion on the expression kinetics of major BHV-1 proteins

An expression kinetics assay was carried out to investigate the effect of US3 deletion on major structural and regulatory BHV-1 proteins. Briefly, MDBK cells were infected at a MOI of 2 to investigate the kinetics of the IE, E, and L BHV-1 proteins in infected cells. Infected cells were harvested from 5-25 hours post-infection at five hour intervals. Whole-cell lysates were generated and frozen at -80˚C. Protein samples were prepared and analyzed by Western blotting with antibodies against each of the BHV-1 proteins of interest. Bands were visualized using the Odyssey system (LiCor) and densitometry was carried out using the LiCor Odyssey software to quantify the amount of normalized proteins over time.

The Western Blots shown in Figure 4.4 demonstrate a number of differences in protein expression between WT and the ΔUS3 BHV-1 infected cells. Any differences in protein expression between samples which were less than 1.5x were deemed not biologically significant. It was demonstrated in two independent experiments that compared to WT BHV-1 infected cells, VP5 was expressed in ΔUS3 BHV-1 infected cells at amounts that were approximately 5x higher early in infection and 1.5x higher at late points of infection; VP16 and VP8 were expressed at

amounts that were approximately 1.5x higher during late stages of infection; gC was expressed at approximately 2x lower amounts beginning at 15 hours post-infection, and although there was a reduction in protein expression at 15 hours post-infection, this was deemed to be an artifact of the gel; bICP4 expression was expressed at 2 hours compared to 3 hours post infection in WT BHV-1 infected cells, and was expressed at approximately 2x higher amounts from 1-10 hours post-infection; Total gB expression was almost 2x that of WT BHV-1 at 10 hours post infection, but was approximately 1.5x lower during late stages of infection (15-25 hours post-infection), with levels decreasing over the course of infection; gD expression was detected earlier at 4 hours post-infection, and; VP22 expression was fairly consistent between both viruses. These data support a role for US3 in efficient protein expression and regulation during the course of infection.

4.4 Effect of US3 on the protein composition of the mature virion

To investigate the role US3 plays in the incorporation of BHV-1 proteins into mature virions, viruses were purified and analyzed by Western blotting for the presence of major BHV-1 structural and regulatory proteins. Initially, WT, ΔUS3 and US3R BHV-1 were propagated in MDBK cells and purified using a 10-60% potassium sodium tartrate gradient. To determine the relative amounts of protein present in each purified virus sample, a BCA assay and Western Blot using a PAb against the capsid protein, VP5 were carried out. After the relative protein concentrations between the viruses were normalized, Western blots were run using antibodies against VP5, gB, gC, gD, VP16, VP8, VP22, and US3.

Figure 4.5a is a composite from one independent experiment that includes all the bands of interest from each Western Blot, including densitometry results. Figure 4.5b is a graphical representation of the averaged relative protein differences between the WT and ΔUS3 BHV-1

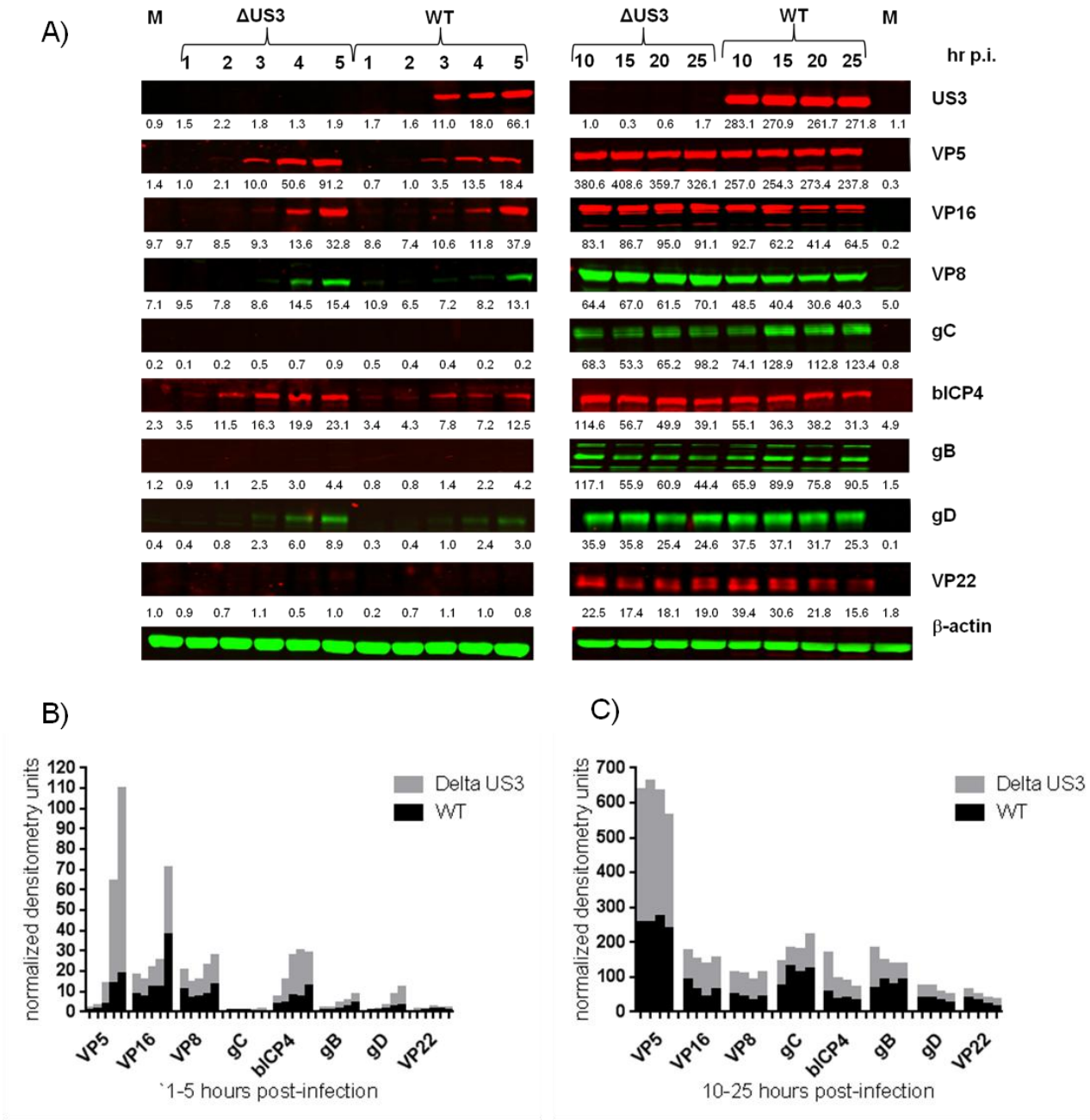

Figure 4.4 a, b, c: Effect of BHV-1 US3 on viral protein expression during infection.

A) MDBK cells were infected at a MOI of 2 and harvested at 5-25 hours post infection at 5 hour intervals. Equal amounts of total cell lysates were analyzed by Western blotting using PAbs specific for VP5, VP22, VP16, US3, or bICP4, and MAbs specific for gC, gB, gD, VP8, or β-actin. Proteins were visualized by probing with goat anti-rabbit IgG IRDye 680-conjugated

secondary antibody (LI-COR Biosciences) or with goat anti-mouse IgG IRDye 800CW-conjugated secondary antibody and visualized using LI-COR's ODYSSEY infrared imaging system (LI-COR Biosciences). The numbers shown below each well represent the normalized fluorescence intensity of each sample relative to β-actin as determined by densitometry using the ODYSSEY system software. All densitometry values were multiplied by 100. This figure is representative of two independent experiments conducted under identical parameters. **B)** Graphical representation of the normalized densitometry values of BHV-1 proteins early during infection (1-5 hours post-infection), and at late times post infection (10-25 hours post-infection), **C)**.

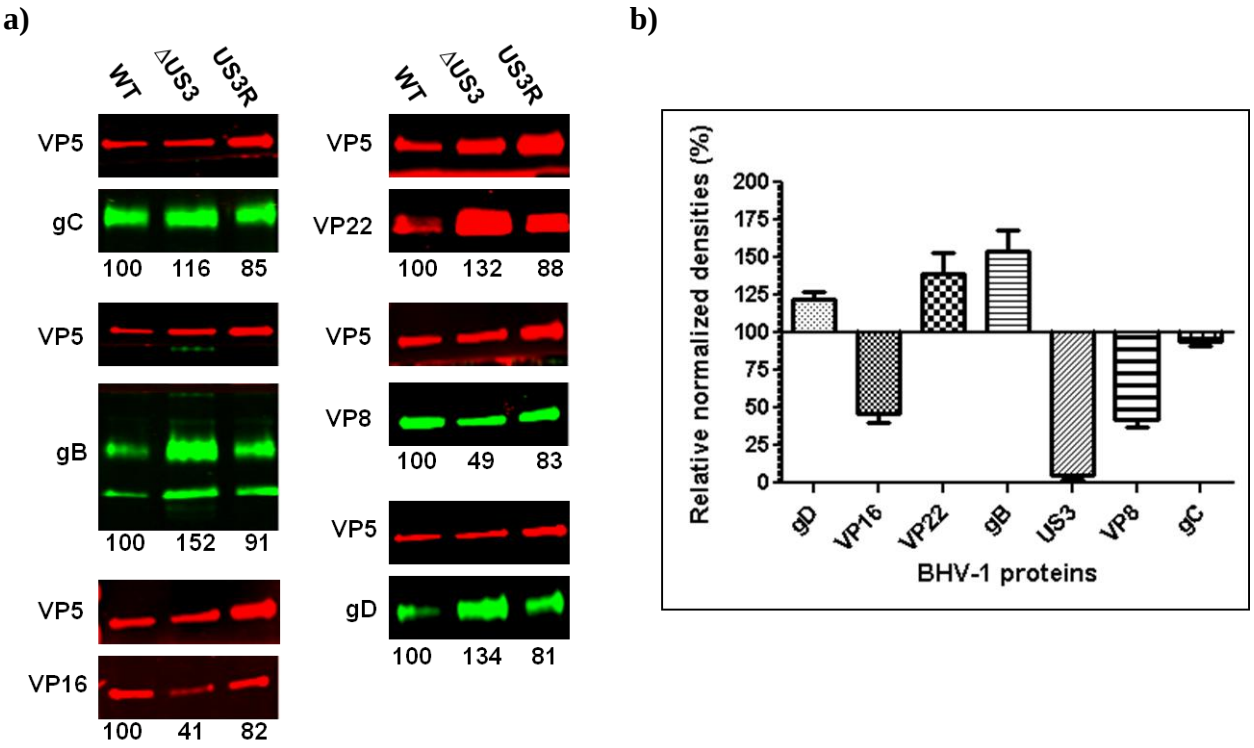

Figure 4.5 a,b: Effect of US3 on the mature virion composition of BHV-1.

Viruses were purified and normalized based on the density of the major capsid protein, VP5. Volumes of solubilised proteins were loaded on a 10% SDS-PAGE gel and used for Western blot. A) Equal amounts of total cell lysates were analyzed by Western blotting using PAbs specific for VP5, VP22, or VP16 or MAbs specific for gC, gB, gD, or VP8. Proteins were visualized by blotting with goat anti-rabbit IgG IRDye 680-conjugated secondary antibody (LI-COR Biosciences) or with goat anti-mouse IgG IRDye 800CW-conjugated secondary antibody and visualized using LI-COR's ODYSSEY infrared imaging system (LI-COR Biosciences). Densitometry was used to analyze the blots and normalized values are shown as percentages of the corresponding values for the WT virus (shown below each blot). **B)** Average densitometry results from two separate experiments using WT and ΔUS3 BHV-1.

from two separate experiments. Based on the Western blots, any difference determined by densitometry that was ≤ 20% was deemed to be not biologically relevant. Therefore, the observed difference in gC incorporation between WT and ΔUS3 BHV-1 was deemed to be non-significant as were the differences in protein concentration between WT BHV-1 and US3R BHV-1. The order of greatest to smallest relative changes in protein incorporation between the WT and ΔUS3 BHV-1 viruses as shown in Figure 4.5b is VP8 (↓ 58%) > gB (↑ 54%) > VP16 (↓ 53%) > VP22 (↑ 40%) > gD (↑ 23%) > gC (↓ 10%).

4.5 The role of US3 in cell to cell spread

To determine whether US3 in BHV-1 is required for efficient cell to cell spread, a plaque-size analysis was carried out using WT, ΔUS3 and US3R BHV-1. Briefly, cells were infected with each virus at 50-100 PFU/well and after ~48 hours, cells were fixed and probed with gB-specific MAbs followed by incubation with alkaline phosphatase-conjugated goat anti-mouse IgG. Plaques were visualized using 5-bromo-4-chloro-3-indolylphosphate and nitroblue tetrazolium and plaque size diameters were quantified and ranked before statistical analysis was done.

As shown in Figure 4.6, the mean plaque diameters resulting from ΔUS3 BHV-1 infection were significantly smaller than those caused by either WT or US3R BHV-1. Additionally, ΔUS3 BHV-1 had a larger number of small plaques compared to WT, which had greater number of larger plaques. The mean plaque diameters resulting from either WT or US3R BHV-1 infection were not significantly different. This study was repeated three times with nearly identical results, confirming that BHV-1 US3 is required for efficient cell to cell spread *in vitro.*

4.6 Effect of US3 on infected monolayers during BHV-1 infection *in vitro*

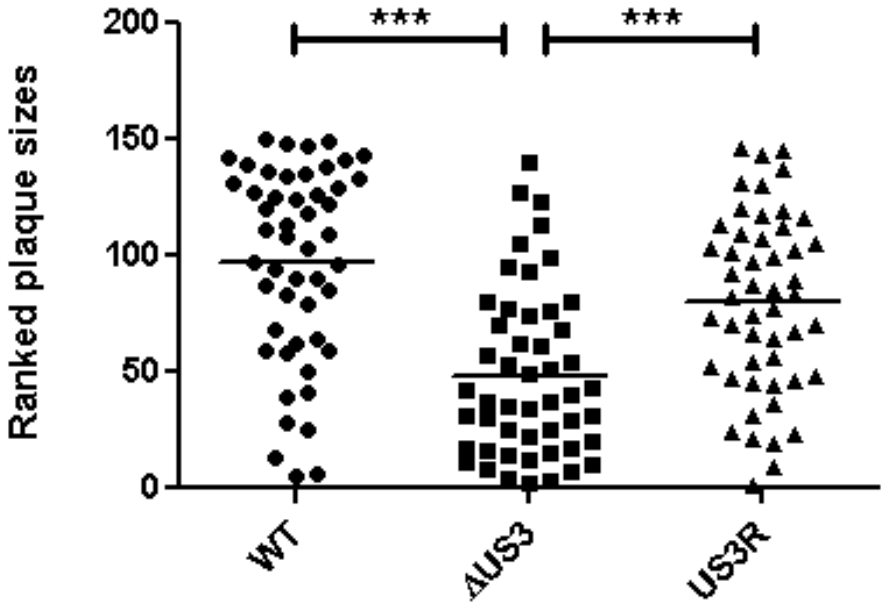

Figure 4.6: Effect of US3 on cell to cell spread *in vitro*.

MDBK cells were infected WT, ΔUS3 or US3R BHV-1 and incubated under semisolid medium for ~48 hours. Once plaques had formed, cells were fixed with ethanol-acetic acid and plaques were detected using a gB-specific MAb. The mean diameters of 50 plaques were photographed and quantified using AxioVision AC 4.5 Software (Zeiss). The plaque sizes were then ranked before a two-tailed *t* test was carried out using Prism 5 software.

In addition to US3 in other alphaherpesviruses (68, 136), BHV-1 US3 has been shown to be responsible for cellular cytoskeleton reorganization outside of the infection context (14). To determine whether US3 is responsible for morphological changes which are indicative of cytoskeleton reorganization in the context of infection, MDBK cells were infected at an MOI of 2 with WT, ΔUS3 and US3R BHV-1, and examined under phase-contrast microscopy after 10 hours of infection. As shown in Figure 4.7, WT and US3R BHV-1 caused identical morphological changes to the host cell, whereas infection with ΔUS3 BHV-1 resulted in a different phenotype.

To investigate the *in vitro* kinetics of the US3-dependent cytoskeleton reorganization, MDBK cells were infected at an MOI of 5 with WT or ΔUS3 BHV-1 and examined under phase-contrast microscopy from 5-35 hours post-infection at 5 hour intervals. As shown in Figure 4.8, infection with ΔUS3 BHV-1 likely results in the abolishment of cellular adhesions compared to WT BHV-1 starting as early as 15 hours post-infection. This effect was delayed until ≥35 hours post infection in cells infected with a MOI of 0.1 (results not shown), demonstrating that US3-dependent morphological changes in BHV-1-infected cells is dependent on the amount of US3 protein present in the cell, which can be manipulated by either increasing the length of infection or by increasing the viral load.

4.7 Effect of US3 on the subcellular localization of tubulin, VP22, VP8, and gB

Since BHV-1 VP22 (66), BHV-1 VP8 (67), and HSV-1 gB (55) have been shown to be substrates for US3, the subcellular localization of these proteins were studied in the absence of US3 in BHV-1infected MDBK cells. Initially, US3 was investigated by infecting MDBK cells in 2-well chamber slides at an MOI of 3. This MOI has been used and balances the integrity of the monolayer while allowing for viral protein expression within a short time frame.

Figure 4.7: Deletion of US3 influences cell morphology in BHV-1 infected MDBK cells.

MDBK cells were infected with WT, ΔUS3 or US3R BHV-1 at a MOI of 2. Ten hours post-infection, monolayers were visualized using a Zeiss Axiovision microscope.

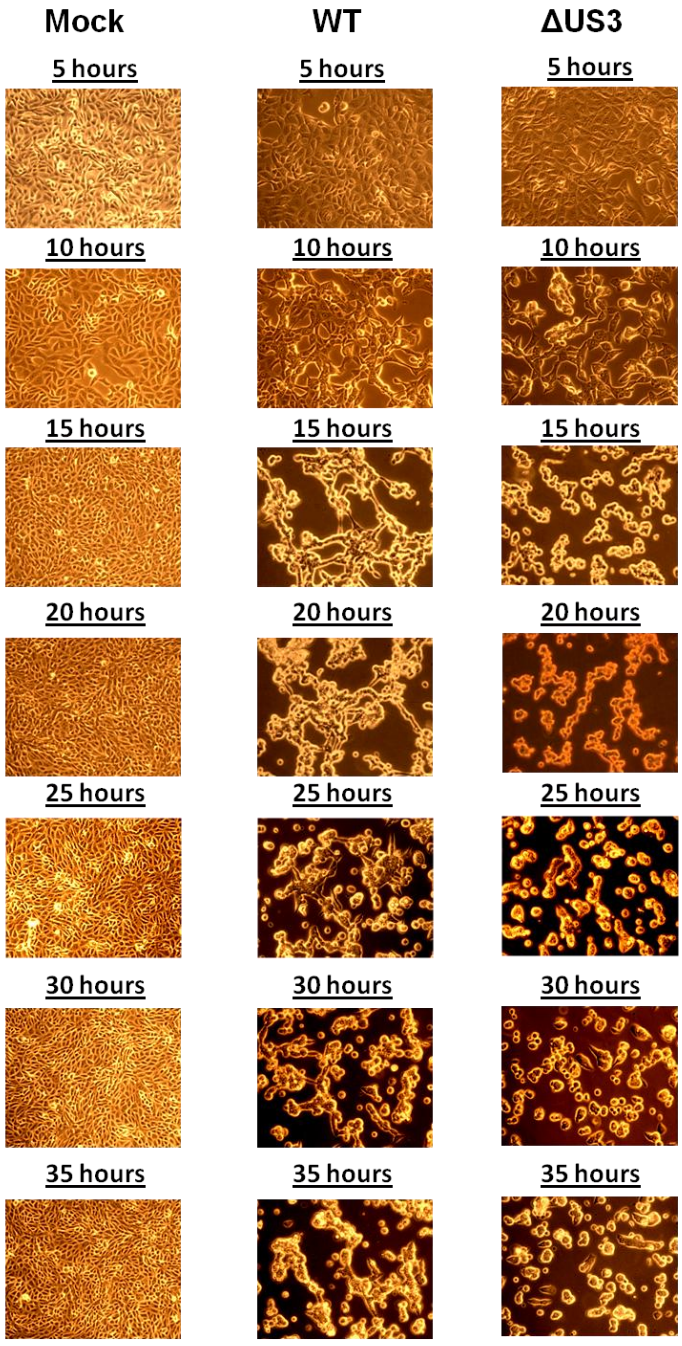

Figure 4.8: US3-dependent changes in cell morphology occur over the course of infection.

MDBK cells were either mock-infected or infected with WT or ΔUS3 BHV-1 at a MOI of 5 and examined using the Zeiss Axiovert 200M microscope from 5 to 35 hours post infection at 5 hour intervals.

At 4 hours post-infection, cells were fixed and US3 was detected with rabbit serum specific for BHV-1 US3. As shown in Figure 4.9, US3 was clearly nuclear 4 hours post-infection in WT BHV-1 infected cells, and was absent throughout the course of infection in either mock-infected or ΔUS3 BHV-1 infected MDBK cells. The nuclear expression of US3 is consistent with results by Labiuk et al. (66).

To investigate the role that BHV-1 US3 plays in cytoskeleton reorganization, tubulin was stained with a specific MAb. As shown in Figure 4.10, a phenotypic difference in cellular morphology was observed between WT and ΔUS3 BHV-1 infected cells. There was some evidence for reorganization of tubulin in WT BHV-1 infected cells but not in ΔUS3 BHV-1 infected MDBK cells, which may be responsible for this phenotypic change. BHV-1 US3 may therefore play an essential role in maintaining adherence between adjacent cells, which could affect intercellular spread of the virus. In the absence of US3, the abolishment of the cellular projections may explain the difference in growth kinetics between ΔUS3 and WT BHV-1 since the virus is unable to spread intercellularly.

Beyond VP22 being a known substrate for US3, the rationale for investigating its subcellular location was that it is involved in cell to cell spread of BHV-1 (54). Since this study has demonstrated that ΔUS3 BHV-1 is impaired in cell to cell spread, it was envisioned that VP22 may be at least partially responsible for this defect. Furthermore, since VP22 was incorporated into the mature BHV-1 virion in higher amounts in ΔUS3 BHV-1 compared to WT BHV-1, it was deemed that US3 may have an effect on VP22 expression and possibly

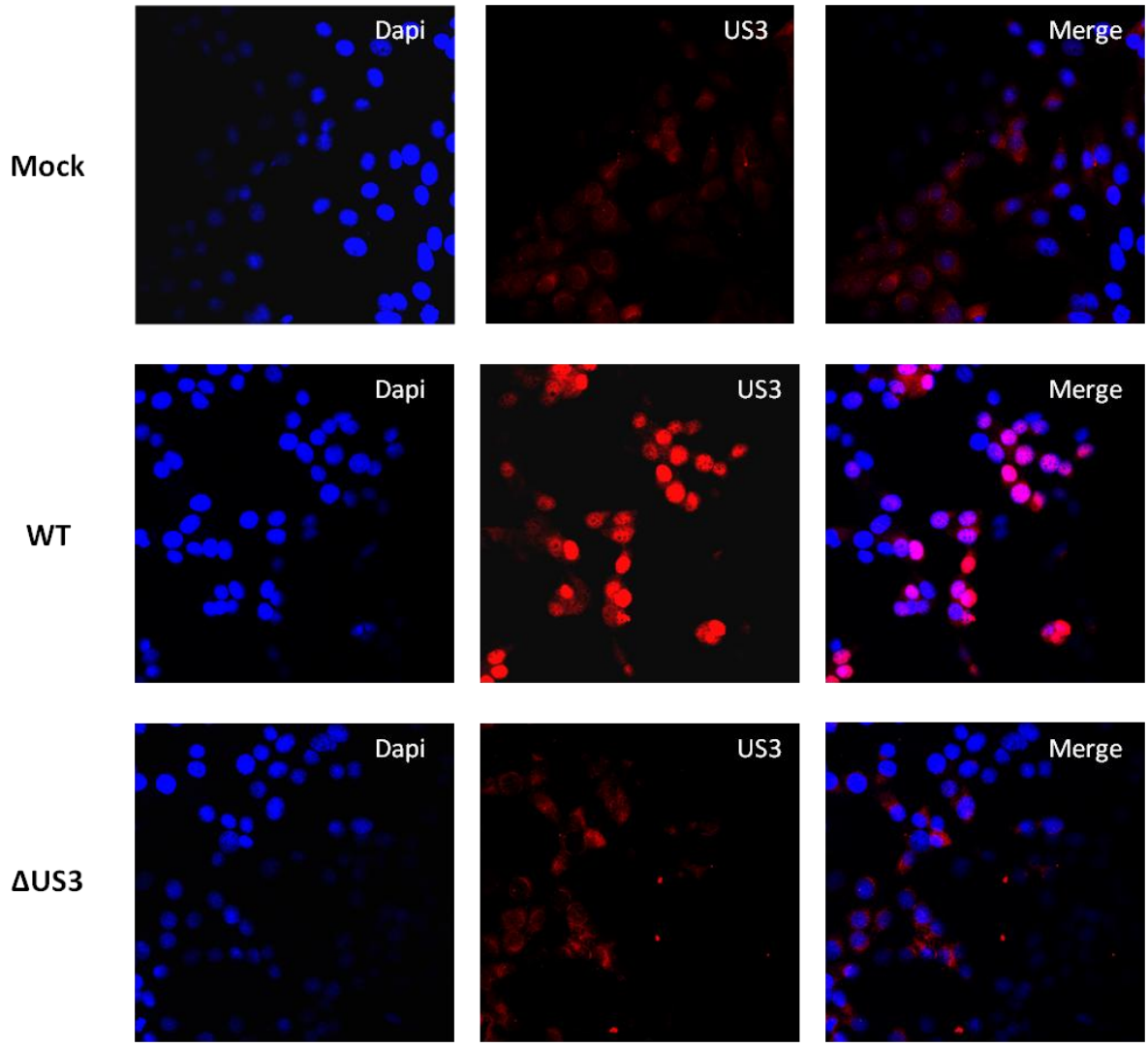

Figure 4.9: US3 localizes to the nucleus during BHV-1 infection and is absent in ΔUS3-infected cells.

MDBK cells were infected with WT or ΔUS3 BHV-1 at a MOI of 3 for 4 hours in 2-well permanox chamber slides before being fixed with paraformaldehyde and permeabilized with acetone. Cells were immunostained using US3-specific PAb and Alexa Fluor 633 goat anti-rabbit IgG, and coverslips were mounted using Prolong Gold Antifade Reagent with Dapi (Invitrogen). Images were acquired using normalized settings on the Zeiss LSM410 confocal microscope and enhanced under identical parameters using the ImageJ software system.

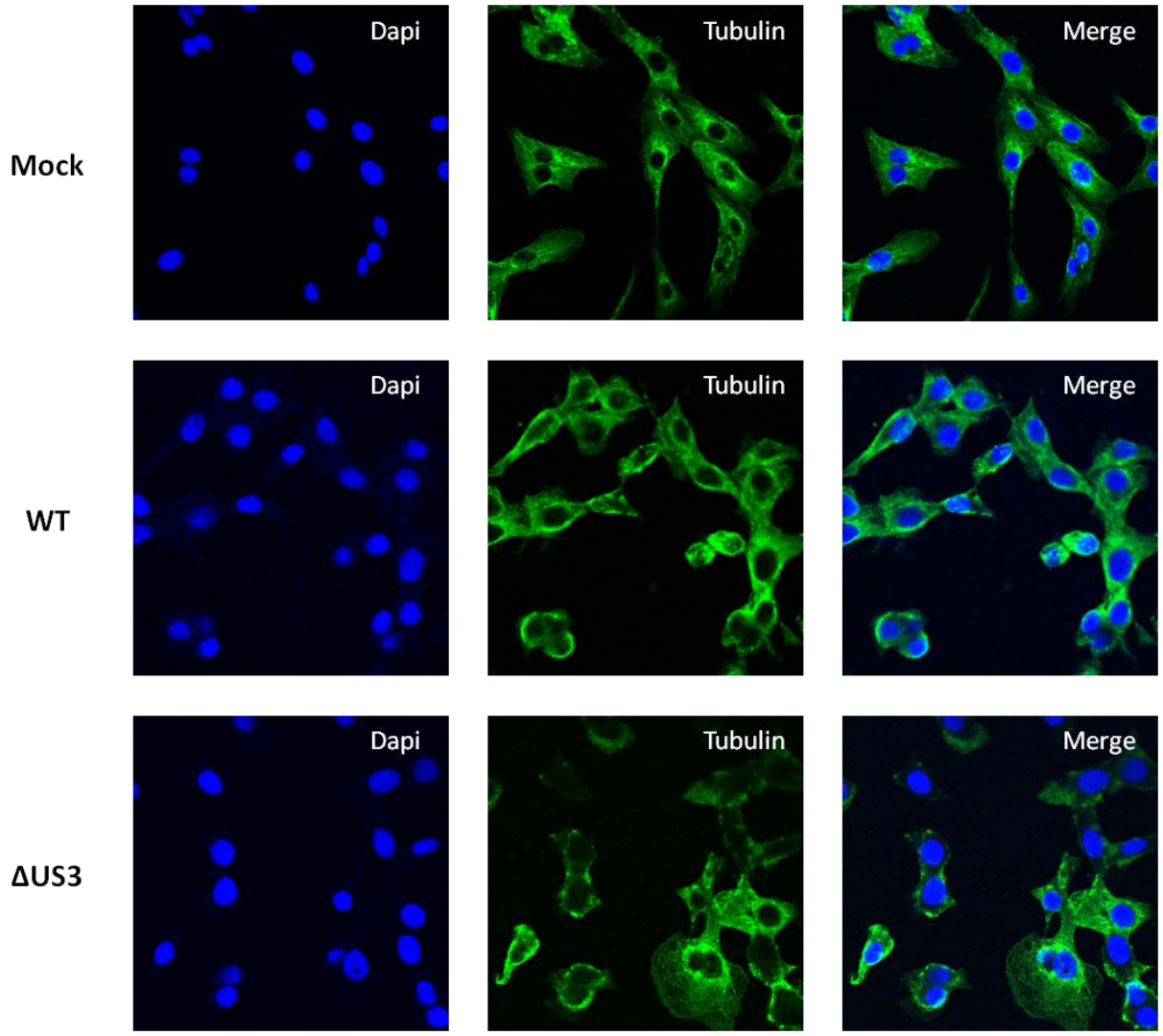

Figure 4.10: BHV-1 US3 may affect maintenance of cellular adhesions that are facilitated through cytoskeleton restructuring.

MDBK cells were infected with WT or ΔUS3 BHV-1 at a MOI of 3 for 4 hours in 2-well permanox chamber slides before being fixed with paraformaldehyde and permeabilized with acetone. Cells were immunostained using tubulin-specific MAb and Alexa Fluor 488 goat anti-mouse IgG, and coverslips were mounted using Prolong Gold Antifade Reagent with Dapi (Invitrogen). Images were acquired using normalized settings on the Leica DMI6000 confocal microscope and enhanced under identical parameters using the ImageJ software system.

intracellular trafficking. To investigate VP22, confocal microscopy was carried out as above, except cells were probed with rabbit VP22-specific PAb serum. Although differences in cell adherence can be seen in Figure 4.11, there is no noticeable difference in VP22 localization between cells infected with either WT or ΔUS3 BHV-1. Namely, at 7 hours post infection VP22 remained cytoplasmic, and was detected in cellular projections in infected cells, irrespective of the presence of US3.

The subcellular localization of VP8 was investigated since our group has previously demonstrated that this viral protein is a substrate of BHV-1 US3 (67), and in HSV-1, US3 and UL47 reciprocally regulate their subcellular location in infected cells. In the current study, an increase in VP8 production in ΔUS3 BHV-1 infected cells and a significant decrease in VP8 incorporation in the mature ΔUS3 BHV-1 virions was demonstrated. Since VP8 is the major tegument protein in BHV-1, decreased incorporation may have an effect on the lifecycle, fitness, and/or pathogenicity of the virus in its host. In WT BHV-1 infected cells, VP8 was expected to be nuclear but may also have some cytoplasmic staining due to the presence of a nuclear export signal (158).

To investigate the subcellular localization of VP8, slides were prepared as above, except cells were fixed and probed with anti-VP8 specific MAb at 7 hours post-infection. Seven hours was chosen as our group has previously shown that VP8 translocates to the nucleus after 5 hours of infection (144). Figure 4.12 clearly demonstrates that the nuclear localization of BHV-1 VP8 is not dependent on US3 phosphorylation for its nuclear translocation. These results are in contrast to those obtained in HSV-1 infection, and could mean that either BHV-1 VP8 does not have to be phosphorylated before nuclear translocation, or could mean that the cellular CK2

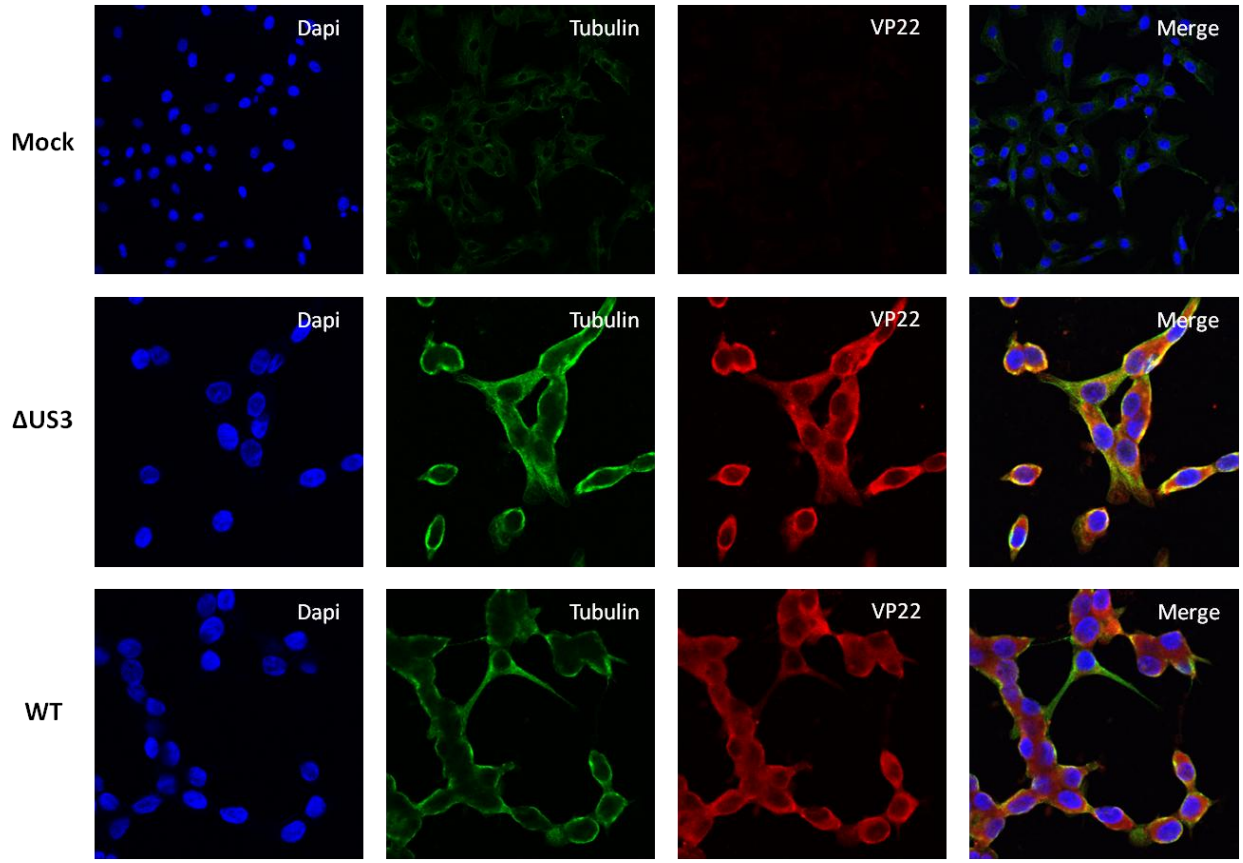

Figure 4.11: The intracellular localization of BHV-1 VP22 is not dependent on US3.

MDBK cells were infected with WT or ΔUS3 BHV-1 at a MOI of 3 for 7 hours in 2-well permanox chamber slides before being fixed with paraformaldehyde and permeabilized with acetone. Cells were immunostained using tubulin-specific MAb and VP22-specific PAb before being incubated with Alexa Fluor 488 goat anti-mouse IgG and Alexa Fluor 622 goat anti-rabbit IgG. Coverslips were mounted using Prolong Gold Antifade Reagent with Dapi (Invitrogen). Images were acquired using normalized settings on the Leica DMI6000 confocal microscope and enhanced under identical parameters using the ImageJ software system.

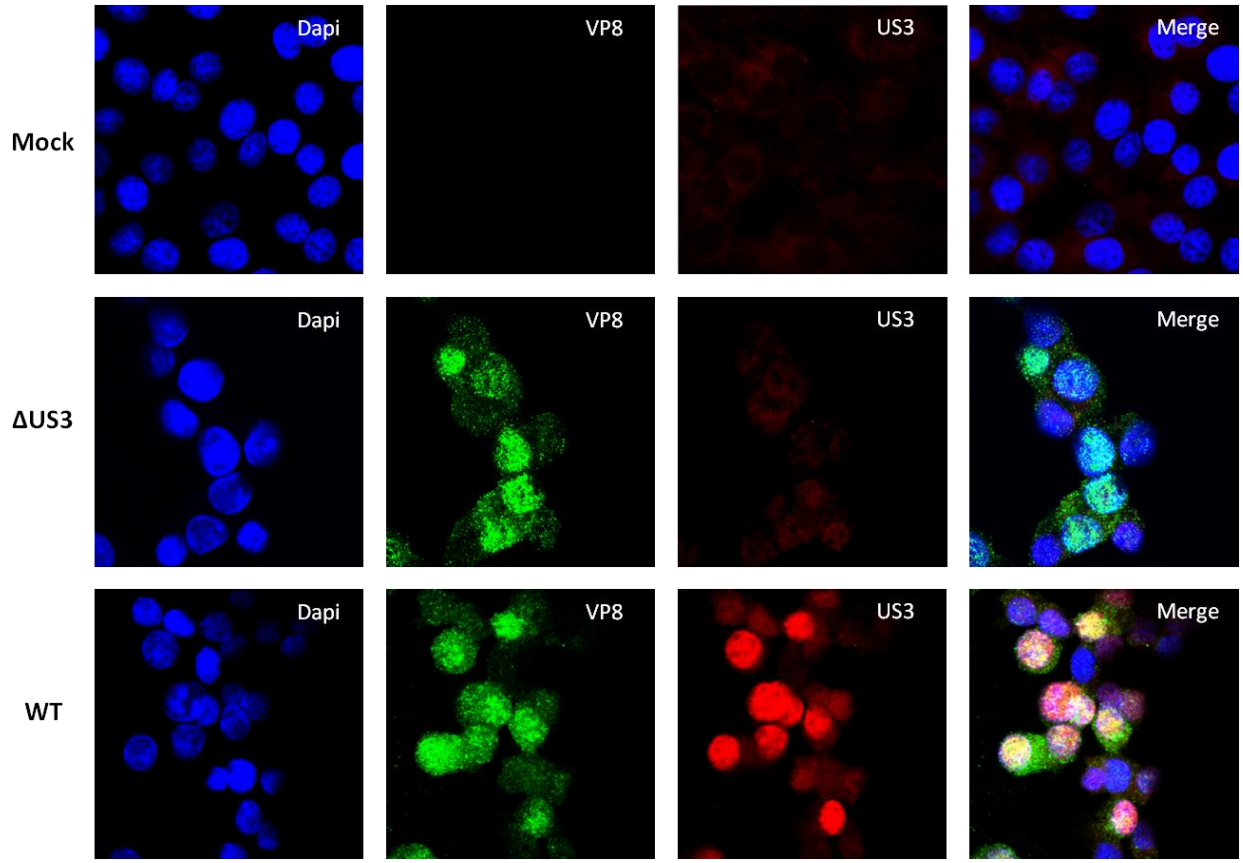

Figure 4.12: BHV-1 VP8 localizes to the nucleus of infected cells independent of US3.

MDBK cells were infected with WT or ΔUS3 BHV-1 at a MOI of 3 for 7 hours in 2-well permanox chamber slides, before being fixed with paraformaldehyde and permeabilized with acetone. Cells were immunostained using VP8-specific MAb and US3-specific PAb before being incubated with Alexa Fluor 488 goat anti-mouse IgG and Alexa Fluor 622 goat anti-rabbit IgG. Coverslips were mounted using Prolong Gold Antifade Reagent with Dapi (Invitrogen). Images were acquired using normalized settings on the Zeiss LSM410 confocal microscope and enhanced under identical parameters using the ImageJ software system.

kinase, which has been shown to be the primary kinase responsible for BHV-1 VP8 phosphorylation, may determine its subcellular location (67).

gB was also investigated by confocal microscopy, since in HSV-1 US3 phosphorylation of gB at residue Thr-887 has been shown to regulate its expression on the surface of infected cells (55). Since the results presented in our study demonstrate that US3 deletion has a significant impact on *in vitro* gB expression and its incorporation into the mature virion, it was envisaged that US3 deletion may also have an effect on gB surface expression in infected cells. MDBK cells were infected with WT or ΔUS3 BHV-1 and fixed at 3 and 6 hours post infection to investigate the kinetics of gB surface expression. Furthermore, to differentiate between total gB cell expression and surface expression of gB, cells were either permeabilized or left unpermeabilized during the staining procedure. Fixed cells were stained with a gB-specific MAb and a US3-specific PAb.

The confocal images shown in Figures 4.13 a and b were taken and enhanced under identical settings. At 3 hours post-infection, the total expression of gB seemed greater in ΔUS3 BHV-1 infected cells compared to WT BHV-1 infected cells, which may reflect impaired endocytosis of gB from the cell surface early in infection. Once the infection progressed, however, it was apparent that the intracellular accumulation of gB is greater in WT BHV-1 infected cells compared to ΔUS3 BHV-1 infected cells, as is shown at 6 hours post-infection.

To investigate the surface expression of gB in ΔUS3 BHV-1 infected cells, non-permeabilized cells which were stained identical to the permeabilized cells were examined using confocal microscopy. Figures 4.14 a and b clearly demonstrate that the surface expression of gB was higher 3 hours post infection in cells infected with ΔUS3 BHV-1 when compared to WT

BHV-1. By 6 hours post infection, however, the difference became difficult to discern which may reflect cells adopting a round morphology at this late time point.

4.8 Effect of US3 on the surface expression of gB *in vitro*

To quantify the differences in gB surface and intracellular expression in MDBK cells infected with either ΔUS3 or WT BHV-1, FACS was carried out. As demonstrated in Figure 4.15, the accumulated intracellular gB was approximately 25% higher in WT BHV-1 infected cells than in cells infected with ΔUS3 BHV-1. This decrease in intracellular gB in ΔUS3 BHV-1 infected cells is associated with a corresponding 25% increase in surface gB expression in cells infected with ΔUS3 BHV-1 compared to cells infected with WT BHV-1. Confirmation of these results through replicate experiments will allow for statistical analysis. Furthermore, FACS analysis comparing WT and US3R BHV-1 infected cells will confirm that the observed effect on gB is due to BHV-1 US3 alone.

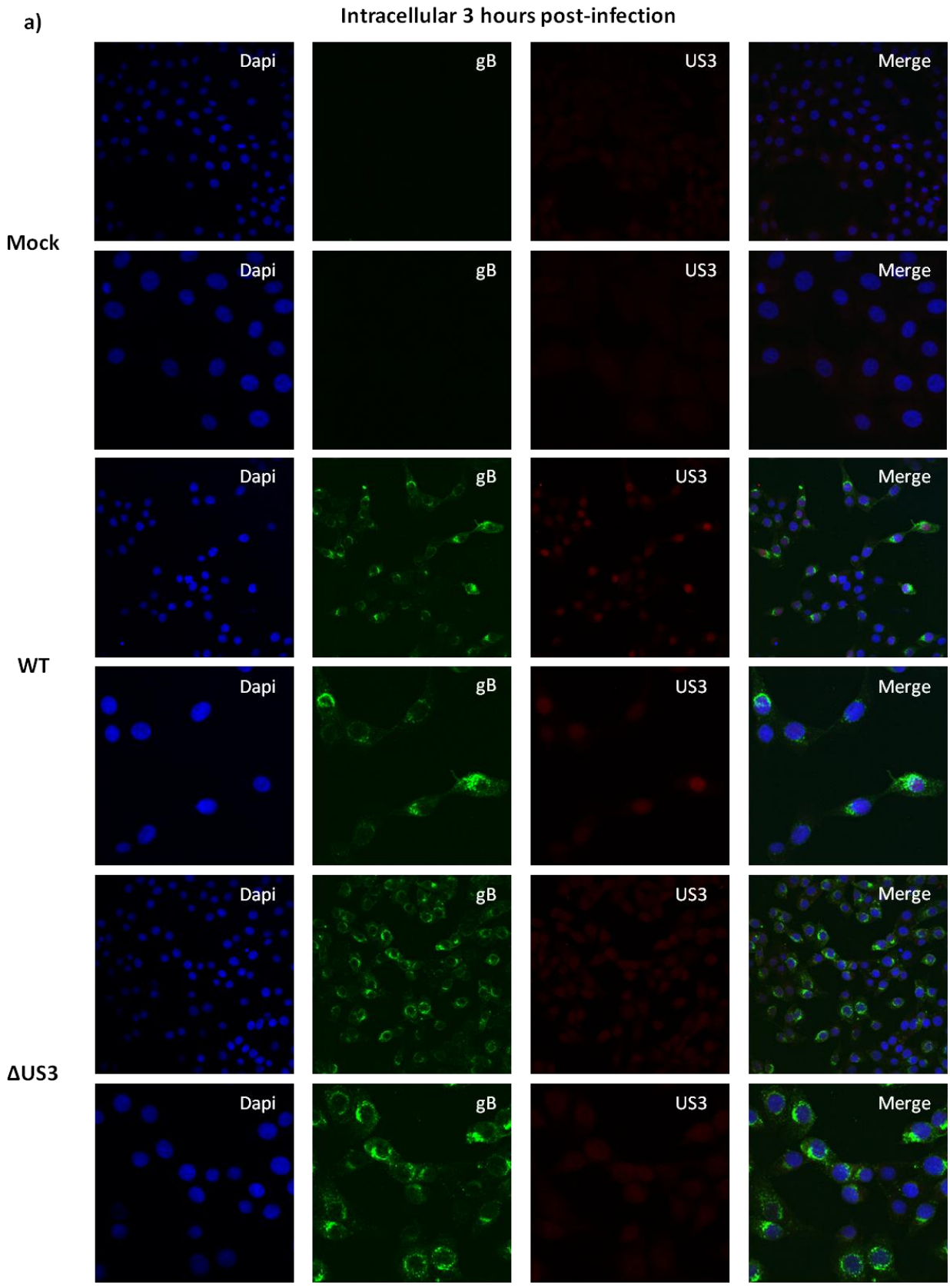
a)
Intracellular 3 hours post-infection
Dapi
gB
US3
Merge
Mock
WT
ΔUS3

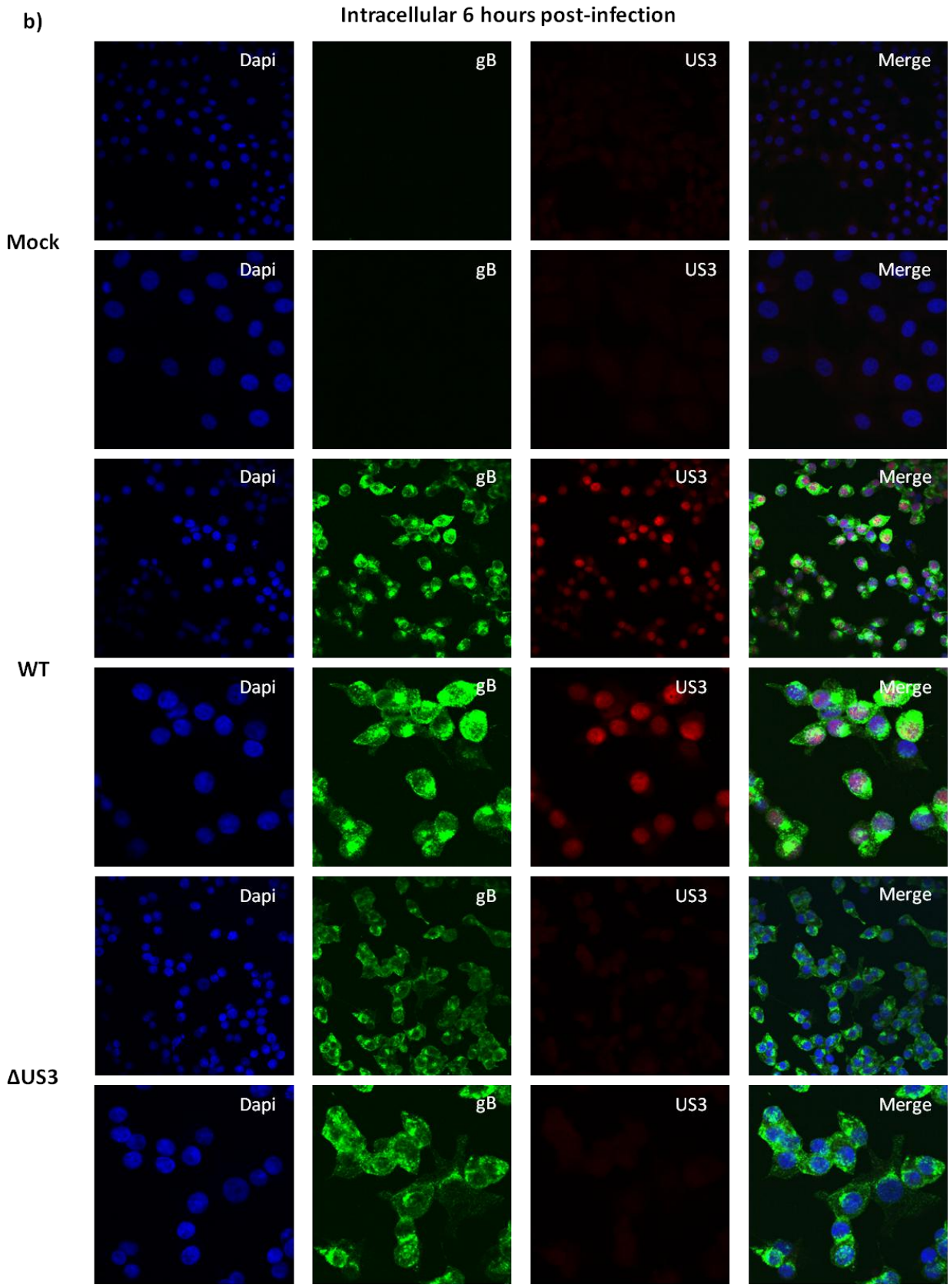
b)
Intracellular 6 hours post-infection
Mock
WT
ΔUS3
Dapi
gB
US3
Merge

Figure 4.13 a,b: Intracellular expression of gB in cells infected with WT and ΔUS3 BHV-1.

MDBK cells were infected with WT or ΔUS3 BHV-1 at a MOI of 3 for 3 (a.) or 6 (b.) hours in 2-well permanox chamber slides, before being fixed with paraformaldehyde and permeabilized with acetone. Cells were immunostained using gB-specific MAb and US3-specific PAb before being incubated with Alexa Fluor 488 goat anti-mouse IgG and Alexa Fluor 633 goat anti-rabbit IgG. Coverslips were mounted using Prolong Gold Antifade Reagent with Dapi (Invitrogen). Images were acquired using normalized settings on the Leica DMI6000 confocal microscope and enhanced under identical parameters using the ImageJ software system.

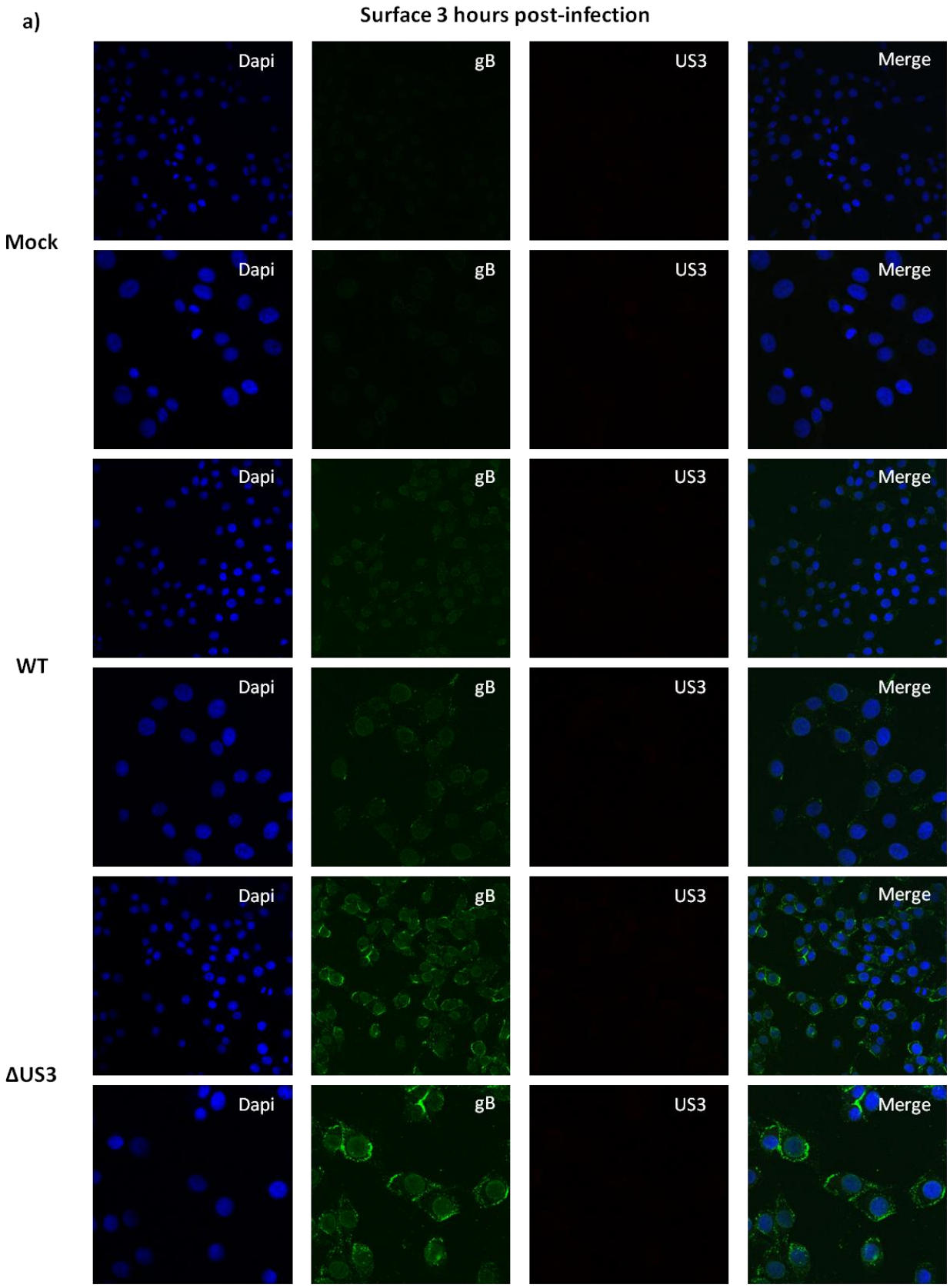
a)
Surface 3 hours post-infection
Dapi
gB
US3
Merge
Mock
WT
ΔUS3

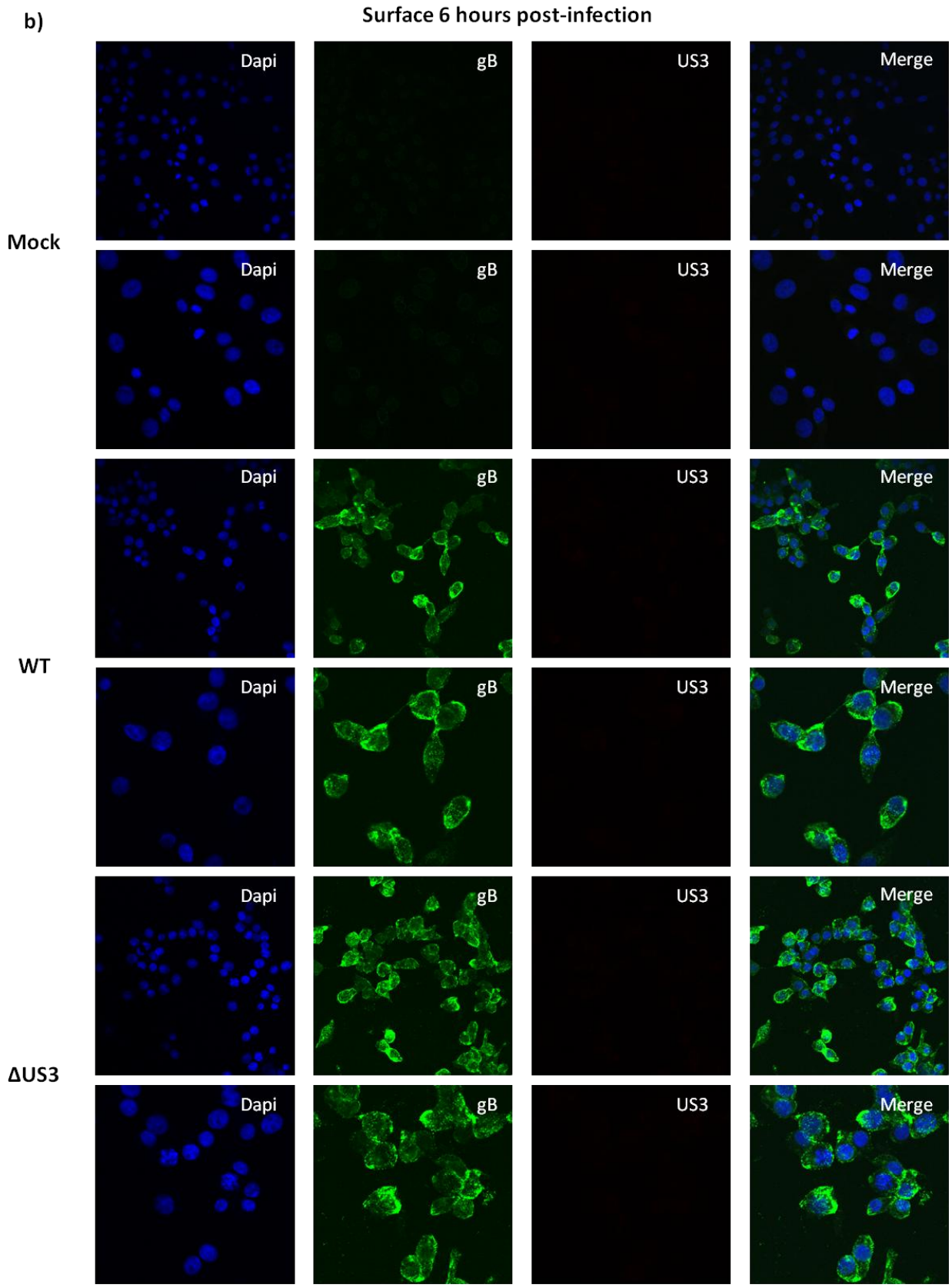
b)
Surface 6 hours post-infection
Dapi
gB
US3
Merge
Mock
WT
ΔUS3

Figure 4.14 a,b: Surface expression of gB in cells infected with WT and ΔUS3 BHV-1.

MDBK cells were infected with WT or ΔUS3 BHV-1 at a MOI of 3 for 3 (a.) or 6 (b.) hours in 2-well permanox chamber slides before being fixed with paraformaldehyde. Cells were immunostained using gB-specific MAb and US3-specific PAb before being incubated with Alexa Fluor 488 goat anti-mouse IgG and Alexa Fluor 633 goat anti-rabbit IgG. Coverslips were mounted using Prolong Gold Antifade Reagent with Dapi (Invitrogen). Images were acquired using normalized settings on the Leica DMI6000 confocal microscope and enhanced under identical parameters using the ImageJ software system.

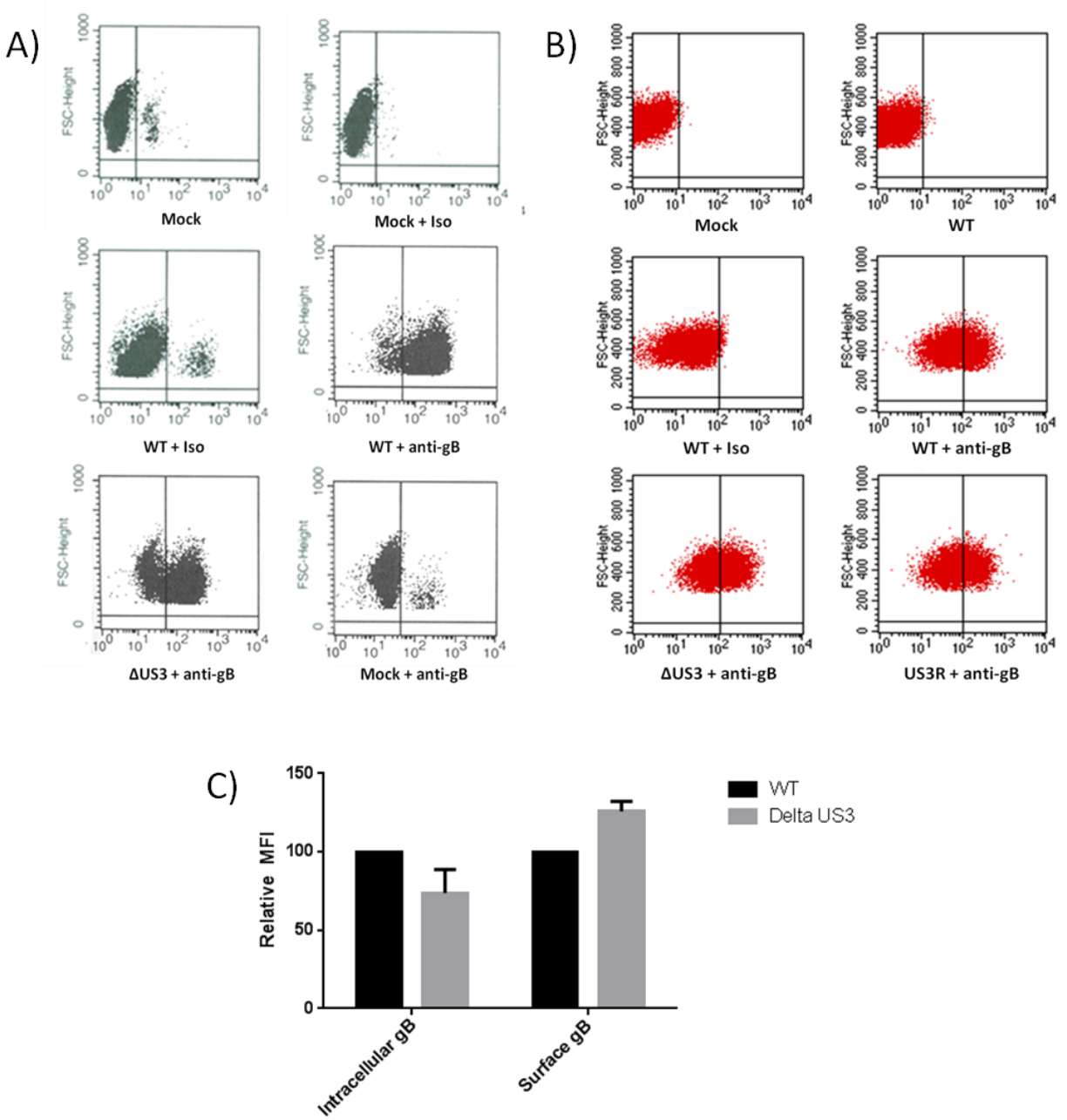

Figure 4.15 a, b, c: Intracellular and surface expression of gB in WT and ΔUS3 BHV-1.

MDBK cells were infected at a MOI of 3 and harvested at 4 hours post-infection. Cells were either permeabilized according to the procedure in Materials and Methods, or nonpermeabilized. Cells were then immunostained with gB-specific MAb and Alexa Fluor 488 goat anti-mouse IgG. A) The MFI of cells expressing intracellular gB was determined by FACS analysis. B) The

MFI of cells expressing gB on the surface was determined by FACS analysis. C) The relative MFI of cells infected with ΔUS3 BHV-1 compared to WT BHV-1 are shown. The bars are represented as the means from two independent experiments after the MFI from mock-infected MDBK cells was subtracted. Standard deviations are presented.

5.0 DISCUSSION AND CONCLUSIONS

BHV-1 causes a range of clinical manifestations in cattle including respiratory and genital infections which range in severity depending on the strain. Of particular economic importance is the role that BHV-1 plays in the development of BRDC, a severe respiratory disease in cattle which may also lead to milk drop, abortions, and death in infected animals. BHV-1-mediated immunosuppression of the host contributes to BRDC by allowing the establishment of secondary infections (51). BHV-1 is an enormous economic concern in countries harboring large cattle populations, such as those in North America. It has been estimated that BRDC or 'shipping fever' costs the US cattle industry close to one billion dollars per year (11, 133).

While culling of seropositive herds has been effective in some European countries, vaccination remains the most effective means of BHV-1 control in countries which harbor large cattle populations. Efforts to develop an inexpensive, safe, and effective vaccine against BHV-1 have been an ongoing since the early 1980's (48). While various vaccines against BHV-1 have been successful at reducing disease severity, transmission, and replication of the virus, none have been able to prevent infection (1). Commercially available vaccines against BHV-1 include MLV and inactivated vaccines, which have issues with safety and efficacy, respectively. Although MLV produce rapid and enduring immune responses, safety issues have prevented these vaccines from being highly successful (139, 150). Alternatively, KV against BHV-1 have outstanding safety profiles, yet fail to elicit appropriate immune responses and often require adjuvants. Due to these issues, genetically engineered gene-deleted, subunit, DNA, and vectored vaccines are being investigated as alternatives to the commercially available vaccines against BHV-1.

To design effective vaccines, more information is required on the contributions of individual BHV-1 gene products to the viral lifecycle and pathogenicity in the host. US3 is one of two serine/threonine kinases which are expressed by the alphaherpesvirus subfamily (114). Although non-essential, US3 has been shown to contribute to viral fitness and pathogenicity in related alphaherpesviruses through multifunctional roles in the viral lifecycle, including efficient viral gene expression, virion morphogenesis, cytoskeleton reorganization and evasion of the antiviral response (22). While the functions of US3 in HSV-1 and PRV infection have been studied extensively, the function(s) of US3 during BHV-1 infection remain poorly understood.

Studies on BHV-1 US3 have elucidated two viral substrates, namely VP8 and VP22 (66, 67). Both of these viral proteins play vital roles in the BHV-1 lifecycle, including efficient viral gene transcription and facilitating intercellular virus spread, respectively. Recently, Brzozowska et al. (14) demonstrated that similar to BHV-5, PRV, and HSV-2 (30, 32, 68, 141), BHV-1 US3 induces cytoskeleton changes that are characteristic of BHV-1 infection. Since this study was conducted using a recombinant baculovirus system, more research is needed to identify the roles of BHV-1 US3 on cytosketon arrangements within the context of infection and also elucidate a reason for this drastic cellular modification. The role of BHV-1 US3 in cell to cell spread was recently shown to be strain-dependent, with the US3 protein playing an integral role in intercellular spread with a highly passaged strain compared to a minimally passaged strain (90). This group also demonstrated that when US3 was deleted, the *in vitro* growth kinetics of the virus were impaired. From these studies, it is clear that while BHV-1 US3 is non-essential, it plays vital roles in viral fitness and potentially in the pathogenicity of the virus in its host.

The objective of our study was to functionally characterize the BHV-1 US3 kinase in an effort to identify roles for US3 in the BHV-1 lifecycle and fitness of BHV-1. To carry out these

studies, a ΔUS3 BHV-1 and corresponding US3R BHV-1 were generated. The viruses were characterized alongside WT BHV-1. *In vitro* growth kinetics, viral protein expression kinetics, and mature virion composition were all investigated. To further elucidate a role for US3 in the BHV-1 lifecycle, the effect that US3 has on cell to cell spread and cellular morphology in the context of infection were determined. Finally, the effect US3 has on the intracellular localization of known substrates, VP8 and VP22, and a putative substrate, gB, were explored through confocal microscopy and flow cytometry (for gB).

After generating a ΔUS3 BHV-1 and the corresponding US3R BHV-1, the growth kinetics of the mutant viruses were investigated. Using a single-step growth assay, we found that ΔUS3 BHV-1 had approximately 10-fold lower intracellular and extracellular titres at late stages of infection compared to either WT or US3R BHV-1. These results are consistent with the work of Minh et al. (90). Additionally, starting at around 15 hours post infection, the titres of ΔUS3 BHV-1 plateaued and remained consistent throughout the course of infection. This is in contrast to the pattern seen with the WT and US3R BHV-1, which had increasing titres throughout the entire time course. The overall observed defect in the growth kinetics of ΔUS3 BHV-1 could be due to a deficiency in cell to cell spread, egress of the virus from the cell, or could reflect lower viral replication rates in the absence of US3. More research is required to identify the mechanism of this impairment.

The effect that US3 has on the expression kinetics of major structural and regulatory proteins was investigated. This analysis was used to identify roles that US3 may play during BHV-1 infection and the viral protein cascade. We found that compared to WT, ΔUS3 BHV-1 infected cells exhibited differences in bICP4 and VP5 protein expression. Specifically, compared to WT BHV-1, the immediate-early protein, bICP4, which was expressed earlier in infection and

the major capsid protein, VP5, was expressed in higher amounts throughout the duration of infection in ΔUS3 BHV-1 infected cells. Since the WT and ΔUS3 BHV-1 stocks were titred in quadruplicate in three independent experiments, we can be confident that the increased production of these proteins was not due to differences in virion input.

Other viral proteins which were most affected by the deletion of US3 included the major tegument proteins, VP16 and VP8, which were expressed in higher amounts during late stages of infection compared to WT infected cells. Also, cellular gB expression was higher with ΔUS3 BHV-1 early in infection, with levels that tapered off over the remainder of infection. gC expression, on the other hand, was reduced by half compared to WT infected cells throughout the course of infection. Viral proteins whose expression seemed unaffected by the deletion of US3 included gD and VP22, which remained fairly consistent in cells infected with either virus throughout the course of infection. These data support a role for US3 in the regulation of major structural and regulatory viral protein expression during the course of infection.

The differences in the cellular expression of these BHV-1 proteins in the absence of US3 could be due to a number of mechanisms. The expression of viral proteins such as VP8, VP16, and gB, were increased in cells infected with ΔUS3 BHV-1 compared to WT BHV-1. It can be speculated that US3 could have a direct effect on the phosphorylation profile of these proteins, and when they are hypophosphorylated, may make them more resistant to degradation. Indeed, phosphorylation by herpesvirus protein kinases has been shown to target cellular and viral proteins for ubiquination and subsequent proteosomal degradation (17, 47). On the contrary, the decreased expression of gC in the absence of BHV-1 US3 could point to an interaction of this protein with BHV-1 US3 (through phosphorylation or other means), which could potentially make gC more stable during normal WT BHV-1 infection. Also, since PRV US3 has been shown

to remain with the capsid until it docks at the nuclear pore, potentially BHV-1 US3 has similar trafficking, and could affect viral protein expression either directly or indirectly (35). Increased intracellular expression of the immediate-early protein, bICP4, suggests that BHV-1 US3 may have a regulatory role in viral gene transcription. It is unclear at this time how BHV-1 US3 affects the expression profiles of various viral proteins; however, it is tempting to believe that either direct phosphorylation of these proteins or other regulatory viral or cellular proteins may be important for efficient viral protein expression.

HSV-1 gB phosphorylation by US3 has been demonstrated to have numerous important roles *in vitro* (44), including influencing gB trafficking and cellular localization. Kato et al. have demonstrated that in HSV-1, US3 is responsible for the direct phosphorylation of gB in infected cells, which regulates its intracellular localization (55). Follow-up studies by Imai et al. have further identified four residues in gB which are required for efficient gB trafficking in cells infected with HSV-1 (43). This group determined that US3-dependent phosphorylation of gB at a position 887 threonine residue is required for efficient downregulation of gB on the surface of infected cells. Although this residue is not present in BHV-1, there are numerous other serine and threonine residues in the cytoplasmic region of gB which are BHV-1 specific, and may play roles in the US3-dependent regulation of gB surface expression in infected cells (151).

Although gB is not a known substrate for BHV-1 US3, our *in vitro* expression kinetics studies have demonstrated that US3 deletion affects the intracellular expression of gB. Namely, in ΔUS3 BHV-1 infected cells, gB levels are increased early in infection and taper off for the remainder of infection compared to WT BHV-1. It is tempting to believe that US3 either directly or indirectly affects its intracellular expression and/or prevents gB degradation. The mechanism for this regulation is likely through phosphorylation of gB by US3, similar to HSV-1 (44).

To determine the effect that BHV-1 US3 has on the integration of viral proteins into the mature virion, we determined the composition of purified WT, ΔUS3 and US3R BHV-1. We found that similar to the effect on viral protein expression kinetics, the incorporation of various viral proteins into the mature virions were different in the ΔUS3 BHV-1 compared to WT or the US3R virus. Quantitative analysis using densitometry demonstrated that compared to WT, ΔUS3 BHV-1 has approximately 50% increased incorporation of gB, 50% decreased incorporation of VP8 and VP16, 40% increased incorporation of VP22, and 25% increased incorporation of gD. gC was the only protein investigated with equal amounts of protein incorporated into the mature virion irrespective of US3. Viral protein incorporation into US3R BHV-1 was approximately the same as that in WT BHV-1, further demonstrating that this virus had reverted to its WT phenotype. These results demonstrate that US3 is required for efficient incorporation of a number of viral proteins into the mature BHV-1 virion.

Similar to what has been demonstrated in a VP8-null BHV-1 (73), the deletion of BHV-1 US3 has resulted in both increased and decreased amounts of certain key proteins in the mature virion. Compared to WT BHV-1, ΔUS3 BHV-1 has increased levels of VP22 and gB, and decreased levels of VP16 and VP8. Besides gB, these trends are not reflected in the expression kinetics profiles of these proteins in the infected cell. To explain these discrepancies, there are a number of possibilities.

Similar to the effect that VP8 deletion has on gC in BHV-1 (73), the incorporation of VP16 and VP8 into the mature virion could be dependent on WT BHV-1 expression levels of US3. Since VP8 is a known substrate of BHV-1 US3, it can be envisaged that reduced phosphorylation of this protein may reduce its assembly into the mature virion. In contrast with this idea, various groups have shown that although alphaherpesvirus VP22 homologues are

phosphorylated during infection, the unphosphorylated form of the protein predominates in the mature virion (26, 37). It is not known if US3 phosphorylates VP16 in BHV-1, however, our results suggest that this is a possibility. Alternatively, US3 in BHV-1 could play a physical role in recruiting VP16 and VP8 into the tegument. Recently, HSV-1 VP22 was shown to play an integral role in the recruitment of various glycoproteins into the tegument (80).

Although VP22 was substantially increased in the virion in the absence of BHV-1 US3, the levels of intracellular VP22 were roughly equal to WT levels. Similar to what has been demonstrated in a VP8-null BHV-1, the decreased incorporation of the major tegument proteins, VP8 and VP16, could drive increased incorporation of VP22 in the absence of BHV-1 US3 (73). Alternatively, similar to what has been found in HSV-1 and HSV-2, hypophosphorylation of VP22 at serine/threonine residues could increase the capacity to which it is incorporated into the tegument (26, 37). More research is obviously needed to identify how BHV-1 US3 physically interacts with VP8, VP16, and VP22, and affects their incorporation into the mature virion. This is a daunting task, as tegumentation of BHV-1 is a complex process that is driven by an intricate cascade of protein-protein interactions.

The marked increase in gB incorporation into mature virions in the absence of US3 points further to a significant role for BHV-1 US3 in the intracellular trafficking and regulation of gB expression *in vitro*. Although HSV-1 gB has been shown to be a substrate for US3, this has not been demonstrated in BHV-1 (55). The corresponding decrease in the major tegument proteins, VP16 and VP8, also point to a role for US3 in their regulation. To date, VP16 has not been identified as a substrate for US3 in BHV-1. Studies in PRV, however, have demonstrated that when US3 is deleted, the incorporation of both the large and small isoforms of VP16 are minimally increased (87).

Our group has previously demonstrated that VP8 is a substrate for US3 (67), however, the function that this plays *in vitro* has not been investigated. To elucidate a potential role for the phosphorylation of VP8 by US3, confocal microscopy was carried out on either WT or ΔUS3 BHV-1 infected cells using antibodies against US3 and VP8. We demonstrated that in both the presence and absence of US3, VP8 localizes to the nucleus during infection. This US3-independent nuclear localization of VP8 was unexpected since a putative phosphorylation residue on VP8 is close to one of the four nuclear import signals (67, 145, 158). This means that the nuclear translocation of VP8 likely occurs through a US3-independent process involving cellular kinases or that this process may not require phosphorylation at all. Furthermore, contrary to what has been found by Kato et al. in HSV-1, BHV-1 US3 and VP8 do not seem to reciprocally regulate their nuclear localization during infection as VP8 is nuclear independent of US3 (56)

US3 deletion also resulted in increased incorporation of VP22, a tegument protein important in BHV-1 cell to cell spread (54). Our group has shown that US3 is involved in phosphorylating VP22 *in vitro*, however, the function of this modification is still unclear (66). To determine whether US3 deletion has an effect on cell to cell spread of the virus, the relative plaque sizes of the WT, ΔUS3, and US3R BHV-1 were determined. We found that relative to WT or US3R BHV-1, the US3-deleted virus was significantly impaired ($p \leq 0.0001$) in cell to cell spread. There was no difference, however, in the cellular localization of VP22 in the presence or absence of US3, with the protein being entirely cytoplasmic at 7 hours post-infection independent of US3. Similarly, phosphorylation of VP22 in HSV-2 has been shown to not be required for its subcellular localization (36). Taken together, our results show that US3-dependent phosphorylation of VP22 is not required for its cytoplasmic localization at early times

post-infection. This localization may be independent of phosphorylation or could be dependent on the cellular casein kinase 2 (CK2), which has been demonstrated to be the major protein which phosphorylates BHV-1 VP22 *in vitro*. It is still possible, however, that the hypophosphorylation of VP22 in the absence of US3 in ΔUS3 BHV-1 may be responsible for the defect in cell to cell spread of this virus.

Consistent with the results from Brzozowska et al., our studies show that US3 causes substantial changes in the host cell morphology during infection (14). Although difficult to discern from our studies, Brzozowska et al. have shown outside of the context of infection that the phenotypic changes are due to US3-dependent actin reorganization, resulting in microtubule formation. In PRV, similar US3-dependent cytoskeleton reorganizations have been shown to be required for efficient intercellular spread of the virus (31). It is tempting to believe that BHV-1 may use a similar intercellular spread mechanism via tubulin. Our studies demonstrated that cells infected with either WT or US3R BHV-1 gradually formed a network of cells which remained connected through long cellular extensions, whereas the extensions were absent during infection with ΔUS3 BHV-1. Using our ΔUS3 BHV-1 mutant, we were able to demonstrate that this phenotype is dependent on US3 and is not compensated for by other viral proteins. Furthermore, cells infected with either WT or ΔUS3 BHV-1 began to show distinct phenotypes as early as 15 hours post infection. Our data also provide some evidence that the US3-dependent cellular changes could be due to tubulin reorganization that results in long cellular extensions produced during WT BHV-1 infection.

In HSV-1, phosphorylation of gB by US3 has been shown to be important for viral egress from the outer nuclear membrane (153). During normal HSV-1 infection, gB and gH cooperate to promote fusion between the viral envelope and the outer nuclear membrane. Wisner et al.

were able to demonstrate that when gB was deleted, HSV-1 virions accumulate in the perinuclear space in large herniations. A similar phenotype is seen when US3 is deleted in HSV-1 or PRV (112, 148). Through mutagenesis studies, Wisner et al. showed that phosphorylation of gB at Thr-887 in the cytoplasmic tail is responsible for mediating fusion between the outer nuclear membrane and the HSV-1 virion. This group suggested that US3 may be packaged in the tegument layer in the perinuclear space, which brings it into close vicinity with the Thr-887 residue on gB, triggering phosphorylation to allow viral egress from the nucleus. Our studies have demonstrated that intracellular expression kinetics and incorporation of gB into mature virions is increased, and that cell to cell spread is impaired in cells infected with ΔUS3 BHV-1. Hypophosphorylation of gB at the cytoplasmic tail may be responsible for this defect in cell to cell spread if the virus is impaired in nuclear egress similar to HSV-1.

In this project, a role for US3 regulation of gB expression was clearly demonstrated both in infected cells and incorporation of the protein into mature virions. Recent studies in HSV-1 have shown that the phosphorylation of gB by US3 regulates its subcellular localization (44, 55, 153). Kato et al. have demonstrated through *in vitro* kinase assays that US3-dependent phosphorylation of gB at threonine residue 887 (Thr-887) is required for efficient downregulation of gB from the surface of infected cells (55). When US3 was rendered kinase-dead or when the Thr-887 residue in gB was mutated, it resulted in a significant increase in gB surface expression in infected cells which corresponded to a downregulation of endocytosed gB from the surface of infected cells (43). Since gB is highly immunogenic, the increased surface expression results in reduced pathogenicity in a mouse model (44). Since the results presented in this study demonstrate that US3-deletion has a significant impact on gB expression and virion

incorporation, we envisaged that US3 deletion may also have an effect on gB surface expression in infected cells.

Therefore, the effect of US3 on gB expression *in vitro* was investigated. Our results show that similar to HSV-1, US3 deletion in BHV-1 results in an increase in gB surface expression, especially at early times post infection (i.e. 3 hours post infection) and a decrease in the intracellular accumulation of gB at late stages of infection (i.e. 6 hours post infection). The difference in surface expression was difficult to ascertain at 6 hours post infection, which may reflect cells rounding up at this later time point. These results were demonstrated through confocal microscopy, and flow cytometry was used to quantify the expression. Using both permeabilized and non-permeabilized cells, the expression levels of intracellular and surface gB were assessed. Intracellular gB expression was approximately 25% higher in the WT BHV-1 infected cells than in cells infected with ΔUS3 BHV-1. This decrease in intracellular gB expression in ΔUS3 BHV-1 infected cells was associated with a corresponding 25% increase in surface gB expression. This inverse relationship is in agreement with what has previously been demonstrated in HSV-1 (43).

These studies in BHV-1 are to our knowledge, the first to demonstrate that US3 (either through direct phosphorylation or by other means) regulates gB expression, incorporation of gB into the mature BHV-1 virion, and intracellular trafficking. More specifically, US3 in BHV-1 was required for efficient endocytosis of gB from the surface of cells, and US3-deletion resulted in an upregulation of gB surface expression and a downregulation of accumulated intracellular gB. Our studies have demonstrated that gB is packaged into ΔUS3 BHV-1 mature virions at levels that are approximately 50% higher than in WT BHV-1, which may reflect more efficient packaging when gB is hypophosphorylated in the absence of US3. Furthermore, the decreased

growth titres and impairment in cell to cell spread of ΔUS3 BHV-1 compared to WT could be due to hypophosphorylation of gB in BHV-1 infected cells, since US3-dependent phosphorylation of gB has been shown to be important in nuclear egress in HSV-1 infected cells (153). Functional analysis by Miethke et al. has demonstrated that BHV-1 gB is responsible for efficient cell to cell spread of the virus, although it has not been elucidated whether US3-dependent phosphorylation is required for this process (88).

Based on our studies, we conclude that BHV-1 US3 plays a key role in the lifecycle and fitness of the virus *in vitro*. We have demonstrated that BHV-1 US3 influences the viral growth kinetics, the expression kinetics of major structural and regulatory proteins, the incorporation of key viral proteins into the mature virion, host-cell morphological changes, and cell to cell spread. The effect that US3-deletion has on viral growth kinetics may reflect a deficiency in cell to cell spread, egress of the virus from the nucleus, or potentially lower replication rates. US3 may influence viral gene expression directly through transcription regulation, or may play a more indirect role through modifying (via phosphorylation or other means) other proteins which interact directly. BHV-1 US3-deletion has a major effect on the intracellular expression and incorporation of two known substrates, VP22 and VP8, into the mature virion. Furthermore the expression and incorporation of VP16 and gB into the mature virion were significantly affected by US3-deletion, which could mean that these proteins are also substrates of BHV-1 US3. Our results also demonstrate that BHV-1 US3 could play a role in the tegumentation process.

These studies have also demonstrated that the cellular localization of VP22 and the nuclear translocation of VP8 at early times post-infection are not dependent on BHV-1 US3. We reasoned that although these proteins are known substrates of US3, US3-dependent phosphorylation is not required for their cellular localization. The localization of BHV-1 VP8

and VP22 may instead be dependent on phosphorylation by other viral and/or cellular proteins, or their localization may be independent of phosphorylation all together. On the other hand, expression and trafficking of gB was affected by the absence of US3, and in cells infected with ΔUS3 BHV-1, the surface expression of gB was increased by approximately 25%. Since gB is plays a major role in viral attachment, this could have a large effect on pathogenicity of the virus *in vivo*.

6.0 GENERAL CONCLUSIONS AND FUTURE DIRECTIONS

Our study has demonstrated a role for US3 in various aspects of the viral lifecycle and has identified potential roles that the protein may play in the fitness of BHV-1. Specifically, US3 has been demonstrated to have an effect on the expression kinetics of a number of major regulatory and structural viral proteins, including bICP4, VP5, gB, VP16, VP8, and gC. Normal incorporation of these proteins, and others, into the mature virion were also shown to be dependent on US3. Of the proteins investigated, the incorporation of the major tegument proteins VP8, VP16, and one of the major glycoproteins, gB, into the mature virion were shown to be most heavily dependent on the presence of US3. In the absence of US3, incorporation of VP8 and VP16 into the mature virion was reduced by 50% and incorporation of gB was increased by 50%. These data likely reflect a significant role for BHV-1 US3 in the expression and trafficking of viral proteins. More research is needed to identify the mechanism(s) by which US3 affects the intracellular expression and incorporation of these major proteins into the mature virion. As most of the proteins investigated are not known substrates of BHV-1 US3, it would also be useful to identify which of these viral proteins are phosphorylated by US3.

The effect that US3 has on BHV-1 growth kinetics and cell to cell spread of the virus was investigated. Using a single-step growth assay, we demonstrated that in the absence of US3, BHV-1 growth was impaired by approximately 10-fold. Furthermore, titres plateaued at 15 hours post infection compared to WT infected cells. We envisaged that viral growth impairment in the absence of US3 could reflect a deficiency in cell to cell spread of the virus, egress of the virus from the cell, or lower replication rates. Through a plaque size analysis, we were also able to identify that US3 plays a major role in cell to cell spread of BHV-1. We demonstrated that cells infected with US3-deleted BHV-1 formed significantly smaller plaques that cells infected with

WT BHV-1. It is clear that more research is required to identify the role(s) that US3 plays in BHV-1 *in vitro* growth kinetics and cell to cell spread.

Although it is unclear how BHV-1 US3 affects cell to cell spread in the virus, we envisaged that it could be through phosphorylation of VP22 and/or a putative substrate, gB. Studies in HSV-1 have shown that US3-dependent phosphorylation of gB at its cytoplasmic tail is required for efficient egress of the virus from the cell (153). VP22 has been identified as a substrate for US3 in BHV-1 and its role in cell to cell spread has been well documented (54, 66). Although we determined that BHV-1 is impaired in intercellular spread in the absence of US3, we could not find any difference in the cellular localization of VP22 in either the presence or absence of US3. We envisaged that the subcellular localization of VP22 could be independent of phosphorylation or could be dependent on CK2 phosphorylation. Follow-up studies could include identifying the residue(s) in gB which are phosphorylated by US3 and carrying out a functional mutagenesis study to determine whether US3-dependent phosphorylation of these residues affects the intercellular spread of BHV-1. Also, examining VP22 localization at late times post-infection in the absence of US3 may determine whether US3-dependent phosphorylation is required for nuclear translocation, as has been investigated by Labiuk et al. (62).

Although VP8 was previously identified as a substrate of US3 in BHV-1, our microscopy studies have demonstrated that the nuclear localization of VP8 is not dependent on phosphorylation by US3 (67). This observation was unexpected, since a putative phosphorylation residue on VP8 is in close proximity to one of the four nuclear import signals (67, 145, 158). This may mean that the nuclear translocation of VP8 occurs through a process that is independent of US3 phosphorylation involving cellular kinases, or that phosphorylation is not

required for the translocation. A systematic mutagenesis study is required to determine which (if any) of the VP8 nuclear import signals require phosphorylation for efficient translocation of the protein into the nucleus.

Our study is, to our knowledge, the first to demonstrate in the context of infection that BHV-1 US3 is required for cellular morphological changes that are characteristic of WT BHV-1 infection. Our microscopy studies have demonstrated a markedly different phenotype in cells infected with WT BHV-1 compared to a US3-deleted BHV-1. The altered phenotype could be rescued in the presence of US3. These cellular morphological differences could be due to tubulin reorganization. Since US3-dependent cytoskeleton changes have been shown to be required for efficient spread of PRV (31), it is tempting to believe that BHV-1 may use a similar mechanism. This could also explain why BHV-1 growth titres and plaque sizes were significantly impaired in the absence of US3. Future directions should involve further studies on cytoskeleton reorganization by US3 during BHV-1 infection, and if confirmed, identifying whether this might be required for efficient cell to cell spread of the virus by comparing intercellular spread of GFP-labeled viruses, similar to studies by Favoreel et al. (28).

Finally, this study provides preliminary evidence that BHV-1 US3 regulates the intracellular trafficking of gB, similar to HSV-1 (43, 44). Using microscopy and flow cytometry in the absence of BHV-1 US3, gB tended to be upregulated at the cell surface by approximately 25%, especially at early times post infection, and the intracellular accumulation of gB was reduced by approximately 25% compared to cells infected with WT BHV-1. Confirmation of these data, as well as inclusion of the US3R BHV-1 virus is required. Similar to Imai et al., a systematic mutational analysis is required to determine which residues in gB which are required for US3-dependent downregulation of gB surface expression (43).

In closing, this study has demonstrated that BHV-1 US3 plays important roles in the viral lifecycle, including *in vitro* growth, expression kinetics of major BHV-1 proteins, intercellular spread of the virus, and integration of major structural viral proteins into the mature virion. Additionally, we have provided evidence that BHV-1 US3 influences cellular morphology during infection, and affects the intracellular localization of a known substrate, VP8, and a putative substrate, gB. Finally, we have demonstrated a novel role for US3 in the intracellular trafficking of gB in BHV-1 infected cells. In the future, determining other viral substrates of BHV-1 US3, including important residues, will shed light on the mechanisms behind how US3 affects the viral lifecycle and fitness of BHV-1. After thorough characterization of BHV-1 US3 *in vitro*, the next step will be determining which roles US3 plays *in vivo* to determine its suitability in BHV-1 vaccine development.

7.0 REFERENCES

1. **Ackermann, M., and M. Engels.** 2006. Pro and contra IBR-eradication. Vet Microbiol **113:**293-302.
2. **Ackermann, M., E. Peterhans, and R. Wyler.** 1982. DNA of bovine herpesvirus type 1 in the trigeminal ganglia of latently infected calves. Am J Vet Res **43:**36-40.
3. **Ackermann, M., and R. Wyler.** 1984. The DNA of an IPV strain of bovid herpesvirus 1 in sacral ganglia during latency after intravaginal infection. Vet Microbiol **9:**53-63.
4. **Asano, S., T. Honda, F. Goshima, Y. Nishiyama, and Y. Sugiura.** 2000. US3 protein kinase of herpes simplex virus protects primary afferent neurons from virus-induced apoptosis in ICR mice. Neurosci Lett **294:**105-8.
5. **Babiuk, L. A., J. L'Italien, S. van Drunen Littel-van den Hurk, T. Zamb, J. P. Lawman, G. Hughes, and G. A. Gifford.** 1987. Protection of cattle from bovine herpesvirus type I (BHV-1) infection by immunization with individual viral glycoproteins. Virology **159:**57-66.
6. **Bello, L. J., J. C. Whitbeck, and W. C. Lawrence.** 1992. Bovine herpesvirus 1 as a live virus vector for expression of foreign genes. Virology **190:**666-73.
7. **Bishop, G. A., Glorioso, J.C., and Schwartz, S.A.** 1983. Relationship between expression of herpes simplex virus glycoproteins and susceptibility target cells to human natural killer activity. J Exp Med **157:**1544-1561.
8. **Bishop, G. A., Marlin, S.D., Schwartz, S.A., Glorioso, J.C.** 1984. Human natural killer cell recognition of herpes simplex virus type I glycoproteins: specificity analysis with the use of monoclonal antibodies and antigenic variants. Journal of Immunology **133:**2206-2214.
9. **Boelaert, F., N. Speybroeck, A. d. Kruif, M. Aerts, T. Burzykowski, G. Molenberghs, and D. L. Berkvens.** 2005. Risk factors for bovine herpesvirus-1 seropositivity. Preventive Veterinary Medicine **69:**285-295.
10. **Bonifacino, J. S., and L.M. Traub.** 2003. Signals for sorting of transmembrane proteins to endosomes and lysosomes. Annual Review in Biochemistry **72:**395-447.
11. **Bowland, S. L., and P. E. Shewen.** 2000. Bovine respiratory disease: commercial vaccines currently available in Canada. The Canadian veterinary journal. La revue vétérinaire canadienne **41:**33.
12. **Bowzard, J. B., R. J. Visalli, C. B. Wilson, J. S. Loomis, E. M. Callahan, R. J. Courtney, and J. W. Wills.** 2000. Membrane Targeting Properties of a Herpesvirus Tegument Protein-Retrovirus Gag Chimera. The Journal of Virology **74:**8692.
13. **Brideau, A. D., Enquist, L.W., and Tirabassi, R.S.** 2000. The role of virion membrane protein endocytosis in the herpesvirus life cycle. J Clin Virol **17:**69-82.

14. **Brzozowska, A., M. Rychlowski, A. D. Lipinska, and K. Bienkowska-Szewczyk.** 2010. Point mutations in BHV-1 Us3 gene abolish its ability to induce cytoskeletal changes in various cell types. Vet Microbiol **143:**8-13.

15. **Campos, F. S., A. C. Franco, S. O. Hubner, M. T. Oliveira, A. D. Silva, P. A. Esteves, P. M. Roehe, and F. A. Rijsewijk.** 2009. High prevalence of co-infections with bovine herpesvirus 1 and 5 found in cattle in southern Brazil. Vet Microbiol **139:**67-73.

16. **Carpenter, D. E., and V. Misra.** 1992. Sequences of the bovine herpesvirus 1 homologue of herpes simplex virus type-1 alpha-trans-inducing factor (UL48). Gene **119:**259-63.

17. **Chaurushiya, M. S., C. E. Lilley, A. Aslanian, J. Meisenhelder, D. C. Scott, S. Landry, S. Ticau, C. Boutell, J. R. Yates, 3rd, B. A. Schulman, T. Hunter, and M. D. Weitzman.** 2012. Viral E3 ubiquitin ligase-mediated degradation of a cellular E3: viral mimicry of a cellular phosphorylation mark targets the RNF8 FHA domain. Mol Cell **46:**79-90.

18. **Chow, T. L., Molello, J.A., Owen, N.V.** 1964. Abortion experimentally induced in cattle by infectious bovine rhinotracheitis virus. J Am Vet Med Assoc **144:**1005-1007.

19. **Connolly, S. A., J. J. Whitbeck, A. H. Rux, C. Krummenacher, S. van Drunen Littel-van den Hurk, G. H. Cohen, and R. J. Eisenberg.** 2001. Glycoprotein D homologs in herpes simplex virus type 1, pseudorabies virus, and bovine herpes virus type 1 bind directly to human HveC(nectin-1) with different affinities. Virology **280:**7-18.

20. **Crump, C. M., B. Bruun, S. Bell, L. E. Pomeranz, T. Minson, and H. M. Browne.** 2004. Alphaherpesvirus glycoprotein M causes the relocalization of plasma membrane proteins. The Journal of general virology **85:**3517.

21. **Del Medico Zajac, M., S. Romera, M. Ladelfa, F. Kotsias, F. Delgado, J. Thiry, F. Meurens, G. Keil, E. Thiry, and B. Muylkens.** 2011. In vitro-generated interspecific recombinants between bovine herpesviruses 1 and 5 show attenuated replication characteristics and establish latency in the natural host. BMC Veterinary Research **7:**19.

22. **Deruelle, M. J., and H. W. Favoreel.** 2011. Keep it in the subfamily: the conserved alphaherpesvirus US3 protein kinase. J Gen Virol **92:**18-30.

23. **Deruelle, M. J., C. Van den Broeke, H. J. Nauwynck, T. C. Mettenleiter, and H. W. Favoreel.** 2009. Pseudorabies virus US3- and UL49.5-dependent and -independent downregulation of MHC I cell surface expression in different cell types. Virology **395:**172-81.

24. **Donnelly, M., and G. Elliott.** 2001. Nuclear localization and shutting of herpes simplex virus tegment protein VP13/14. J Virol **75:**2566-2574.

25. **Donnelly, M., J. Verhagen, and G. Elliott.** 2007. RNA binding by the herpes simplex virus type 1 nucleocytoplasmic shuttling protein UL47 is mediated by an N-terminal arginine-rich domain that also functions as its nuclear localization signal. J Virol **81:**2283-96.

26. **Elliott, G., D. O'Reilly, and P. O'Hare.** 1996. Phosphorylation of the herpes simplex virus type 1 tegument protein VP22. Virology **226:**140-5.

27. **Endsley, J. J., M. J. Quade, B. Terhaar, and J. A. Roth.** 2002. BHV-1-Specific CD4+, CD8+, and gammadelta T cells in calves vaccinated with one dose of a modified live BHV-1 vaccine. Viral Immunol **15:**385-93.

28. **Engels, M., and M. Ackermann.** 1996. Pathogenesis of ruminant herpesvirus infections. Vet Microbiol **53:**3-15.

29. **Farnsworth, A., Goldsmith, K., Johnson, D.C.** 2003. Herpes simplex virus glycoproteins gD and gE/gI serve essential but redundant functions during acquisition of the virion envelope in the cytoplasm. Journal of Virology **77:**8481-8494.

30. **Favoreel, H. W., G. Van Minnebruggen, D. Adriaensen, and H. J. Nauwynck.** 2005. Cytoskeletal rearrangements and cell extensions induced by the US3 kinase of an alphaherpesvirus are associated with enhanced spread. Proc Natl Acad Sci U S A **102:**8990-5.

31. **Favoreel, H. W., Van Minnebruggen, G., Adriaensen, D., Nauwynck, H.J.** 2005. Cytoskeletal rearrangements and cell extensions induced by the US3 kinase of an alphaherpesvirus are associated with enhanced spread. Proc. Natl. Acad. Sci. U.S.A. **102:**8990-8995.

32. **Finnen, R. L., B. B. Roy, H. Zhang, and B. W. Banfield.** 2009. Analysis of filamentous process induction and nuclear localization properties of the HSV-2 serine/threonine kinase Us3. Virology.

33. **Fuchs, W., H. Granzow, and T. C. Mettenleiter.** 1997. Functional complementation of UL3.5-negative pseudorabies virus by the bovine herpesvirus 1 UL3.5 homolog. J Virol **71:**8886-92.

34. **Fuchs, W., Klupp, B.G., Granzow, H., Hengartner, C., Brack, A., Mundt, A., Enquist, L.W., Mettenleiter, T.C.** 2002c. Physical interaction between envelope glycoproteins E and M of pseudorabies virus and the major tegument protein UL49. Journal of Virology **76:**8208-8217.

35. **Geenen, K., H. W. Favoreel, L. Olsen, L. W. Enquist, and H. J. Nauwynck.** 2005. The pseudorabies virus US3 protein kinase possesses anti-apoptotic activity that protects cells from apoptosis during infection and after treatment with sorbitol or staurosporine. Virology **331:**144-50.

36. **Geiss, B. J., G. L. Cano, J. E. Tavis, and L. A. Morrison.** 2004. Herpes simplex virus 2 VP22 phosphorylation induced by cellular and viral kinases does not influence intracellular localization. Virology **330:**74-81.

37. **Geiss, B. J., J. E. Tavis, L. M. Metzger, D. A. Leib, and L. A. Morrison.** 2001. Temporal regulation of herpes simplex virus type 2 VP22 expression and phosphorylation. J Virol **75:**10721-9.

38. **Granzow, H., B. G. Klupp, and T. C. Mettenleiter.** 2005. Entry of pseudorabies virus: an immunogold-labeling study. J Virol **79:**3200-5.

39. **Granzow, H., B. G. Klupp, and T. C. Mettenleiter.** 2004. The pseudorabies virus US3 protein is a component of primary and of mature virions. J Virol **78:**1314-23.

40. **Hariharan, M. J., C. Nataraj, and S. Srikumaran.** 1993. Down regulation of murine MHC class I expression by bovine herpesvirus 1. Viral Immunol **6:**273-84.

41. **Harms, J. S., X. Ren, S. C. Oliveira, and G. A. Splitter.** 2000. Distinctions between bovine herpesvirus 1 and herpes simplex virus type 1 VP22 tegument protein subcellular associations. J Virol **74:**3301-12.

42. **Higgins, R. J., Edwards, S.** 1986. Systemic neonatal infectious bovine rhinotracheitis virus infection in suckler calves. Vet. Rec. **119:**177-178.

43. **Imai, T., J. Arii, A. Minowa, A. Kakimoto, N. Koyanagi, A. Kato, and Y. Kawaguchi.** 2011. Role of the herpes simplex virus 1 Us3 kinase phosphorylation site and endocytosis motifs in the intracellular transport and neurovirulence of envelope glycoprotein B. J Virol **85:**5003-15.

44. **Imai, T., K. Sagou, J. Arii, and Y. Kawaguchi.** 2010. Effects of phosphorylation of herpes simplex virus 1 envelope glycoprotein B by Us3 kinase in vivo and in vitro. J Virol **84:**153-62.

45. **Inman, M., J. Zhou, H. Webb, and C. Jones.** 2004. Identification of a novel bovine herpesvirus 1 transcript containing a small open reading frame that is expressed in trigeminal ganglia of latently infected cattle. J Virol **78:**5438-47.

46. **Ioannou, X. P., P. Griebel, R. Hecker, L. A. Babiuk, and S. van Drunen Littel-van den Hurk.** 2002. The immunogenicity and protective efficacy of bovine herpesvirus 1 glycoprotein D plus Emulsigen are increased by formulation with CpG oligodeoxynucleotides. J Virol **76:**9002-10.

47. **Iwahori, S., T. Murata, A. Kudoh, Y. Sato, S. Nakayama, H. Isomura, T. Kanda, and T. Tsurumi.** 2009. Phosphorylation of p27Kip1 by Epstein-Barr virus protein kinase induces its degradation through SCFSkp2 ubiquitin ligase actions during viral lytic replication. J Biol Chem **284:**18923-31.

48. **Jericho, K. W., W. D. Yates, and L. A. Babiuk.** 1982. Bovine herpesvirus-1 vaccination against experimental bovine herpesvirus-1 and Pasteurella haemolytica respiratory tract infection: onset of protection. Am J Vet Res **43:**1776-80.

49. **Jones, C.** 2003. Herpes simplex virus type 1 and bovine herpesvirus 1 latency. Clin Microbiol Rev **16:**79-95.

50. **Jones, C., and S. Chowdhury.** 2010. Bovine Herpesvirus Type 1 (BHV-1) is an Important Cofactor in the Bovine Respiratory Disease Complex. Veterinary Clinics of North America: Food Animal Practice **26:**303-321.

51. **Jones, C., and S. Chowdhury.** 2007. A review of the biology of bovine herpesvirus type 1 (BHV-1), its role as a cofactor in the bovine respiratory disease complex and development of improved vaccines. Anim Health Res Rev **8:**187-205.

52. **Jones, C., V. Geiser, G. Henderson, Y. Jiang, F. Meyer, S. Perez, and Y. Zhang.** 2006. Functional analysis of bovine herpesvirus 1 (BHV-1) genes expressed during latency. Vet Microbiol **113:**199-210.

53. **Kaashoek, M. J., F. A. Rijsewijk, R. C. Ruuls, G. M. Keil, E. Thiry, P. P. Pastoret, and J. T. Van Oirschot.** 1998. Virulence, immunogenicity and reactivation of bovine herpesvirus 1 mutants with a deletion in the gC, gG, gI, gE, or in both the gI and gE gene. Vaccine **16:**802-9.

54. **Kalthoff, D., H. Granzow, S. Trapp, and M. Beer.** 2008. The UL49 gene product of BoHV-1: a major factor in efficient cell-to-cell spread. J Gen Virol **89:**2269-74.

55. **Kato, A., J. Arii, I. Shiratori, H. Akashi, H. Arase, and Y. Kawaguchi.** 2009. Herpes simplex virus 1 protein kinase Us3 phosphorylates viral envelope glycoprotein B and regulates its expression on the cell surface. J Virol **83:**250-61.

56. **Kato, A., Z. Liu, A. Minowa, T. Imai, M. Tanaka, K. Sugimoto, Y. Nishiyama, J. Arii, and Y. Kawaguchi.** 2011. Herpes simplex virus 1 protein kinase Us3 and major tegument protein UL47 reciprocally regulate their subcellular localization in infected cells. J Virol **85:**9599-613.

57. **Kato, A., M. Yamamoto, T. Ohno, H. Kodaira, Y. Nishiyama, and Y. Kawaguchi.** 2005. Identification of proteins phosphorylated directly by the Us3 protein kinase encoded by herpes simplex virus 1. J Virol **79:**9325-31.

58. **Kato, A., M. Yamamoto, T. Ohno, M. Tanaka, T. Sata, Y. Nishiyama, and Y. Kawaguchi.** 2006. Herpes simplex virus 1-encoded protein kinase UL13 phosphorylates viral Us3 protein kinase and regulates nuclear localization of viral envelopment factors UL34 and UL31. J Virol **80:**1476-86.

59. **Klupp, B. G., H. Granzow, and T. C. Mettenleiter.** 2001. Effect of the pseudorabies virus US3 protein on nuclear membrane localization of the UL34 protein and virus egress from the nucleus. J Gen Virol **82:**2363-71.

60. **Kopp, M., Granzow, H., Fuchs, W., Klupp, B.G., Mettenleiter, T.C.** 2004. Simultaneous deletion of pseudorabies virus tegument protein UL11 and glycoprotein M severely impairs secondary envelopment. Journal of Virology **78:**3024-3034.

61. **Koppel, R., B. Vogt, and M. Schwyzer.** 1997. Immediate-early protein BICP22 of bovine herpesvirus 1 trans-represses viral promoters of different kinetic classes and is itself regulated by BICP0 at transcriptional and posttranscriptional levels. Arch Virol **142:**2447-64.

62. **Koppers-Lalic, D., F. A. Rijsewijk, S. B. Verschuren, J. A. van Gaans-Van den Brink, A. Neisig, M. E. Ressing, J. Neefjes, and E. J. Wiertz.** 2001. The UL41-encoded virion host shutoff (vhs) protein and vhs-independent mechanisms are responsible for down-regulation of MHC class I molecules by bovine herpesvirus 1. J Gen Virol **82:**2071-81.

63. **Kupferschmied, H. U., U. Kihm, P. Bachmann, K. H. Müller, and M. Ackermann.** 1986. Transmission of IBR/IPV virus in bovine semen: A case report. Theriogenology **25:**439-443.

64. **Kweon, C. H., S. W. Kang, E. J. Choi, and Y. B. Kang.** 1999. Bovine herpes virus expressing envelope protein (E2) of bovine viral diarrhea virus as a vaccine candidate. J Vet Med Sci **61:**395-401.

65. **Kwong, A., Frenkel, N.** 1989. The herpes simplex virus virion host shutoff function. Journal of Virology **63:**4834-4839.

66. **Labiuk, S., V. Lobanov, Z. Lawman, M. Snider, L. Babiuk, and S. van Drunen Littel-van den Hurk.** 2009. Bovine Herpesvirus-1 US3 Protein Kinase: Critical Residues and Involvement in the Phosphorylation of VP22. J Gen Virol.

67. **Labiuk, S. L., L. A. Babiuk, and S. van Drunen Littel-van den Hurk.** 2009. Major tegument protein VP8 of bovine herpesvirus 1 is phosphorylated by viral US3 and cellular CK2 protein kinases. J Gen Virol **90:**2829-39.

68. **Ladelfa, M. F., F. Kotsias, M. P. Del Medico Zajac, C. Van den Broeke, H. Favoreel, S. A. Romera, and G. Calamante.** Effect of the US3 protein of bovine herpesvirus 5 on the actin cytoskeleton and apoptosis. Vet Microbiol **153:**361-6.

69. **Lam, N., and G. J. Letchworth.** 2000. Bovine herpesvirus 1 U(L)3.5 interacts with bovine herpesvirus 1 alpha-transinducing factor. J Virol **74:**2876-84.

70. **Leach, N., S. L. Bjerke, D. K. Christensen, J. M. Bouchard, F. Mou, R. Park, J. Baines, T. Haraguchi, and R. J. Roller.** 2007. Emerin is hyperphosphorylated and redistributed in herpes simplex virus type 1-infected cells in a manner dependent on both UL34 and US3. J Virol **81:**10792-803.

71. **Lehman, I. R., and P. E. Boehmer.** 1999. Replication of herpes simplex virus DNA. The Journal of biological chemistry **274:**28059.

72. **Li, Y., S. van Drunen Littel-van den Hurk, L. A. Babiuk, and X. Liang.** 1995. Characterization of cell-binding properties of bovine herpesvirus 1 glycoproteins B, C, and D: identification of a dual cell-binding function of gB. J Virol **69:**4758-68.

73. **Liang, L., and B. Roizman.** 2008. Expression of gamma interferon-dependent genes is blocked independently by virion host shutoff RNase and by US3 protein kinase. J Virol **82:**4688-96.

74. **Liang, X., B. Chow, and L. A. Babiuk.** 1997. Study of immunogenicity and virulence of bovine herpesvirus 1 mutants deficient in the UL49 homolog, UL49.5 homolog and dUTPase genes in cattle. Vaccine **15:**1057-64.

75. **Liang, X. P., L. A. Babiuk, S. van Drunen Littel-van den Hurk, D. R. Fitzpatrick, and T. J. Zamb.** 1991. Bovine herpesvirus 1 attachment to permissive cells is mediated by its major glycoproteins gI, gIII, and gIV. J Virol **65:**1124-32.

76. **Liu, Z. F., M. C. Brum, A. Doster, C. Jones, and S. I. Chowdhury.** 2008. A bovine herpesvirus type 1 mutant virus specifying a carboxyl-terminal truncation of glycoprotein E is defective in anterograde neuronal transport in rabbits and calves. J Virol **82:**7432-42.

77. **Lobanov, V. A., S. L. Maher-Sturgess, M. G. Snider, Z. Lawman, L. A. Babiuk, and S. van Drunen Littel-van den Hurk.** 2010. A UL47 gene deletion mutant of bovine

herpesvirus type 1 exhibits impaired growth in cell culture and lack of virulence in cattle. J Virol **84:**445-58.

78. **Longnecker, R., and B. Roizman.** 1987. Clustering of genes dispensable for growth in culture in the S component of the HSV-1 genome. Science **236:**573-6.

79. **Mahony, T. J., F. M. McCarthy, J. L. Gravel, and P. L. Young.** 2003. Rapid and efficient construction of recombinant bovine herpesvirus 1 genomes. J Virol Methods **107:**269-74.

80. **Maringer, K., Stylianou, J., Elliot, G.** 2012. A network of protein interactions around the herpes simplex virus tegument protein VP22. Journal of Virology **86:**12971-12982.

81. **Mars, M. H., M. C. de Jong, C. van Maanen, J. J. Hage, and J. T. van Oirschot.** 2000. Airborne transmission of bovine herpesvirus 1 infections in calves under field conditions. Vet Microbiol **76:**1-13.

82. **Mechor, G. D., C. G. Rousseaux, O. M. Radostits, L. A. Babiuk, and L. Petrie.** 1987. Protection of newborn calves against fatal multisystemic infectious bovine rhinotracheitis by feeding colostrum from vaccinated cows. Can J Vet Res **51:**452-9.

83. **Mettenleiter, T. C.** 2002. Brief overview on cellular virus receptors. Virus Research **82:**3-8.

84. **Mettenleiter, T. C.** 2004. Budding Events in herpesvirus morphogenesis. Virus Research **106:**167-180.

85. **Mettenleiter, T. C.** 2006. Intriguing interplay between viral proteins during herpesvirus assembly or: the herpesvirus assembly puzzle. Veterinary Microbiology **113:**163-169.

86. **Mettenleiter, T. C. B. G. K. a. H. G.** 2006. Herpesvirus assembly: a tale of two membranes. Current Opinion in Microbiology **9:**423-429.

87. **Michael, K., B. G. Klupp, T. C. Mettenleiter, and A. Karger.** 2006. Composition of pseudorabies virus particles lacking tegument protein US3, UL47, or UL49 or envelope glycoprotein E. J Virol **80:**1332-9.

88. **Miethke, A., G. M. Keil, F. Weiland, and T. C. Mettenleiter.** 1995. Unidirectional complementation between glycoprotein B homologues of pseudorabies virus and bovine herpesvirus 1 is determined by the carboxy-terminal part of the molecule. J Gen Virol **76 (Pt 7):**1623-35.

89. **Miller, J. M., C. A. Whetstone, and M. J. Van der Maaten.** 1991. Abortifacient property of bovine herpesvirus type 1 isolates that represent three subtypes determined by restriction endonuclease analysis of viral DNA. Am J Vet Res **52:**458-61.

90. **Minh, L. Q.** 2011. Studies on the bovine herpesvirus 1 US3 protein kinase (BHV-1pUS3). Dissertation. Ernst-Moritz-Arndt-Universität Greifswald, Greifswald, Insel Riems.

91. **Misra, V., R. M. Blumenthal, and L. A. Babiuk.** 1981. Proteins Specified by bovine herpesvirus 1 (infectious bovine rhinotracheitis virus). J Virol **40:**367-78.

92. **Misra, V., A. C. Bratanich, D. Carpenter, and P. O'Hare.** 1994. Protein and DNA elements involved in transactivation of the promoter of the bovine herpesvirus (BHV) 1

IE-1 transcription unit by the BHV alpha gene trans-inducing factor. J Virol **68:**4898-909.

93. **Misra, V., S. Walker, S. Hayes, and P. O'Hare.** 1995. The bovine herpesvirus alpha gene trans-inducing factor activates transcription by mechanisms different from those of its herpes simplex virus type 1 counterpart VP16. J Virol **69:**5209-16.

94. **Morris, J. B., H. Hofemeister, and P. O'Hare.** 2007. Herpes simplex virus infection induces phosphorylation and delocalization of emerin, a key inner nuclear membrane protein. J Virol **81:**4429-37.

95. **Mou, F., T. Forest, and J. D. Baines.** 2007. US3 of herpes simplex virus type 1 encodes a promiscuous protein kinase that phosphorylates and alters localization of lamin A/C in infected cells. J Virol **81:**6459-70.

96. **Mou, F., E. Wills, and J. D. Baines.** 2009. Phosphorylation of the U(L)31 protein of herpes simplex virus 1 by the U(S)3-encoded kinase regulates localization of the nuclear envelopment complex and egress of nucleocapsids. J Virol **83:**5181-91.

97. **Mou, F., E. G. Wills, R. Park, and J. D. Baines.** 2008. Effects of lamin A/C, lamin B1, and viral US3 kinase activity on viral infectivity, virion egress, and the targeting of herpes simplex virus U(L)34-encoded protein to the inner nuclear membrane. J Virol **82:**8094-104.

98. **Muylkens, B., J. Thiry, P. Kirten, F. Schynts, and E. Thiry.** 2007. Bovine herpesvirus 1 infection and infectious bovine rhinotracheitis. Vet Res **38:**181-209.

99. **Nakamichi, K., K. Ohara, D. Kuroki, and H. Otsuka.** 2000. Bovine herpesvirus 1 glycoprotein G is required for viral growth by cell-to-cell infection. Virus Res **68:**175-81.

100. **Nandi, S., M. Kumar, M. Manohar, and R. S. Chauhan.** 2009. Bovine herpes virus infections in cattle. Anim Health Res Rev **10:**85-98.

101. **Nataraj, C., S. Eidmann, M. J. Hariharan, J. H. Sur, G. A. Perry, and S. Srikumaran.** 1997. Bovine herpesvirus 1 downregulates the expression of bovine MHC class I molecules. Viral Immunol **10:**21-34.

102. **OIE.** 2010. OIE Terrestrial Manual, Chapter 2.4.13 Infectious Bovine Rhinotracheitis/Infectious Pustular Vulvovaginitis.

103. **Oien, N. L., D. R. Thomsen, M. W. Wathen, W. W. Newcomb, J. C. Brown, and F. L. Homa.** 1997. Assembly of herpes simplex virus capsids using the human cytomegalovirus scaffold protein: critical role of the C terminus. J Virol **71:**1281-91.

104. **Okazaki, K., T. Matsuzaki, Y. Sugahara, J. Okada, M. Hasebe, Y. Iwamura, M. Ohnishi, T. Kanno, M. Shimizu, E. Honda, and et al.** 1991. BHV-1 adsorption is mediated by the interaction of glycoprotein gIII with heparinlike moiety on the cell surface. Virology **181:**666-70.

105. **Pastoret, P. P., E. Thiry, B. Brochier, and G. Derboven.** 1982. Bovid herpesvirus 1 infection of cattle: pathogenesis, latency, consequences of latency. Ann Rech Vet **13:**221-35.

106. **Peri, P., R. K. Mattila, H. Kantola, E. Broberg, H. S. Karttunen, M. Waris, T. Vuorinen, and V. Hukkanen.** 2008. Herpes simplex virus type 1 Us3 gene deletion influences toll-like receptor responses in cultured monocytic cells. Virol J **5:**140.

107. **Poon, A. P., H. Gu, and B. Roizman.** 2006. ICP0 and the US3 protein kinase of herpes simplex virus 1 independently block histone deacetylation to enable gene expression. Proc Natl Acad Sci U S A **103:**9993-8.

108. **Preston, C. M., and M. J. Nicholl.** Induction of Cellular Stress Overcomes the Requirement of Herpes Simplex Virus Type 1 for Immediate-Early Protein ICP0 and Reactivates Expression from Quiescent Viral Genomes. The Journal of Virology **82:**11775.

109. **Purves, F. C., D. Spector, and B. Roizman.** 1991. The herpes simplex virus 1 protein kinase encoded by the US3 gene mediates posttranslational modification of the phosphoprotein encoded by the UL34 gene. J Virol **65:**5757-64.

110. **Rebordosa, X., J. Pinol, J. A. Perez-Pons, J. Lloberas, J. Naval, X. Serra-Hartmann, E. Espuna, and E. Querol.** 1996. Glycoprotein E of bovine herpesvirus type 1 is involved in virus transmission by direct cell-to-cell spread. Virus Res **45:**59-68.

111. **Reynolds, A. E., B. J. Ryckman, J. D. Baines, Y. Zhou, L. Liang, and R. J. Roller.** 2001. U(L)31 and U(L)34 proteins of herpes simplex virus type 1 form a complex that accumulates at the nuclear rim and is required for envelopment of nucleocapsids. J Virol **75:**8803-17.

112. **Reynolds, A. E., E. G. Wills, R. J. Roller, B. J. Ryckman, and J. D. Baines.** 2002. Ultrastructural localization of the herpes simplex virus type 1 UL31, UL34, and US3 proteins suggests specific roles in primary envelopment and egress of nucleocapsids. J Virol **76:**8939-52.

113. **Robinson, K. E., J. Meers, J. L. Gravel, F. M. McCarthy, and T. J. Mahony.** 2008. The essential and non-essential genes of Bovine herpesvirus 1. J Gen Virol **89:**2851-63.

114. **Roizman, B., Knipe, D.** 2001. Herpes simplex viruses and their replication., p. 2399-2460. *In* D. Knipe, Howley, P.M. (ed.), Fields Virology, vol. fourth ed.

115. **Roizman, B., Pellett, P.E.** 2001. The family Herpesviridae: a brief introduction., p. 2381-2397. *In* D. M. Knipe, Howley, P.M. (ed.), Fields Virology, 4 ed, vol. fourth ed.

116. **Roller, R. J., Y. Zhou, R. Schnetzer, J. Ferguson, and D. DeSalvo.** 2000. Herpes Simplex Virus Type 1 UL34 Gene Product Is Required for Viral Envelopment. The Journal of Virology **74:**117.

117. **Ryckman, B. J., and R. J. Roller.** 2004. Herpes simplex virus type 1 primary envelopment: UL34 protein modification and the US3-UL34 catalytic relationship. J Virol **78:**399-412.

118. **Sagou, K., T. Imai, H. Sagara, M. Uema, and Y. Kawaguchi.** 2009. Regulation of the catalytic activity of herpes simplex virus 1 protein kinase Us3 by autophosphorylation and its role in pathogenesis. J Virol **83:**5773-83.

119. **Sanchez-Pescador, L., Paz, P., Navarro, D., Pereira, L., Kohl, S.** 1992. Epitopes of herpes simplex virus type 1 glycoprotein B that bind type-common neutralizing antibodies elicit type-specific antibody-dependent cellular cytotoxicity. J Infect Dis **166:**623-627.

120. **Schrijver, R. S., J. P. Langedijk, G. M. Keil, W. G. Middel, M. Maris-Veldhuis, J. T. Van Oirschot, and F. A. Rijsewijk.** 1997. Immunization of cattle with a BHV1 vector vaccine or a DNA vaccine both coding for the G protein of BRSV. Vaccine **15:**1908-16.

121. **Schroder, C., and G. M. Keil.** 1999. Bovine herpesvirus 1 requires glycoprotein H for infectivity and direct spreading and glycoproteins gH(W450) and gB for glycoprotein D-independent cell-to-cell spread. J Gen Virol **80 (Pt 1):**57-61.

122. **Schroder, C., G. Linde, F. Fehler, and G. M. Keil.** 1997. From essential to beneficial: glycoprotein D loses importance for replication of bovine herpesvirus 1 in cell culture. J Virol **71:**25-33.

123. **Schroeder, R. J., and M. D. Moys.** 1954. An acute upper respiratory infection of dairy cattle. J Am Vet Med Assoc **125:**471-2.

124. **Schumacher, D., B. K. Tischer, S. Trapp, and N. Osterrieder.** 2005. The protein encoded by the US3 orthologue of Marek's disease virus is required for efficient de-envelopment of perinuclear virions and involved in actin stress fiber breakdown. J Virol **79:**3987-97.

125. **Schwyzer, M., and M. Ackermann.** 1996. Molecular virology of ruminant herpesviruses. Vet Microbiol **53:**17-29.

126. **Schwyzer, M., D. Styger, B. Vogt, D. E. Lowery, C. Simard, S. LaBoissiere, V. Misra, C. Vlcek, and V. Paces.** 1996. Gene contents in a 31-kb segment at the left genome end of bovine herpesvirus-1. Vet Microbiol **53:**67-77.

127. **Schynts, F., M. A. McVoy, F. Meurens, B. Detry, A. L. Epstein, and E. Thiry.** 2003. The structures of bovine herpesvirus 1 virion and concatemeric DNA: implications for cleavage and packaging of herpesvirus genomes. Virology **314:**326-35.

128. **Simpson-Holley, M., Colgrove, R.C., Nalepa, G., Harper, J.W., Knipe, D.M.** 2005. Identification and functional evaluation of cellular and viral factors involved in the alteration of nuclear architecture during herpes simplex virus 1 infection. Journal of Virology **79:**12840-12851.

129. **Solis-Calderon, J. J., V. M. Segura-Correa, J. C. Segura-Correa, and A. Alvarado-Islas.** 2003. Seroprevalence of and risk factors for infectious bovine rhinotracheitis in beef cattle herds of Yucatan, Mexico. Prev Vet Med **57:**199-208.

130. **Straub, O. C.** 1991. BHV1 infections: relevance and spread in Europe. Comp Immunol Microbiol Infect Dis **14:**175-86.

131. **Takashima, Y., H. Tamura, X. Xuan, and H. Otsuka.** 1999. Identification of the US3 gene product of BHV-1 as a protein kinase and characterization of BHV-1 mutants of the US3 gene. Virus Res **59:**23-34.

132. **Thiry, J., V. Keuser, B. Muylkens, F. Meurens, S. Gogev, A. Vanderplasschen, and E. Thiry.** 2006. Ruminant alphaherpesviruses related to bovine herpesvirus 1. Vet Res **37:**169-90.

133. **Tikoo, S. K., M. Campos, and L. A. Babiuk.** 1995. Bovine herpesvirus 1 (BHV-1): biology, pathogenesis, and control. Adv Virus Res **45:**191-223.

134. **Tischer, B. K., G. A. Smith, and N. Osterrieder.** 2010. En passant mutagenesis: a two step markerless red recombination system. Methods Mol Biol **634:**421-30.

135. **Tyborowska, J., K. Bienkowska-Szewczyk, M. Rychlowski, J. T. Van Oirschot, and F. A. Rijsewijk.** 2000. The extracellular part of glycoprotein E of bovine herpesvirus 1 is sufficient for complex formation with glycoprotein I but not for cell-to-cell spread. Arch Virol **145:**333-51.

136. **Van den Broeke, C., M. Radu, M. Deruelle, H. Nauwynck, C. Hofmann, Z. M. Jaffer, J. Chernoff, and H. W. Favoreel.** 2009. Alphaherpesvirus US3-mediated reorganization of the actin cytoskeleton is mediated by group A p21-activated kinases. Proc Natl Acad Sci U S A **106:**8707-12.

137. **Van Drunen Littel-van den Hurk, S., R. P. Braun, P. J. Lewis, B. C. Karvonen, L. A. Babiuk, and P. J. Griebel.** 1999. Immunization of neonates with DNA encoding a bovine herpesvirus glycoprotein is effective in the presence of maternal antibodies. Viral Immunol **12:**67-77.

138. **van Drunen Littel-van den Hurk, S., S. Garzon, J. V. van den Hurk, L. A. Babiuk, and P. Tijssen.** 1995. The role of the major tegument protein VP8 of bovine herpesvirus-1 in infection and immunity. Virology **206:**413-25.

139. **van Drunen Littel-van den Hurk, S., D. Myers, P. A. Doig, B. Karvonen, M. Habermehl, L. A. Babiuk, M. Jelinski, J. Van Donkersgoed, K. Schlesinger, and C. Rinehart.** 2001. Identification of a mutant bovine herpesvirus-1 (BHV-1) in post-arrival outbreaks of IBR in feedlot calves and protection with conventional vaccination. Can J Vet Res **65:**81-8.

140. **van Drunen Littel-van den Hurk, S., J. Van Donkersgoed, J. Kowalski, J. V. van den Hurk, R. Harland, L. A. Babiuk, and T. J. Zamb.** 1994. A subunit gIV vaccine, produced by transfected mammalian cells in culture, induces mucosal immunity against bovine herpesvirus-1 in cattle. Vaccine **12:**1295-302.

141. **Van Minnebruggen, G., H. W. Favoreel, L. Jacobs, and H. J. Nauwynck.** 2003. Pseudorabies virus US3 protein kinase mediates actin stress fiber breakdown. J Virol **77:**9074-80.

142. **van Oirschot, J. T.** 1995. Bovine herpesvirus 1 in semen of bulls and the risk of transmission: a brief review. Vet Q **17:**29-33.

143. **van Schaik, G., Y. H. Schukken, M. Nielen, A. A. Dijkhuizen, H. W. Barkema, and G. Benedictus.** 2002. Probability of and risk factors for introduction of infectious diseases into Dutch SPF dairy farms: a cohort study. Prev Vet Med **54:**279-89.

144. **Vasilenko, N. L., M. Snider, S. L. Labiuk, V. A. Lobanov, L. A. Babiuk, and S. van Drunen Littel-van den Hurk.** Bovine herpesvirus-1 VP8 interacts with DNA damage binding protein-1 (DDB1) and is monoubiquitinated during infection. Virus Res **167:**56-66.

145. **Verhagen, J., I. Hutchinson, and G. Elliott.** 2006. Nucleocytoplasmic shuttling of bovine herpesvirus 1 UL47 protein in infected cells. J Virol **80:**1059-63.

146. **Vlcek, C., V. Benes, Z. Lu, G. F. Kutish, V. Paces, D. Rock, G. J. Letchworth, and M. Schwyzer.** 1995. Nucleotide sequence analysis of a 30-kb region of the bovine herpesvirus 1 genome which exhibits a colinear gene arrangement with the UL21 to UL4 genes of herpes simplex virus. Virology **210:**100-8.

147. **Vonk Noordegraaf, A., A. Labrovic, K. Frankena, D. U. Pfeiffer, and M. Nielen.** 2004. Simulated hazards of loosing infection-free status in a Dutch BHV1 model. Prev Vet Med **62:**51-8.

148. **Wagenaar, F., J. M. Pol, B. Peeters, A. L. Gielkens, N. de Wind, and T. G. Kimman.** 1995. The US3-encoded protein kinase from pseudorabies virus affects egress of virions from the nucleus. J Gen Virol **76 (Pt 7):**1851-9.

149. **Wang, X., C. Patenode, and B. Roizman.** US3 protein kinase of HSV-1 cycles between the cytoplasm and nucleus and interacts with programmed cell death protein 4 (PDCD4) to block apoptosis. Proc Natl Acad Sci U S A **108:**14632-6.

150. **Whetstone, C. A., J. G. Wheeler, and D. E. Reed.** 1986. Investigation of possible vaccine-induced epizootics of infectious bovine rhinotracheitis, using restriction endonuclease analysis of viral DNA. Am J Vet Res **47:**1789-95.

151. **Whitbeck, J. C., L. J. Bello, and W. C. Lawrence.** 1988. Comparison of the bovine herpesvirus 1 gI gene and the herpes simplex virus type 1 gB gene. J Virol **62:**3319-27.

152. **Winkler, M. T., A. Doster, and C. Jones.** 1999. Bovine herpesvirus 1 can infect CD4(+) T lymphocytes and induce programmed cell death during acute infection of cattle. J Virol **73:**8657-68.

153. **Wisner, T. W., C. C. Wright, A. Kato, Y. Kawaguchi, F. Mou, J. D. Baines, R. J. Roller, and D. C. Johnson.** 2009. Herpesvirus gB-induced fusion between the virion envelope and outer nuclear membrane during virus egress is regulated by the viral US3 kinase. J Virol **83:**3115-26.

154. **Wussow, F., Tanja Spieckermann, Anne Brunnemann, Linda Huske, Tuna Toptan and Helmut Fickenscher.** 2011. Bacterial Genetics of Large Mammalian DNA Viruses: Bacterial Artificial Chromosomes as a Prerequisite for Efficiently Studying Viral DNA Replication and Functions. *In* H. Seligmann (ed.), DNA Replication - Current Advances. InTech.

155. **Yates, W. D.** 1982. A review of infectious bovine rhinotracheitis, shipping fever pneumonia and viral-bacterial synergism in respiratory disease of cattle. Can J Comp Med **46:**225-63.

156. **Zakhartchouk, A. N., C. Pyne, G. K. Mutwiri, Z. Papp, M. E. Baca-Estrada, P. Griebel, L. A. Babiuk, and S. K. Tikoo.** 1999. Mucosal immunization of calves with recombinant bovine adenovirus-3: induction of protective immunity to bovine herpesvirus-1. J Gen Virol **80 (Pt 5):**1263-9.

157. **Zhang, Y. D., Sirko, A., and J.L. McKnight.** 1991. Role of herpes simplex virus type 1 UL47 and UL47 in alpha TIF-mediated transcriptional induction: characterization of three viral deletion mutants. Journal of Virology **65:**829-841.

158. **Zheng, C., R. Brownlie, L. A. Babiuk, and S. van Drunen Littel-van den Hurk.** 2004. Characterization of nuclear localization and export signals of the major tegument protein VP8 of bovine herpesvirus-1. Virology **324:**327-39.

159. **Zhou, Z., Chen, D., Jakana, J., Rixon, F.J., Chiu, W.** 1999. Visualization of tegument-capsid interactions and DNA in intact herpes simplex virus type 1 virions. Journal of Virology **73:**3210-3218.